# The last tenascin: Insights on tenascin-W functions and regulation

**INAUGURALDISSERTATION**

zur
Erlangung der Würde eines Doktors der Philosophie
vorgelegt der
Philosophisch-Naturwissenschaftlichen Fakultät
der Universität Basel

von

**Enrico Martina**

aus Italien

Basel, 2012

Genehmigt von der Philosophisch-Naturwissenschaftlichen Fakultät auf Antrag von

Prof. Dr. Ruth Chiquet-Ehrismann

Prof. Dr. Gerhard Christofori

Dr. Mohamed Bentires-Alj

Basel, den 22/05/2012

Prof. Dr. Martin Spiess
(Dekan)

*Ai miei genitori, Silvano e Marisa:*
*Grazie per avermi sempre sostenuto e amato.*

# ACKNOWLEDGMENTS

Many people supported and positively influenced me during these years at the FMI, and I would like to thank them all, for this thesis would not have been possible without them.

First of all, I would like to thank Ruth Chiquet-Ehrismann, for giving me the opportunity to work in her lab. She continually supported me, advised me, gave me the independence to pursue my ideas, and she was always there smiling when I needed her help.

My deepest gratitude goes to Florence Brellier: she taught me everything, and if I was ever able to do something good in the lab, it is because of her teachings. Her limitless patience and unbelievable kindness made things so much better.

Many thanks to all the past and present lab members, especially Martin Degen, on which shoulder I climbed to produce this thesis; Roman Lutz, that provided me with true friendship and help and a snowboard; Jan Beckmann, that always gave me good and precious advices; Jacqueline Ferralli, that gave me so much help that it would be ridiculous to try quantify; and Marianne, Daniela, Michaela, Ulrike, Irem, Francesca, Maria, Matthias, Jonas, Ismail and Dominik, for the nice atmosphere.

I would like to thank Matthias Chiquet and Richard P. Tucker, for the scientific discussions and advices, and Arnaud Scherberich, Paul Bourgine, Nathalie Heuzé-Vourc'h, Falk Saupe, Michael Van Der Heyden, Gertraud Orend, Natsuko Imaizumi, Curzio Rüegg for the collaborations we had.

I am grateful to Gerard Christofori and Mohamed Bentires-Alj for being in my thesis committee and for the good advices and scientific input.

At the end, I want to deeply thank all the wonderful people I met at the FMI throughout these years: you made these the best years of my life. Thank you!

# TABLE OF CONTENTS

**I. Summary ..... 3**

**II. Introduction ..... 4**

II.1 – The importance of tumor microenvironment ..... 5

II.2 – Tenascin-W: an extracellular matrix protein associated with osteogenesis and cancer. ..... 7

II.3 – Aim of this work ..... 12

**III. Results ..... 13**

III.1 Published papers ..... 14

III.1.1 – Tenascin-W is a specific marker of glioma-associated blood vessels and stimulates angiogenesis *in vitro* ..... 14

III.1.2 – The adhesion modulating properties of tenascin-W ..... 25

III.2 Submitted manuscript ..... 34

III.2.1 – Tenascin-W is a better cancer biomarker than tenascin-C for most human solid tumors ..... 34

III.3 Unpublished results ..... 56

III.3.1 – Tenascin-W gene is repressed by the NuRD complex ..... 56

III.3.1.1 – The genomic location of the human tenascin-W gene ..... 56

III.3.1.2 – Characterization of the human tenascin-W promoter ..... 57

III.3.1.3 – In silico prediction of transcription factor binding sites ..... 62

III.3.1.4 – DNA pull-down of complexes binding to the repressor region ..... 64

III.3.1.5 – Chromatin immunoprecipitation ..... 66

III.3.2 – Bone marrow-derived stem cells differentiated to osteoblasts express tenascin-W *in vitro* ..... 71

**IV. Discussion ..... 74**

IV.1 – Tenascin-W in the context of tumors ..... 75

IV.2 – Regulation of tenascin-W ..... 78

IV.3 – Tenascin-W and bone marrow-derived mesenchymal stem cells ..... 82

**V. Appendix ..... 84**

V.1 Experimental procedures (unpublished results) ..... 85

SEAP constructs ..... 85

Cell culture and transfection ..... 86

Reporter gene assay ..... 87

In silico analysis for conserved sequences and transcription factor binding sites ..... 87

DNA pull-down ..... 88

Mass spectrometry ..... 89

qPCR ..... 90

Antibodies ..... 90

Chromatin immunoprecipitation ..... 90

Primary BMSC culture and differentiation ..... 92

Immunofluorescence ..... 92

V.2 Supplementary data ..... 93

V.3 References ..... 94

# I. SUMMARY

Over the last decade, it became clear that the tumor stroma plays an active role in the process of tumor progression, by interacting with the transformed cells and providing a permissive microenvironment for malignant growth. The tumor microenvironment is a complex system comprised of extracellular matrix and the different cell populations within it. The extracellular matrix that surrounds solid tumors is very different from the healthy counterpart. Various proteins are upregulated in the tumor stroma, among them two members of the tenascin family, tenascin-C and tenascin-W. Similar to tenascin-C, tenascin-W is mainly expressed during development and in the adult its expression is restricted. Tenascin-W has previously been found in the stroma of breast cancer and colon carcinoma. We have extended the range of human solid tumors that express tenascin-W to brain tumor, melanoma, lung and kidney carcinoma, and we show that tenascin-W is not detectable in the corresponding normal tissues. Moreover, we demonstrate that tenascin-W is often localized in close proximity with tumor blood vessels. Our in vitro studies reveal that tenascin-W has an antiadhesive, pro-migratory effect on a variety of cultured cells, in particular endothelial cells. We therefore postulate a pro-angiogenic role for tenascin-W in tumors. Due to its specific expression in solid tumors, we propose tenascin-W as a tumor biomarker.

We also report that tenascin-W is upregulated during osteogenic differentiation of human bone marrow derived mesenchymal stem cells, fitting with its expression during bone development reported in chicken and mice.

In order to shed light on the mechanism of regulation, we studied the human tenascin-W promoter. We found a putative GATA binding site in this promoter that enhances reporter gene activity when deleted or mutated. We used a labeled DNA probe harboring the binding site in pulldown experiments, followed by mass spec identification of the binding proteins. We identified four members of the NuRD repressor complex among the proteins pulled down. The specific binding of the CHD4 core component of the complex to the human tenascin-W promoter was confirmed by chromatin immunoprecipitation. We therefore speculate that the human tenascin-W gene is silenced by NuRD-mediated chromatin remodeling.

# INTRODUCTION

# II. INTRODUCTION

## II.1 – The importance of tumor microenvironment

Carcinogenesis is a multistep process characterized by the progressive acquisition and accumulation by cancer cells of genetic and epigenetic alterations that eventually allow them to escape the controls and constraints of tissue homeostasis, proliferating and disseminate *(1–4)*. According to Hanahan and Weinberg *(1, 5)*, the six traits ("hallmark") common to all types of cancer cells and that together allow malignant growth are: (I) ability to sustain chronic proliferation, (II) resistance to growth suppressive signals, (III) resistance to cell death, (IV) achieved unlimited replicative potential, (V) induction of angiogenesis, and (VI) ability to invade the surrounding tissue and metastasize. A great deal of research has been carried out to unveil the molecular mechanisms underlying malignant growth. The knowledge of the signaling pathways aberrantly activated in cancer led to discovery of better drugs and new therapeutical approaches *(6)*. Nevertheless, due to the complex nature of the disease and its intrinsic heterogeneity, therapeutic approaches that focused exclusively on cancer cells are insufficient to effectively control the pathology.

Over the last years, new evidences of the deep influence that the surrounding stroma exerts on any aspect of carcinogenesis shifted the attention of the cancer biology community on the tumor microenvironment *(7, 8)*. The emerging view is tumor as a complex tissue, in which neoplastic cells interact with different neighbor cell types and by these interactions the outcome of tumor progression is determined *(9, 10)*.

The tumor microenvironment is a heterogenic system comprised by extracellular matrix and the cellular populations within it *(11)* (Fig. II.1). The non-tumoral cell populations present in the tumor stroma include inflammatory cells *(12)*, vascular-associated cells like endothelial cells and pericytes *(13)*, and activated fibroblasts *(14, 15)*.

Many solid tumors exhibit a very different profile of extracellular matrix protein in their stroma, when compared to their normal counterparts *(16)*. A number of proteins is upregulated specifically in solid tumors, like tenascin-C *(17)* and

fibronectin *(18)*. As well as its composition, the mechanical properties of the extracellular matrix also have an impact on its function, as the stiffness of tumor stroma stimulate cancer cells growth and invasion *(19)*.

A consequence of acknowledging the role of tumor microenvironment on the process of carcinogenesis is the development of new therapeutical strategies, that target the tumor-permissive microenvironment rather than the transformed epithelial cells *(20–22)*.

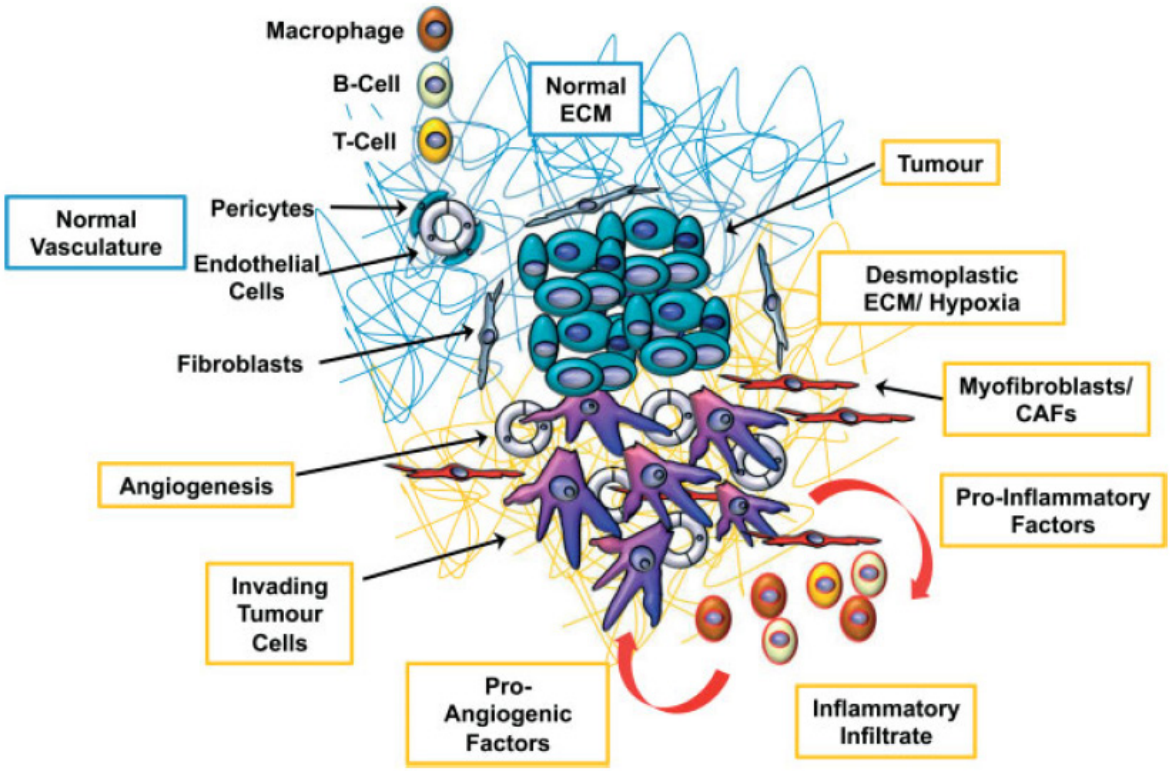


***Figure II.1*** *– Changes to the normal microenvironment promote tumor invasion. Activation of carcinoma-associated fibroblasts and induction of an inflammatory infiltrate lead to release of pro-angiogenic factors. Development of an altered extracellular matrix (ECM) leads to tumor-specific interactions with tumor cells and enhance invasion (16)*

## II.2 – Tenascin-W: an extracellular matrix protein associated with osteogenesis and cancer.

Enrico Martina, Ruth Chiquet-Ehrismann, Florence Brellier

Int J Biochem Cell Biol. 2010 Sep;42(9):1412-5 (Review)

The International Journal of Biochemistry & Cell Biology 42 (2010) 1412–1415

Contents lists available at ScienceDirect

The International Journal of Biochemistry & Cell Biology

journal homepage: www.elsevier.com/locate/biocel

Molecules in focus

# Tenascin-W: An extracellular matrix protein associated with osteogenesis and cancer

Enrico Martina, Ruth Chiquet-Ehrismann*, Florence Brellier

*Friedrich Miescher Institute for Biomedical Research, Novartis Research Foundation, Maulbeerstrasse 66, CH-4058 Basel, Switzerland*

ARTICLE INFO

*Article history:*
Received 19 May 2010
Received in revised form 1 June 2010
Accepted 2 June 2010
Available online 9 June 2010

*Keywords:*
Tenascin-W
Tumor marker
Bone
Cell adhesion

ABSTRACT

Tenascin-W was the last member of a family of four large extracellular matrix glycoproteins to be discovered. The original member of the tenascin family, tenascin-C, has been widely studied due to its association with asthma, fibrosis, infection, inflammation and cancer. Recent studies report multiple common features between tenascin-W and tenascin-C in terms of structure, expression and function, especially in the context of tumorigenesis. Furthermore, specific functions for tenascin-W in osteogenesis have been revealed. This review presents an update on our current knowledge concerning tenascin-W and discusses potential medical applications of this cancer-enriched extracellular matrix protein.



## 1. Introduction

Tenascins are a family of four large extracellular matrix glycoproteins (Chiquet-Ehrismann and Tucker, 2004). The best described member is tenascin-C, which is mostly expressed in the embryo at sites of epithelial–mesenchymal interactions and in developing connective tissue. Tenascin-C persists in some connective tissues in the adult organism and reappears most notably during pathological conditions such as cancer, inflammation and wounds (Orend and Chiquet-Ehrismann, 2006; Brellier et al., 2009). Tenascin-X is widely expressed in loose connective tissue both during development and in the adult, while tenascin-R is confined to the nervous system. This review will focus on the final member of tenascin family, tenascin-W.

Tenascin-W was originally cloned from zebrafish (Weber et al., 1998). In 2003, the murine tenascin-W gene was independently cloned by two groups: Neidhardt et al. (2003) named it tenascin-N, while Scherberich et al. (2004) recognized it as the mouse orthologue of zebrafish tenascin-W. Although phylogenetic analysis revealed that there are only four members of the tenascin family in vertebrates (i.e. tenascin-C, tenascin-R, tenascin-X and tenascin-W) (Tucker et al., 2006), mammalian tenascin-W is still listed in the major databases as tenascin-N (TNN). In 2007, the human gene of tenascin-W was cloned and characterized by Degen et al. (2007).

## 2. Structure

Tenascin-W shares with the other tenascins a characteristic modular structure (Fig. 1A). At the N-terminus, three-and-a-half heptad repeats are flanked by cysteine residues that covalently crosslink three subunits by disulphide bridges. Similarly to tenascin-C, a hexameric form of tenascin-W can be assembled through dimerization of two trimers (Scherberich et al., 2004) (Fig. 1B). This N-terminal oligomerization region is followed by three-and-a-half EGF-like repeats, a species-specific number of fibronectin (FN) type III repeats, and a large C-terminal fibrinogen-related domain. Tenascin-W FN type III repeats originated from duplication events occurring during vertebrate evolution (Tucker et al., 2006): Zebrafish and chicken have 6 repeats, mouse 12 and man 9. While in the case of tenascin-C some of the FN type III repeats are subjected to alternative splicing mechanisms that lead to multiple isoforms (Orend and Chiquet-Ehrismann, 2006), no alternatively spliced isoforms of tenascin-W have been observed so far.

The FN type III repeat structure of tenascin-C predicts an exposed loop between the F and G strands (Leahy et al., 1992). Interestingly, this loop is the site of conserved RGD or KGD integrin-binding motifs in some of the FN type III repeats of tenascin-W of different organisms (Tucker et al., 2006) (Fig. 1A).

## 3. Expression

### 3.1. Tenascin-W in development

In all species analyzed, zebrafish, chicken and mouse, tenascin-W is expressed transiently during embryonic development of

* Corresponding author. Tel.: +41 61 697 24 94; fax: +41 61 697 39 76.
*E-mail address:* chiquet@fmi.ch (R. Chiquet-Ehrismann).

1357-2725/$ – see front matter © 2010 Elsevier Ltd. All rights reserved.
doi:10.1016/j.biocel.2010.06.004

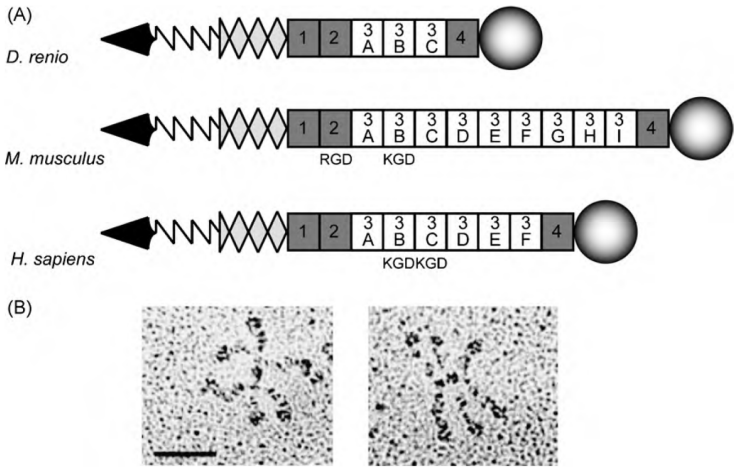


**Fig. 1.** Tenascin-W structure. (A) Repeat and domain organization of tenascin-W in zebrafish, mouse and human. The shapes in the scheme symbolize different domains: N-terminal linker domain (black arrowhead), heptad repeats (zigzag), EGF-like repeats (diamonds and partial diamond), FN type III repeats (dark rectangles = conserved; white rectangles = recently duplicated), and C-terminal fibrinogen-like globular domain (circle). The positions of the putative integrin-binding RGD and KGD residues are indicated. (B) Hexamers of mouse recombinant tenascin-W as revealed by electron microscopy. Scale bar = 50 nm (Scherberich et al., 2004).

smooth muscle, tendons and ligaments, but the primary site of expression is the extracellular matrix of periosteal bone (Weber et al., 1998; Scherberich et al., 2004; Meloty-Kapella et al., 2006). In situ hybridization performed on zebrafish embryos at different stages of development revealed that tenascin-W is expressed in differentiating somites, by migrating neural crest cells as well by cells of sclerotome origin (Weber et al., 1998). During mouse embryonic development, tenascin-W has a very specific pattern of expression that is much more restricted than tenascin-C (Scherberich et al., 2004). It is found in the maxillary process at embryonic day 11.5 (E11.5), in smooth muscle cells of stomach and intestine at E14.5 (Scherberich et al., 2004) and in various developing bones, most notably mandible, palate, teeth starting from E15 (Scherberich et al., 2004). Similarly to mouse embryo, avian tenascin-W immunoreactivity first appears at E8 in the mandible, ribs and developing calvarial bones (Meloty-Kapella et al., 2006), where it colocalizes with tenascin-C staining. A transient expression of tenascin-W was also reported in the smooth muscle of the digestive tract (Meloty-Kapella et al., 2006).

### 3.2. Tenascin-W in the adult

Tenascin-W expression is strongly reduced in the adult stage of all the model organisms examined so far: zebrafish, mouse and chicken. In adult zebrafish, tenascin-W mRNA is limited to non-neuronal cells in the dorsal root ganglia derived from the neural crest and to mesenchymal cells in the somites (Weber et al., 1998). In the mature rooster, tenascin-W was found in testis, in the matrix that surrounds each seminiferous tubule, and lining the ventricular surfaces of the central nervous system (Meloty-Kapella et al., 2006). In adult mouse, tenascin-W is expressed in kidney, aortic valve, cornea and periosteum (Scherberich et al., 2004), as well as in the fully differentiated mouse periodontal ligament (Nishida et al., 2007).

### 3.3. Tenascin-W in cancer

The frequent co-expression of tenascin-C and tenascin-W during development prompted the investigation for similar expression in disease. Because of the well-established role of tenascin-C as a tumor marker (Orend and Chiquet-Ehrismann, 2006), expression of tenascin-W in tumors was investigated. The analysis of different mouse mammary tumor models revealed that tenascin-W was overexpressed only in the tumor stroma of the mice models known to develop metastases and, unlike tenascin-C, was absent both from nonmetastatic tumors and from normal mammary tissue (Scherberich et al., 2005). This seems to be different in human breast cancer. Degen et al. (2007) found tenascin-W expression in a large majority of human breast tumors; however, low-grade breast tumors were enriched in tenascin-W compared to high-grade ones, and again normal tissues were devoid of tenascin-W. Tenascin-W is also overexpressed in colon carcinoma, but not in healthy colon tissues (Degen et al., 2008). As far as brain tumors are concerned, all glioma subtypes tested (oligodendroglioma, astrocytoma and glioblastoma) are enriched in tenascin-W compared to healthy control brain tissue, where tenascin-W is not detectable (Martina et al., 2010). The cellular source of tenascin-W differs in different types of tumors. In breast and colon carcinomas tenascin-W is exclusively stromal, whereas in gliomas tenascin-W is restricted to blood vessels where it colocalizes with von Willebrand factor (Martina et al., 2010) (Fig. 2). In contrast to tenascin-C, tenascin-W does not appear to be produced by brain tumor cells themselves.

## 4. Biological functions

Similarly to tenascin-C, tenascin-W does not sustain cell adhesion in vitro when used as a single substratum. However, in contrast to tenascin-C, tenascin-W neither inhibits spreading of tumor cells on fibronectin (Degen et al., 2007) nor promotes their proliferation (Scherberich et al., 2005). Fibroblasts (Degen et al., 2007), C2C12 osteoblast precursors (Scherberich et al., 2004), human umbilical vein endothelial cells (HUVEC) (Martina et al., 2010), breast cancer cells (Degen et al., 2007), and other cell types cultured on tenascin-W attach loosely and fail to spread. They exhibit round cell bodies, lack stress fibers, and display elongated actin-rich protrusions. A similar morphology is displayed by osteoblasts cultured on circular peptides containing the KGD motif present in FN type III repeats (Meloty-Kapella et al., 2008). This suggests that the characteristic morphology of cells cultured on tenascin-W is mediated by the interaction between the conserved KGD sequence and potential integrin receptors. Several integrin heterodimers such as integrin

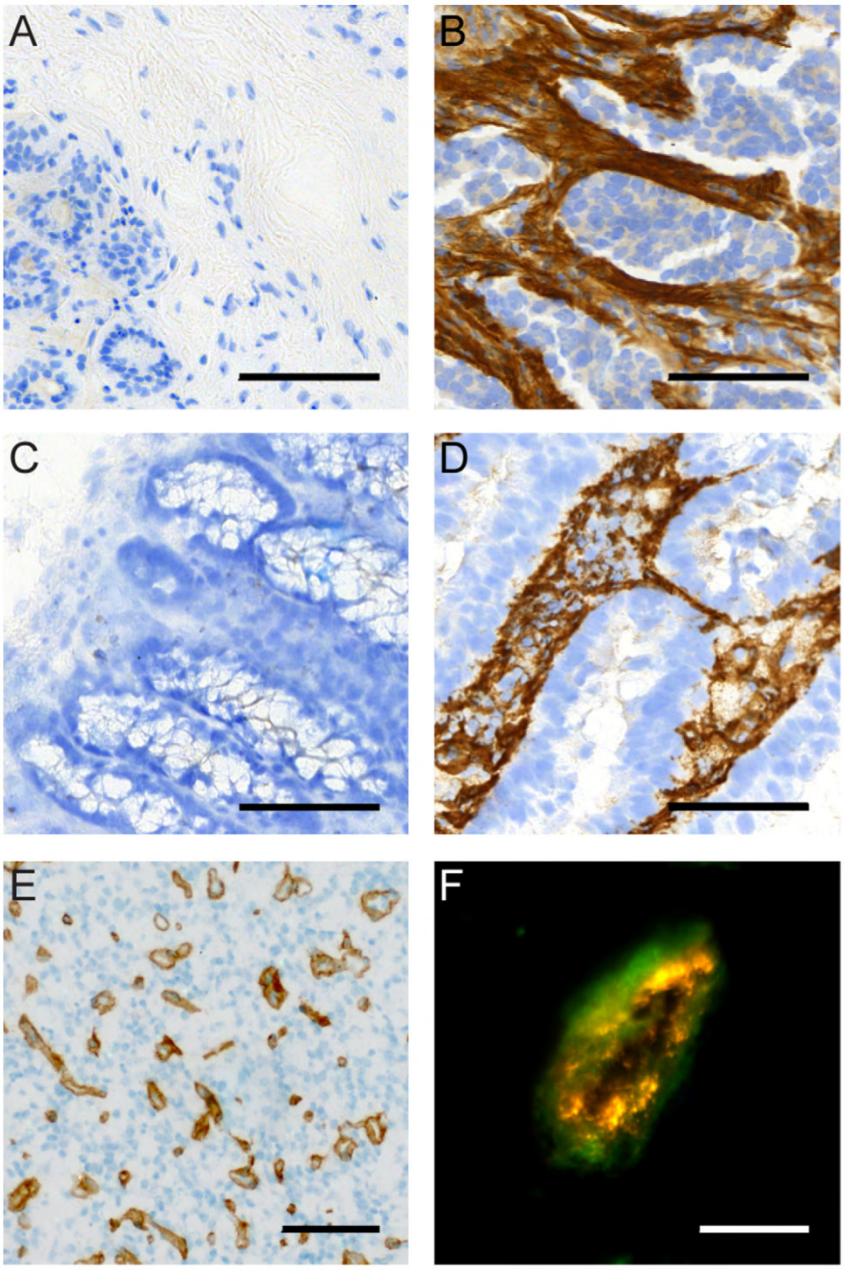


**Fig. 2.** Tenascin-W staining in normal and cancer tissues. Normal breast (A) and normal colon (C) show no tenascin-W expression, while the stroma of breast (B) and colon (D) cancers are positive (scale bars = 100 μm). In glioblastoma (E) tenascin-W staining is restricted to vessel-like structures (scale bar = 100 μm). Double immunofluorescence staining (F) of tenascin-W (green) and von Willebrand factor (red) in glioblastoma reveals the co-localization of tenascin-W and blood vessels (scale bar = 20 μm). (For interpretation of the references to color in the figure caption, the reader is referred to the web version of the article.)

α8β1 (Scherberich et al., 2004), α4β1 and αVβ1 (Degen et al., 2007) have been shown to influence the behavior of cells cultured on tenascin-W substrates.

Adhesion and migration are tightly linked processes and an intermediate state of adhesion is required for cells to be able to move (Murphy-Ullrich, 2001). Not surprisingly, tenascin-W can stimulate cell migration. Mammary tumor cells both from mouse (Scherberich et al., 2005) and from human (Degen et al., 2007) showed increased transfilter migration in the presence of tenascin-W. When endothelial cells are cultured on a substratum of tenascin-W mixed with collagen type I the average speed of the random movement of the cells is increased (Martina et al., 2010). Furthermore, in a well-established in vitro angiogenesis assay, tenascin-W is able to induce sprouting of HUVEC spheroids embedded in collagen gel to an extent comparable with the pro-angiogenic tenascin-C (Martina et al., 2010). The observation that tenascin-W is localized around glioma-associated blood vessels, its effect on the migration of endothelial cells in vitro, and the induced

sprouting of HUVEC spheroids, all suggest a role for tenascin-W in angiogenesis.

The prominent expression of tenascin-W in the developing skeleton encouraged different studies of tenascin-W role in osteogenesis. Screening of Bmp2 target genes in ATDC5 osteochondroprogenitor cells interestingly identified tenascin-W as a candidate (Kimura et al., 2007), in agreement with previous observations that tenascin-W is induced following Bmp2 stimulation in osteoblast precursors C2C12 (Scherberich et al., 2004) and in primary mouse embryonic fibroblasts (Scherberich et al., 2005). Kimura et al. (2007) reported an inhibiting effect on cell proliferation and differentiation of osteoblasts by conditioned medium containing tenascin-W, in contrast to more recent studies reporting that recombinant purified tenascin-W can promote osteoblast migration and stimulate in vitro mineralization (Meloty-Kapella et al., 2008). Interestingly, short circular peptides that contain the conserved KGD sequence from the sixth FN type III repeat of chicken tenascin-W were sufficient to induce in vitro osteoblast proliferation (Meloty-Kapella et al., 2008). Furthermore, frontal bones explanted from chicken embryos and cultured in the presence of tenascin-W for 24 h were thicker, indicating that tenascin-W is able to stimulate bone growth ex vivo (Meloty-Kapella et al., 2008). In agreement with these observation, analysis of the Kusa-A1 osteoblastic cell line revealed induction of tenascin-W compared to the control when in vitro mineralization is induced (Mikura et al., 2009). Moreover, Fgf2 application inhibited mineralization and completely abolished tenascin-W expression in the E15 mouse fetal coronal suture within 24 h, also pointing to a role of tenascin-W in promoting osteoblast maturation (Mikura et al., 2009).

Intriguingly, the expression of tenascin-W at sites like the edge of growing bones, cranial sutures (Mikura et al., 2009) and the periodontal ligament (Nishida et al., 2007), all non-ossified aspects of tissues subjected to compression, allows one to speculate about an additional mechanism of tenascin-W induction in response to mechanical compression. The family member tenascin-C is already well known to be induced by mechanical stimulation of cells (Chiquet et al., 2009). Further studies are needed to investigate a parallel mechanism for the regulation of tenascin-W expression by mechanical forces.

## 5. Possible medical applications

The newly established role of tenascin-W in osteogenesis may imply therapeutic use for this extracellular matrix protein. Tenascin-W may be considered as a tool to reestablish the balance between bone synthesis and resorption during osteoporosis or to promote healing following bone trauma. Since tenascin-W-derived KGD peptides show similar properties as the full-length protein itself, these small molecules could also be promising candidates for such an application (Meloty-Kapella et al., 2008).

As discussed above, the expression of both tenascin-C and tenascin-W is induced in different types of cancer. Normal breast tissue, colon mucosa and healthy brain show no expression of tenascin-W, while the protein can be found in the stroma of breast cancer (Degen et al., 2007), colon carcinoma (Degen et al., 2008), and various types of brain tumors (Martina et al., 2010). In contrast to tenascin-C, which is found in some healthy tissues and can be induced under different pathological conditions (i.e. asthma, inflammation) (Orend and Chiquet-Ehrismann, 2006), tenascin-W expression is more strictly associated with tumorigenesis. Moreover, elevated tenascin-W levels can be reliably detected in the serum of patients with breast or colon cancer (Degen et al., 2008). Taken together, these observations suggest that the detection of tenascin-W in body fluids from patients may become a convenient method for cancer detection.

Another medical application for tenascin-W is to use it as a "tumor flag" for the selective delivery of anticancer drugs at the site of tumors (Kaspar et al., 2006). Such an approach has been successfully applied using tenascin-C (Brack et al., 2006; Silacci et al., 2006) and a tumor-specific splicing isoform of fibronectin (Villa et al., 2008) as target. The presence of tenascin-W in the tumor vasculature of gliomas (Martina et al., 2010), but potentially also in blood vessels of other types of tumors, makes it easily accessible from the blood stream, and turns it into an appealing candidate for such a therapeutic approach.

## Acknowledgment

We thank Richard P. Tucker for the critical reading of this manuscript and the many useful suggestions for improvements.

## References

Brack SS, Silacci M, Birchler M, Neri D. Tumor-targeting properties of novel antibodies specific to the large isoform of tenascin-C. Clin Cancer Res 2006;12:3200–8.
Brellier F, Tucker RP, Chiquet-Ehrismann R. Tenascins and their implications in diseases and tissue mechanics. Scand J Med Sci Sports 2009;19:511–9.
Chiquet-Ehrismann R, Tucker RP. Connective tissues: signalling by tenascins. Int J Biochem Cell Biol 2004;36:1085–9.
Chiquet M, Gelman L, Lutz R, Maier S. From mechanotransduction to extracellular matrix gene expression in fibroblasts. Biochim Biophys Acta 2009;1793:911–20.
Degen M, Brellier F, Kain R, Ruiz C, Terracciano L, Orend G, et al. Tenascin-W is a novel marker for activated tumor stroma in low-grade human breast cancer and influences cell behavior. Cancer Res 2007;67:9169–79.
Degen M, Brellier F, Schenk S, Driscoll R, Zaman K, Stupp R, et al. Tenascin-W, a new marker of cancer stroma, is elevated in sera of colon and breast cancer patients. Int J Cancer 2008;122:2454–61.
Kaspar M, Zardi L, Neri D. Fibronectin as target for tumor therapy. Int J Cancer 2006;118:1331–9.
Kimura H, Akiyama H, Nakamura T, de Crombrugghe B. Tenascin-W inhibits proliferation and differentiation of preosteoblasts during endochondral bone formation. Biochem Biophys Res Commun 2007;356:935–41.
Leahy DJ, Hendrickson WA, Aukhil I, Erickson HP. Structure of a fibronectin type III domain from tenascin phased by MAD analysis of the selenomethionyl protein. Science 1992;258:987–91.
Martina E, Degen M, Ruegg C, Merlo A, Lino MM, Chiquet-Ehrismann R, et al. Tenascin-W is a specific marker of glioma-associated blood vessels and stimulates angiogenesis in vitro. FASEB J 2010;24:778–87.
Meloty-Kapella CV, Degen M, Chiquet-Ehrismann R, Tucker RP. Avian tenascin-W: expression in smooth muscle and bone, and effects on calvarial cell spreading and adhesion in vitro. Dev Dyn 2006;235:1532–42.
Meloty-Kapella CV, Degen M, Chiquet-Ehrismann R, Tucker RP. Effects of tenascin-W on osteoblasts in vitro. Cell Tissue Res 2008;334:445–55.
Mikura A, Okuhara S, Saito M, Ota M, Ueda K, Iseki S. Association of tenascin-W expression with mineralization in mouse calvarial development. Congenit Anom (Kyoto) 2009;49:77–84.
Murphy-Ullrich JE. The de-adhesive activity of matricellular proteins: is intermediate cell adhesion an adaptive state? J Clin Invest 2001;107:785–90.
Neidhardt J, Fehr S, Kutsche M, Lohler J, Schachner M. Tenascin-N: characterization of a novel member of the tenascin family that mediates neurite repulsion from hippocampal explants. Mol Cell Neurosci 2003;23:193–209.
Nishida E, Sasaki T, Ishikawa SK, Kosaka K, Aino M, Noguchi T, et al. Transcriptome database KK-Periome for periodontal ligament development: expression profiles of the extracellular matrix genes. Gene 2007;404:70–9.
Orend G, Chiquet-Ehrismann R. Tenascin-C induced signaling in cancer. Cancer Lett 2006;244:143–63.
Scherberich A, Tucker RP, Degen M, Brown-Luedi M, Andres AC, Chiquet-Ehrismann R. Tenascin-W is found in malignant mammary tumors, promotes alpha8 integrin-dependent motility and requires p38MAPK activity for BMP-2 and TNF-alpha induced expression in vitro. Oncogene 2005;24:1525–32.
Scherberich A, Tucker RP, Samandari E, Brown-Luedi M, Martin D, Chiquet-Ehrismann R. Murine tenascin-W: a novel mammalian tenascin expressed in kidney and at sites of bone and smooth muscle development. J Cell Sci 2004;117:571–81.
Silacci M, Brack SS, Spath N, Buck A, Hillinger S, Arni S, et al. Human monoclonal antibodies to domain C of tenascin-C selectively target solid tumors in vivo. Protein Eng Des Sel 2006;19:471–8.
Tucker RP, Drabikowski K, Hess JF, Ferralli J, Chiquet-Ehrismann R, Adams JC. Phylogenetic analysis of the tenascin gene family: evidence of origin early in the chordate lineage. BMC Evol Biol 2006;6:60.
Villa A, Trachsel E, Kaspar M, Schliemann C, Sommavilla R, Rybak JN, et al. A high-affinity human monoclonal antibody specific to the alternatively spliced EDA domain of fibronectin efficiently targets tumor neo-vasculature in vivo. Int J Cancer 2008;122:2405–13.
Weber P, Montag D, Schachner M, Bernhardt RR. Zebrafish tenascin-W, a new member of the tenascin family. J Neurobiol 1998;35:1–16.

## II.3 – Aim of this work

Tenascin-W was the fourth tenascin to be discovered, and most likely there are no other members of the tenascin family in the genome *(23)*. Being “the last tenascin”, tenascin-W remains poorly understood in its functions and regulation.

The primary goal of this work is to further deepen the knowledge of tenascin-W. We will study its expression pattern in different human tumors, to test whether tenascin-W is a suitable tumor biomarker. In order to understand tenascin-W functions, we will investigate its effect on different types of cells in culture, employing a wide panel of in vitro assays. Furthermore, the tenascin-W promoter will be identified and described. From its characterization we hope to shed light on the gene regulatory mechanisms controlling its expression.

# RESULTS

# III. RESULTS

# III.1 Published papers

## III.1.1 – Tenascin-W is a specific marker of glioma-associated blood vessels and stimulates angiogenesis *in vitro*

Enrico Martina, Martin Degen, Curzio Rüegg, Adrian Merlo, Maddalena Lino, Ruth Chiquet-Ehrismann and Florence Brellier

FASEB J. 2010 Mar;24(3):778-87

My contribution:
I performed the experiments of double immunofluorescence staining that confirmed the co-localization of tenascin-W and blood vessels in glioblastoma samples (described in the paper figure 3 and 4). I performed the adhesion assays and the migration assays on HUVEC cells that demonstrate the effect of tenascin-W on cell morphology and motility (paper figure 5). I carried out the experiments that showed that tenascin-W induces the sprouting of HUVEC spheroids embedded in collagen gel (paper figures 6 and 7). Finally, I contributed to the preparation of the manuscript.

The FASEB Journal article fj.09-140491. Published online November 2, 2009.
*The FASEB Journal* • Research Communication

# Tenascin-W is a specific marker of glioma-associated blood vessels and stimulates angiogenesis *in vitro*

**Enrico Martina,* Martin Degen,*,[1] Curzio Rüegg,[†,‡] Adrian Merlo,[§] Maddalena M. Lino,[§] Ruth Chiquet-Ehrismann,* and Florence Brellier*,[2]**

*Friedrich Miescher Institute for Biomedical Research, Novartis Research Foundation, Basel, Switzerland; [†]Division of Experimental Oncology, Centre Pluridisciplinaire d'Oncologie, Centre Hospitalier Universitaire Vaudois, University of Lausanne, Lausanne, Switzerland; [‡]Swiss Institute for Experimental Cancer Research, NCCR Molecular Oncology, Epalinges, Switzerland; and [§]Laboratory of Molecular Neuro-Oncology, Department of Research, University Hospital, Basel, Switzerland

ABSTRACT **The microenvironment hosting a tumor actively participates in regulating tumor cell proliferation, migration, and invasion. Among the extracellular matrix proteins enriched in the stroma of carcinomas are the tenascin family members tenascin-C and tenascin-W. Whereas tenascin-C overexpression in gliomas is known to correlate with poor prognosis, the status of tenascin-W in brain tumors has not been investigated so far. In the present study, we analyzed protein levels of tenascin-W in 38 human gliomas and found expression of tenascin-W in 80% of the tumor samples, whereas no tenascin-W could be detected in control, nontumoral brain tissues. Double immunohistochemical staining of tenascin-W and von Willebrand factor revealed that tenascin-W is localized around blood vessels, exclusively in tumor samples. *In vitro*, the presence of tenascin-W increased the proportion of elongated human umbilical vein endothelial cells (HUVECs) and augmented the mean speed of cell migration. Furthermore, tenascin-W triggered sprouting of HUVEC spheroids to a similar extent as the proangiogenic factor tenascin-C. In conclusion, our study identifies tenascin-W as a candidate biomarker for brain tumor angiogenesis that could be used as a molecular target for therapy irrespective of the glioma subtype.—Martina, E., Degen, M., Rüegg, C., Merlo, A., Lino, M. M., Chiquet-Ehrismann, R., Brellier, F. Tenascin-W is a specific marker of glioma-associated blood vessels and stimulates angiogenesis *in vitro*. *FASEB J.* 24, 000–000 (2010). www.fasebj.org**

*Key Words: neovascularization · secreted glycoproteins*

TUMORIGENESIS HAS LONG BEEN considered as a cell-autonomous process. However, it is now well recognized that progressive steps of tumorigenesis are largely influenced by the tumor microenvironment (for reviews, see refs. 1–3). This microenvironment consists both of a rich extracellular matrix (ECM) called stroma and of all nontumoral cells populating the tumor, such as fibroblasts, macrophages, and endothelial cells. The stroma is mainly produced by mesenchymal cells and provides a physical support for tissue architecture. In addition to this structural role, it also affects tumor cell behavior through activation of signaling pathways. Stroma associated with normal and tumor tissues strongly differ in their composition (for review, see ref. 4). For instance, being the site where tumor angiogenesis occurs, tumor stroma is on the one hand enriched in proangiogenic factors, such as vascular endothelial growth factor (VEGF) (5) and tumor necrosis factor alpha (TNF-α) (6), and on the other hand deprived of antiangiogenic factors, such as thrombospondin-1 (7). Unbalancing the preestablished equilibrium toward angiogenesis is crucial for the tumor, since these newly formed capillaries will supply oxygen and nutrients necessary for its expansion and growth.

Among the proteins known to be enriched in tumor stroma are members of the tenascin family. Tenascins are large extracellular glycoproteins participating in tissue modeling processes and are thus mainly expressed during embryogenesis. In adults, expression of tenascins becomes more restricted, at least in normal conditions (8). However, as with oncogenic proteins, two tenascin members can be reexpressed in tumors: tenascin-C and tenascin-W. Since its discovery 25 yr ago (9), many laboratories have confirmed the significance of tenascin-C as a tumor biomarker in various organs and have described its key role in tumorigenesis (for review, see ref. 10). Tenascin-C contributes to tumor development at many levels. First, it modulates the properties of tumor cells in terms of adhesion (9, 11), proliferation (9, 11), migration (12), and invasion (13). Second, it stimulates tumor angiogenesis (14–18), and third, it is associated with the metastatic potential of cancer cells (19, 20). More recently characterized (21), tenascin-W constitutes a novel and efficient biomarker for human breast tumors (22) and colorectal tumors

[1] Present address: Department of Dermatology, Brigham and Women's Hospital, Harvard Skin Disease Research Center, Harvard Medical School, Boston, MA 02115, USA.
[2] Correspondence: Friedrich Miescher Institute for Biomedical Research, Novartis Research Foundation, Maulbeerstrasse 66, CH-4058 Basel, Switzerland. E-mail: florence.brellier@fmi.ch
doi: 10.1096/fj.09-140491

(23). Notably, and in contrast to tenascin-C, tenascin-W was undetectable in healthy colon tissues, suggesting that tenascin-W may have a better potential as a colon tumor biomarker.

In the present study, we focused on gliomas, which represent the most common primary brain tumors in humans. The characterization of gliomas depends on the type of cells from which they develop. Oligodendrogliomas are derived from oligodendrocytes and represent 4% of all brain tumors, while astrocyte-derived astrocytomas are much more common. Astrocytomas are graded from I to IV, the highest grade being also known as glioblastoma multiforme or glioblastoma. Patients suffering from glioblastoma, which are highly aggressive and invasive tumors, have a median survival time of only 10 mo. This very short survival time may be explained by the extreme adaptability of glioblastoma cells to antiproliferative or antiangiogenic treatments (for review, see ref. 24). In contrast, the median survival time for patients with oligodendroglioma is 10 yr (25).

Many studies have reported tenascin-C overexpression in brain tumors (for review, see refs. 26, 27). Tenascin-C levels are higher in glioblastoma than in oligodendroglioma (28). High expression levels of perivascular tenascin-C in glioma were shown to correlate with shorter progression-free survival (12), and expression of stromal tenascin-C was shown to be increased in higher tumor grades with poor prognosis (29). In contrast, nothing is known concerning the status of tenascin-W in these tumors.

Because the key role played by tenascin-C in brain tumorigenesis made it a recognized target for glioma treatment (30), we tested whether tenascin-W expression correlates with tumorigenesis in the brain as well, and we investigated its potential function during glioma development.

## MATERIALS AND METHODS

### Glioma biopsies

Gliomas, as well as healthy control brain samples, were obtained from the University Hospital of Basel in accordance with the guidelines of the ethical committee of the University of Basel. Glioblastoma samples were from patients aged 39 to 84 yr (mean age 60 yr), astrocytomas from patients aged 40 to 63 (mean age 45 yr) and oligodendrogliomas from patients aged 38 to 67 (mean age 57 yr). Healthy control samples were obtained from independent individuals. One part of each biopsy was used for protein extraction, and another part was embedded in optimal cutting temperature (OCT) compound (Tissue Tek; Miles Laboratories, Naperville, IL, USA) for the preparation of cryosections. Tumors were diagnosed and graded according to the World Health Organization classification of tumors of the nervous system.

### Western blot analysis

Tissue samples were thawed on ice, minced, and homogenized in RIPA lysis buffer. After measuring the protein concentration with the Bio-Rad protein assay (Bio-Rad, Munich, Germany), samples were separated by SDS-PAGE (6%) and electroblotted to polyvinyldifluoride membranes (Millipore, Billerica, MA, USA). Equal protein loading was confirmed by staining the membrane with amido black. After a blocking step in 5% milk, membranes were incubated overnight with the rabbit polyclonal antiserum pAb (3F/4) raised against human tenascin-W (1:750) (22), the mouse monoclonal antibody B28-13 raised against human tenascin-C (1:100), a mouse monoclonal antibody against vinculin (V-9131; 1:2000; Sigma, Schnelldorf, Germany), or a rabbit polyclonal antibody against actin (1:2000; A-5060, Sigma). They were then incubated for 1 h with anti-mouse IgG or anti-rabbit IgG coupled to horseradish peroxidase. Blots were developed using Super Signal (Pierce, Rockford, IL, USA) for tenascin-C and tenascin-W and ECL reagent (GE Healthcare, Otelfingen, Switzerland) for vinculin and actin. They were then exposed to Kodak BioMax MR Films (Kodak, Rochester, NY, USA).

### Omnibus database search

Using the Gene Expression Omnibus database in PubMed, we imported the values corresponding to *tenascin-W* (found as "*tenascin N*") of the dataset record GDS1813. This dataset was generated to study gliomagenesis by analyzing a set of 50 human gliomas of various histogenesis (31). The values imported from the dataset correspond to the ratio between values obtained for each sample and those obtained for a common human reference, expressed in binary logarithm (see Supplemental Table 1). The ratio was then calculated in a linear basis for each sample (see Supplemental Table 1) or as a mean for each disease state (see **Table 1**). The "fold change over normal" is the ratio between the mean values found in each disease state and in the normal brain.

### Immunostaining

Chromogenic and fluorescent detection was performed on 9- or 12-μm-thick cryosections using the Discovery XT automated stainer (Ventana Medical Systems, Tucson, AZ, USA) with a standard and a customized procedure, respectively. Frozen tissue slides were dried for 1 h at room temperature, fixed for 10 min at −20°C in acetone, and then introduced into the automate. For chromogenic stainings, slides were incubated for 1 h at 37°C with the mouse monoclonal 56O antibody raised against human tenascin-W (1:1000) (23), the B28-13 antitenascin-C antibody (1:1000), or a rabbit polyclonal antibody against von Willebrand factor (1:25,000; A0082, Dako Corp., Carpinteria, CA, USA). They were then treated for 32 min at 37°C with a biotinylated anti-mouse or anti-rabbit secondary antibody (1:200; 715-065-150 and 711-065-152, respectively; Jackson Immunoresearch Laboratories, West Grove, PA, USA) and developed with the DAB Map detection kit (Ventana). Counterstainings were obtained with hematoxylin and bluing reagent (Ventana). For immunofluorescence stainings, slides were incubated for 1 h at 37°C with anti-tenascin-W mAb 56O (1:50), anti-tenascin-C mAb B28-13 (1:50), anti-von Willebrand factor (1:200), rabbit polyclonal anti-desmin antibody (1:100, RB-9014-P1, Neomarkers, Fremont, CA, USA), or rabbit polyclonal anti-laminin antibody (1:200; Life Technologies, Gaithersburg, MD, USA). The slides were then treated for 32 min at 37°C with Alexa Fluor 488 donkey anti-mouse IgG and Alexa Fluor 568 donkey anti-rabbit IgG or Alexa Fluor 647 goat anti-rabbit IgG secondary antibodies (1:200; A21202, A10042, and A21245, respectively; Invitrogen, Basel, Switzerland), carefully rinsed by hand, and mounted with prolong gold reagent (Invitrogen). Wide-field images were acquired using a Zeiss Axiovert 200 microscope equipped with a charge-coupled de-

vice Cool Snap HQ camera, using a ×20/0.50 or a ×40/1.3 oil objective (Carl Zeiss, Oberkochen, Germany). Confocal laser scanning microscopy was performed using a Zeiss Axioplan 2-LSM510meta, using a ×63/1.4 oil objective. Images were processed using ImageJ software (http://rsb.info.nih.gov/ij/).

### Cell culture

Human umbilical vein endothelial cells (HUVECs) were a kind gift of Grégory Bieler (Division of Experimental Oncology, University of Lausanne). The cells were isolated from 3 independent umbilical cords and pooled. HUVECs were cultured in endothelial growth medium consisting of medium 199 (Life Technologies) supplemented with 10% FCS (Hyclone, Lausanne, Switzerland), 12 μg/ml bovine brain extract (Clonetics, Walkersville, MD, USA), 10 ng/ml human recombinant EGF (Peprotech, Rocky Hill, NJ, USA), 25 U/ml heparin (Sigma), 1 μg/ml hydrocortisone (Sigma), 2 mM L-glutamine, 100 U/ml streptomycin, and 100 U/ml penicillin. Cells were used between passages 4 and 8.

Human embryonic kidney-293 (HEK-293) cells used in this study were either mock transfected or transfected to stably express His-tagged full-length human tenascin-W (22), His-tagged full-length human tenascin-C (32) or His-tagged EGF-repeats of human teneurin-4 (D. Kenzelmann, unpublished data). HEK-293 cells were cultured in DMEM/10% FCS with 2 μg/ml puromycin.

### Purification of tenascins and fibronectin

HEK-293 cells stably transfected to express either His-tagged human tenascin-W or His-tagged human tenascin-C were grown to confluence. Serum-free culture medium containing the secreted recombinant human tenascins was collected, and after ammonium sulfate precipitation (0–38%) and dialysis against PBS containing 0.01% Tween-20, the protein was passed over a gelatin-agarose column to remove fibronectin, followed by affinity purification on an Ni-NTA resin (Invitrogen) in the presence of 0.5 M urea, as described previously (22). The protein eluates were then dialyzed against PBS containing 0.01% Tween using 100-kDa-cutoff dialysis bags (Spectrumlabs, Greensboro, NC, USA) to limit potential copurification of small molecules. Purified tenascins appeared as single bands on Coomassie-stained acrylamide gels. Fibronectin was purified from horse serum as described previously (33).

### Cell adhesion assay

Seventy-two-well MicroWell Mini Trays (Nunc, Roskilde, Denmark) were coated for 90 min at 37°C with 10 μl/well of 20 μg/ml of rat tail collagen type I (BD Biosciences, San Jose, CA, USA). After 3 washes with PBS, the wells were coated overnight at 4°C with PBS containing 0.01% Tween, 200 ng of human tenascin-W, human tenascin-C, or fibronectin. The wells were blocked for 1 h at room temperature with PBS containing 1% BSA. HUVECs were trypsinized and resuspended in serum-free medium, and 1500 cells were seeded in each well. For the dose-response experiment, wells were coated with collagen and washed and blocked with BSA. Cells were then seeded in serum-free medium containing a different concentration of soluble tenascin-W, or BSA as a control. After 3 h at 37°C, cells were washed 3 times with PBS, fixed with 4% formaldehyde, and stained with 0.1% crystal violet. Pictures of the entire wells were taken at ×2.5 under an inverted microscope, and the cells were counted. The ratio between the number of elongated cells and the total number of cells was calculated. Experiments were done in triplicate wells, in 3 independent experiments.

### Cell motility assay

Twenty-four-well plates were coated as described above. HUVECs were trypsinized and resuspended in serum-free medium, and $5 \times 10^4$ cells were seeded in each well. Cells were allowed to adhere for 2 h at 37°C. Time-lapse microscopy was then performed using an inverted microscope with a ×5 objective, acquiring a picture every 10 min for 10 h. During this time, the plate was maintained at 37°C in 6% $CO_2$ and 100% humidity. Cell motility was quantified manually, tracking ≥35 cells/condition throughout the time stack, using the ImageJ software. The experiment was repeated twice.

### Generation of spheroids

Spheroids of HEK-293 cells and HUVECs were prepared, as described previously, as "random" and "standard" spheroids, respectively (34). HEK-293 cells were labeled with fluorescent vibrant dye DiL (Invitrogen), trypsinized, and resuspended in DMEM/10% FCS containing 0.42% (w/v) carboxymethylcellulose. Three million cells were seeded in a nonadherent Petri dish for bacterial culture and incubated overnight at 37°C. Under these conditions, cells aggregate spontaneously to form random spheroids of similar sizes. To obtain HUVEC spheroids of defined size and cell number (standard spheroids), subconfluent monolayers of HUVECs were labeled with the fluorescent vibrant dye DiO (Invitrogen), trypsinized, and resuspended in endothelial growth medium containing 0.24% (w/v) carboxymethylcellulose (Sigma). Four hundred cells were seeded in each well of a nonadherent round-bottom 96-well plate (Greiner Bio-One, St. Gallen, Switzerland) to form spheroids, which were collected the next day.

### Spheroid sprouting assay

An *in vitro* angiogenesis assay described previously (35) was adapted as follows: HUVEC spheroids were transferred into a rat type I collagen gel (1.2 mg/ml), containing purified tenascin-W, purified tenascin-C, or BSA at a final concentration of 20 μg/ml. In coculture experiments, HEK-293 cells expressing tenascin-W, tenascin-C, or an unrelated teneurin-4 fragment, or mock-transfected HEK-293 cells were incorporated into the gel either as single cells (8000 cells/ml gel) or as random spheroids (250 μl random spheroid suspension/ml gel). The fluid spheroid-containing gel was transferred into prewarmed 24-well suspension plates (Greiner Bio-One) and incubated for 30 min at 37°C. After polymerization of the gel, spheroids were fed with 100 μl of endothelial growth medium, with or without 10 ng/ml of VEGF-165 (R&D Systems, Minneapolis, MN, USA) and incubated for 48 h at 37°C. For each condition, pictures of 10 spheroids were acquired under an inverted microscope at ×100 and analyzed. Cumulative sprout length (CSL) was quantified by measuring the total length of all sprouting processes originating from each single spheroid, using the ImageJ software. Three independent experiments were performed.

## RESULTS

### Brain tumors overexpress tenascin-W

We first assessed tenascin-W and tenascin-C protein content in extracts of normal brain by immunoblot analysis. No tenascin-W could be detected in normal brain, while tenascin-C was present (**Fig. 1*A***, lanes N1 and N2). We

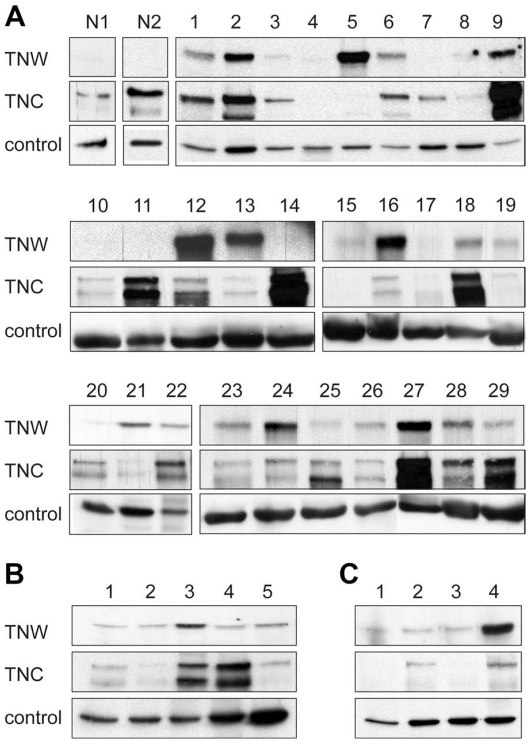


**Figure 1.** Immunoblot analysis of tenascin-W and tenascin-C expression in glioma protein extracts. Protein extracts of glioma or healthy brain tissues were separated by SDS-PAGE and immunoblotted for tenascin-W and tenascin-C. Blots were also probed for actin or vinculin to check equal loadings of the samples. *A*) Healthy brain tissue extracts (N1 and N2) and glioblastoma extracts (lanes 1–29). *B*) astrocytoma extracts (lanes 1–5). *C*) Oligodendroglioma extracts (lanes 1–4). Note the absence of tenascin-W in healthy brain tissues. In contrast, the majority of the glioma extracts show expression of tenascin-W. Tenascin-C is also expressed in most of the glioblastomas and astrocytomas, but much less in oligodendrogliomas. Tenascin-C is also detectable in healthy brain tissues.

then analyzed 29 glioblastoma samples. Almost all samples contained tenascin-C, as well as tenascin-W at various levels (Fig. 1*A*, lanes 1–29). We could detect tenascin-W in 21 extracts (*i.e.*, >70% of the samples) and among them, 8 expressed tenascin-W at high or very high levels. We also analyzed tenascin-W and tenascin-C expression in 5 astrocytomas and 4 oligodendrogliomas (Fig. 1*B*, *C*). Tenascin-W was present in all of these samples tested. In contrast to tenascin-C, which is overexpressed in glioblastoma and astrocytomas, but not in oligodendrogliomas (as described previously in ref. 28), no glioma subtype specificity for tenascin-W expression was observed. Altogether, ~80% of the glioma samples tested were tenascin-W-positive.

Using the Gene Expression Omnibus database accessible on PubMed, we extracted raw transcript data from a transcript profiling study of gliomas by Bredel *et al.* (31). This revealed that 27 of the 30 glioblastoma samples tested showed overexpression of *tenascin-W* mRNA compared to 4 healthy brain samples (see Supplemental Table 1). The fold change increase in *tenascin-W* transcript level between healthy brain and glioblastoma was almost 2.5 (Table 1). This increase was statistically significant ($P<0.05$, ANOVA test), thereby confirming our protein expression data at the RNA level and in an independent dataset.

### Blood vessels in brain tumors are stained for tenascin-W

To identify the cellular source of tenascin-W in gliomas, we performed immunohistochemical analyses on glioblastoma and oligodendroglioma cryosections. Tenascin-W immunostaining revealed circular structures histologically reminiscent of blood vessels, similarly to tenascin-C, which, in addition, was present around the glioblastoma cells throughout the tissue section (**Fig. 2**). We then costained the sections for the tenascins and von Willebrand factor, an established marker of blood vessels. We observed complete overlap between tenascin-W immunostaining and blood vessel structures marked by von Willebrand factor (**Fig. 3*C*, *E***), suggesting that the cellular source of tenascin-W could be tumor endothelial cells. Immunohistochemical analyses of healthy brain tissues showed, as expected, a typical, sparser network of blood vessels compared to tumor tissues. Consistent with our immunoblot analyses, tenascin-W was not detectable in healthy brain tissue, even around vessels (Fig. 3*A*), suggesting that tenascin-W expression is tumor-endothelial specific. Tenascin-C and von Willebrand double staining showed only a partial overlap, as the tenascin-C staining mainly surrounded the staining for von Willebrand factor (Fig. 3*D*, *F*). Tenascin-C may thus not be secreted solely by

TABLE 1. *Tenascin-W levels in an independent RNA profiling*

| Disease state | Tenascin-W mRNA level (tissue of interest/common reference) | Fold change over normal |
|---|---|---|
| Normal ($n$=4) | 0.745 ± 0.093 | 1 |
| Oligodendroglioma ($n$=8) | 0.969 ± 0.061 | 1.3 |
| Anaplastic oligoastrocytoma ($n$=6) | 0.992 ± 0.093 | 1.3 |
| Glioblastoma ($n$=30) | 1.831 ± 0.188 | 2.5* |
| Astrocytic tumors ($n$=4) | 1.305 ± 0.437 | 1.8 |
| Glioneuronal neoplasm ($n$=1) | 1.496 | 2 |

$n$ = number of samples in each category. *$P < 0.05$; ANOVA test.

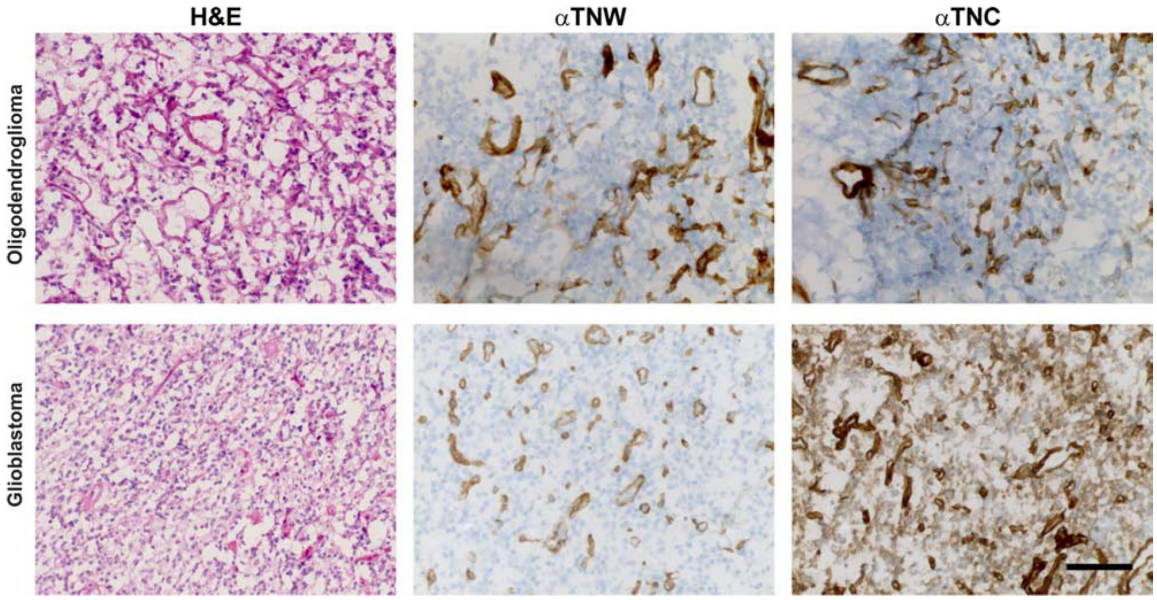


**Figure 2.** Immunohistochemical detection of tenascin-W and tenascin-C in gliomas. Cryosections of oligodendroglioma (top panels) and glioblastoma (bottom panels) were stained with hematoxylin and eosin (H&E), as well as with tenascin-W (αTNW) and tenascin-C (αTNC) antibodies. Cell nuclei are counterstained in blue in middle and right panels. Note the circular structures, reminiscent of blood vessels, stained by tenascin-W and tenascin-C. In glioblastoma, tenascin-C stains all cells throughout the section, while tenascin-W is present only in the vessel-like structures. Scale bar = 50 μm.

the endothelial cells themselves. In healthy brain tissue sections, tenascin-C remained undetectable (Fig. 3*B*), suggesting that tenascin-C may not be expressed in the entire brain.

To assess more precisely the localization of tenascin-W, we then stained sections of glioblastoma with anti-desmin and anti-pan-laminin antibodies. The former is known to stain pericytes at the periphery of blood vessels, and the latter stains the basement membrane shared by the endothelial and surrounding pericyte cell layers. Tenascin-W staining was adjacent to desmin staining and rarely enclosed the pericytes (a typical picture is shown in **Fig. 4*A***), in contrast to tenascin-C, which clearly enclosed all the pericytes surrounding the blood vessels (Fig. 4*B*). Furthermore, tenascin-W staining was restricted to the area delimited by the laminin staining (Fig. 4*C*), whereas tenascin-C staining clearly extended beyond the periphery of the basement membrane (Fig. 4*D*). These experiments show that tenascin-W is present in and around the endothelial cell layer but does not overlap with the pericyte cell layer.

### Tenascin-W promotes elongation and migration of endothelial cells

A characteristic feature of angiogenic endothelial cells is their migratory capacity associated with the acquisition of an elongated cell shape (36). To investigate whether tenascin-W influences the morphology of endothelial cells, we compared HUVECs seeded on collagen substrata, including tenascin-W, tenascin-C, or fibronectin. Cells seeded in serum-free conditions on a mixture of collagen I/fibronectin were polygonal and well spread, with a regular cobblestone-like shape (**Fig. 5*A***, left panel). When the cells were cultured on collagen I/tenascin-C or collagen I/tenascin-W mixtures, a fraction of the cells exhibited an elongated cell shape. The cells were mostly bipolar with long, thin, protrusions (Fig. 5*A*, middle and right panels), a morphology reminiscent of migrating cells. The number of elongated cells was significantly higher in the presence of tenascin-C and tenascin-W than in the presence of fibronectin (Fig. 5*B*), suggesting that tenascin-W, as it has been shown before for tenascin-C (17), promotes endothelial cell elongation. When used in solution rather than coated on the surface, tenascin-W triggered a similar change of morphology. It increased the proportion of elongated HUVECs with an $EC_{50}$ of 2.5 μg/ml and reached a maximal effect at 20 μg/ml concentration (Fig. 5*C*), which was used subsequently in all experiments.

The typical morphology of HUVECs when cultured on a mixed collagen I/tenascin-W substratum suggested that these cells may acquire a motile phenotype in the presence of tenascin-W (37). To test this hypothesis, we tracked the movement of the cells by live imaging over a period of 10 h. On each substratum tested, we observed random movements of the cells. When we measured the mean speed of HUVECs, we observed a higher speed on collagen I/tenascin-W and collagen I/tenascin-C compared to collagen I/fibronectin (Fig. 5*D*). Cell speed comparisons between collagen I/fibronectin *vs.* collagen I alone revealed no difference (data not shown). Although a large hetero-

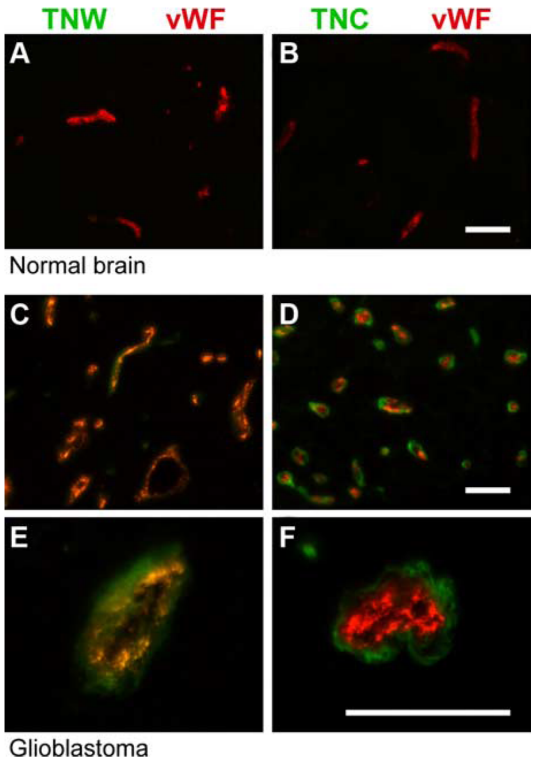


**Figure 3.** Double immunofluorescence staining of tenascin-W or tenascin-C with von Willebrand factor in normal brain and glioblastoma. Cryosections of control brain (*A*, *B*) and glioblastomas (*C*–*F*) were used for fluorescent detection of tenascin-W (TNW; green; *A*, *C*, *E*), tenascin-C (TNC; green; *B*, *D*, *F*) and von Willebrand factor (vWF; red). Note the normal, typical network of capillaries in normal brain (*A*, *B*), compared to the dense network observed in glioblastomas (*C*, *D*). There is a complete overlap between TNW and vWF stainings (*E*), in contrast to the partial overlap between TNC and vWF (*F*). Scale bars = 50 μm.

geneity between individual cells within each condition was observed, statistical analyses confirmed a significant effect of tenascin-C and tenascin-W on the motility of HUVECs ($P<0.0001$, ANOVA test).

### Tenascin-W promotes endothelial cell sprouting

To collect further evidence for a potential angiogenic activity of tenascin-W, we monitored its effect on the endothelial sprouting capacity of HUVECs, using a collagen gel-embedded spheroid-based *in vitro* angiogenesis assay. Incorporation of tenascin-C into the gel promoted endothelial cell sprouting, as described previously (38). Similarly, when HUVEC spheroids were incorporated in a tenascin-W-containing gel, we observed a significant induction of endothelial cell sprouts (**Fig. 6*A***, top panels). The extensions formed by the sprouting cells were similar to the ones triggered by tenascin-C. The measurement of the CSLs confirmed the increase in the presence of tenascin-W and tenascin-C to be statistically significant (Fig. 6*B*, open bars). Interestingly, the addition of VEGF, a potent proangiogenic factor, further increased the HUVEC sprouting capacities triggered by tenascin-C and tenascin-W (Fig. 6*A*, bottom panels; *B*, solid bars), suggesting an additive effect of tenascins and VEGF.

To exclude the possibility of an indirect effect mediated by contaminating proangiogenic factors copurified with tenascins, we established a coculture system. We cultured HUVEC spheroids in the presence of stably transfected HEK-293 cells as a source of tenascin-W, tenascin-C, or a teneurin-4 fragment, the latter serving as a negative control. Simultaneous incorporation in the gel of independently prepared HUVEC spheroids labeled with a green vital dye and HEK-293 spheroids labeled in red led to the formation of HUVEC sprouting in the presence of VEGF, only when the HEK-293 spheroids were expressing tenascin-C or tenascin-W (**Fig. 7*A***). For quantification, we prepared collagen gels populated with dissociated HEK-293 cells and measured the CSL of HUVEC spheroids under each condition. The presence of HEK-293 cells secreting tenascin-W strongly increased the sprouting capac-

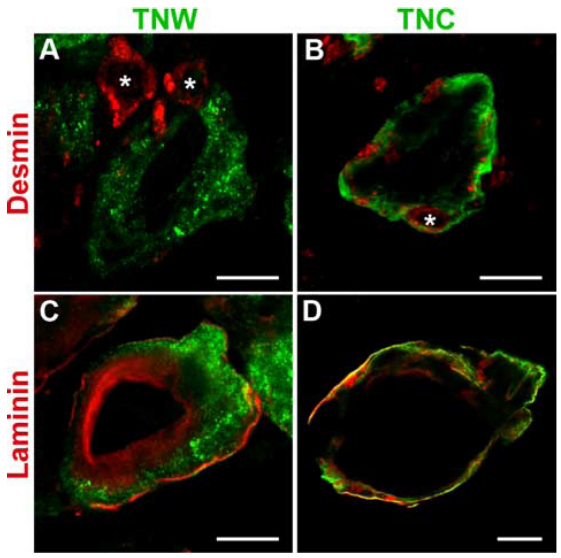


**Figure 4.** Double immunofluorescence staining of tenascin-W or tenascin-C with desmin and laminin in glioblastoma. Cryosections of glioblastomas were used for fluorescent detection of tenascin-W (TNW; green; *A*, *C*), tenascin-C (TNC; green; *B*, *D*), desmin (red; *A*, *B*), and laminin (red; *C*, *D*). Pictures were acquired by confocal laser scanning microscopy. Pericytes can be clearly identified by desmin staining and are present as expected at the periphery of the blood vessels (*A*, *B*; asterisks). Note that TNW staining is adjacent to the pericytes but does not encircle them (*A*). In contrast, TNC staining clearly encloses all pericytes present around the blood vessel (*B*). Laminin staining localizes the basement membrane shared by endothelial and pericytes cell layers (*C*, *D*). TNW is present only within the area delimitated by the laminin staining (*C*), whereas TNC is not restricted to this basement membrane and clearly extends beyond the laminin staining (*D*). Scale bars = 10 μm.

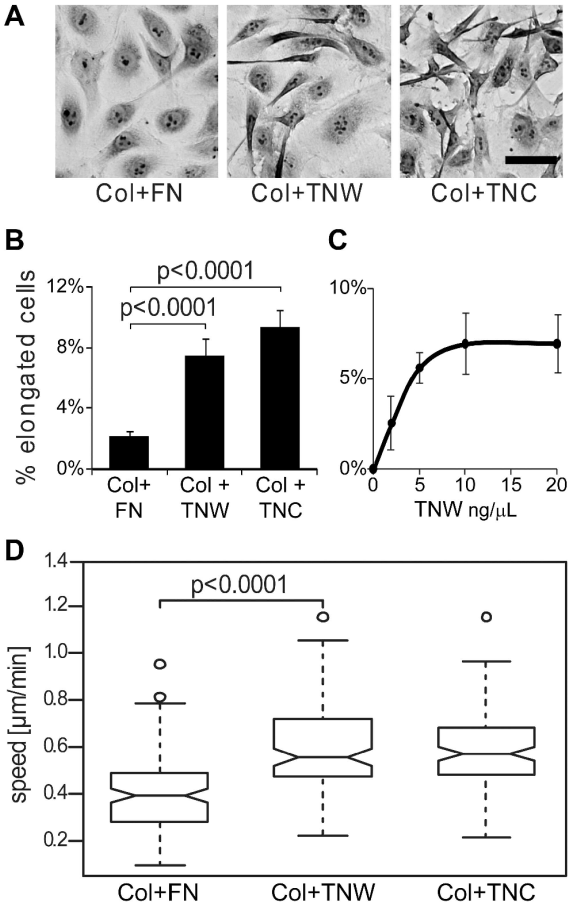


**Figure 5.** Morphology and motility of HUVECs seeded on fibronectin, tenascin-W, or tenascin-C in combination with type I collagen. *A*) Culture plates were coated with type I collagen, followed by fibronectin (FN), tenascin-W (TNW) or tenascin-C (TNC). HUVECs were seeded on these mixed substrata and incubated for 3 h at 37°C. Cells were then fixed and stained with crystal violet, and morphology of the cells was observed. Morphology of HUVEC populations observed on the different substrata is shown. Note the emergence of elongated cells in the presence of TNW and TNC. Scale bar = 50 μm. *B*) Percentage of elongated cells on total number of adherent cells in each condition described in *A*. Statistical analyses were performed with ANOVA. *C*) Culture plates were coated with type I collagen. HUVECs were then seeded in serum-free medium containing increasing concentrations of soluble TNW or BSA as a control. After 3 h incubation at 37°C, cells were fixed, stained with crystal violet and analyzed. For each concentration of TNW, the number of HUVEC elongated cells was assessed, and the percentage of the total number of cells was calculated. Background, evaluated as percentage of HUVEC elongated cells observed in control conditions (*i.e.*, BSA at the same concentration), was then deduced. *D*) Culture plates were coated with type I collagen, followed by FN, TNW, or TNC. After 2 h of incubation at 37°C, the movement of HUVECs was recorded by time-lapse microscopy. Cell motility was quantified, tracking ≥35 cells/condition throughout the time stack. Results are represented with a box plot; thicker line represents median value. Ten percent of the values are composed within the notch surrounding the median line. Bottom and top extensions of the box identify the first and the fourth quartile, respectively. Extreme lines represent the minimal and the maximal values of each dataset. Outliers are individually plotted as small circles. Note the significant increase ($P<0.0001$, ANOVA test) of cell motility in the presence of TNW and TNC.

ity of HUVEC spheroids (Fig. 7*B*), thus confirming a proangiogenic role for tenascin-W.

## DISCUSSION

In the present study, we found overexpression of tenascin-W in 80% of the glioma samples tested. In contrast, we could not detect tenascin-W in healthy human brain tissue, confirming previous studies in mice (21). This differential expression of tenascin-W in healthy brain *vs.* tumor tissues reveals a high potential for tenascin-W as a brain tumor biomarker. Our protein data paralleled an independent study on the transcript level performed by Bredel *et al.* (31). As yet we have no evidence that tenascin-W expression could be used as a predictor of the severity and the aggressiveness of gliomas, since oligodendrogliomas express tenascin-W to a similar extent as glioblastomas. Also, we were unable to find any correlation between patient survival data and the level of expression of tenascin-W, but extending the number of samples would be necessary to establish firmly whether a correlation exists.

Previous studies performed in our laboratory reported overexpression of tenascin-W, as well as tenascin-C in breast (22) and colon (23) tumors, two organs characterized by an absence of tenascin-W in normal, nonpathological conditions. In these carcinomas, the source of tenascin-C is the stromal or cancer-associated fibroblasts, shown to play an active role in the progression of the tumor (for review, see ref. 2). Like tenascin-C, tenascin-W is also present in the stroma of these carcinomas. The situation is different in glioblastomas and melanomas, in which the tumor cells themselves express tenascin-C. In contrast to tenascin-C, we could neither observe tenascin-W in brain cancer cells themselves after immunostaining glioma sections, nor detect expression of tenascin-W in the culture medium of glioma cell lines (data not shown). The present study shows that tenascin-W expression in gliomas is confined to blood vessels. Together with the induction of endothelial cell sprouting in *in vitro* functional angiogenesis assays, these observations point to a proangiogenic function of tenascin-W. This result is in agreement with a transcriptome study analyzing microvascular endothelial cells from patients suffering from impaired angiogenesis due to systemic sclerosis (39). *Tenascin-W* was among the genes down-regulated in these samples. Since proangiogenic features have also been described for tenascin-C in several studies (14, 16–18), our results reveal a common role between tenascin-C and tenascin-W. However, the blood vessel-associated expression pattern of tenascin-W and tenascin-C differs slightly.

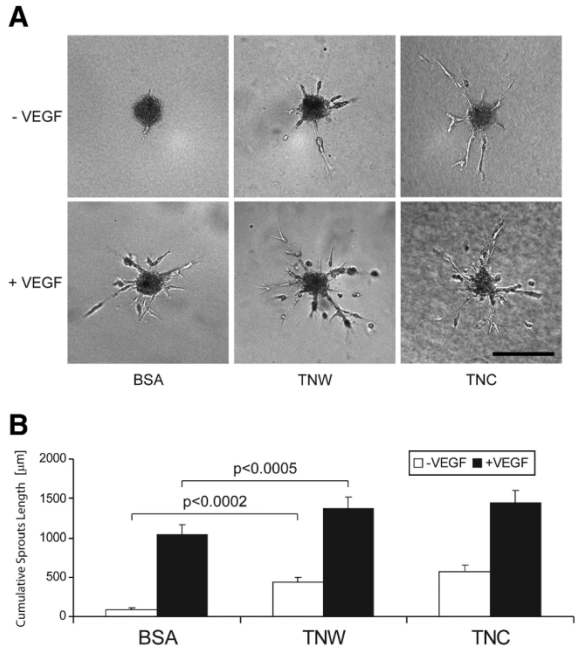


**Figure 6.** Sprouting capacity of HUVEC spheroids in a type I collagen gel containing purified tenascin-W and tenascin-C. HUVEC spheroids were added in a type I collagen gel containing BSA, tenascin-W (TNW), or tenascin-C (TNC) at a concentration of 20 μg/ml. Cultures were fed with endothelial growth medium in the presence or absence of VEGF at a concentration of 10 ng/ml (+VEGF or −VEGF, respectively). After 48 h, pictures of 10 randomly chosen spheroids/condition were acquired. *A*) Representative pictures of each condition. Scale bar = 200 μm. *B*) CSLs were quantified, measuring the total length of all sprouting processes originating from a single spheroid. Note the significant increase of HUVEC sprouting capacity in the presence of both TNW and TNC. This holds true in the absence of VEGF (open bars), as well as in the presence of VEGF (solid bars).

Tenascin-C and tenascin-W are not solely restricted to the blood vessels themselves but are also visible in the perivascular space. Tenascin-C can be detected in association with desmin-positive pericytes, while tenascin-W was interior of the desmin-stained cells and seemed to be associated with endothelial cells. This suggests different cellular sources of the two proteins, such as pericytes for the production of tenascin-C and endothelial cells as the source of tenascin-W. This is supported by the observation that pericytes can secrete tenascin-C *in vitro* (data not shown), and *tenascin-W* transcripts have been observed in endothelial cells (39). The distinct expression patterns of tenascin-C and tenascin-W may, in addition, reveal specificities in the regulation of each tenascin. Some glioblastomas express both tenascins, some express either tenascin-C or tenascin-W, and some of them express neither. Unfortunately, analysis of clinical data did not enable us to link any of these combinations with a given patient outcome. Considering that tenascin-C and tenascin-W may be regulated differently, that bone morphogenic proteins (BMPs) mainly induce tenascin-W (21, 40), and that several BMP members promote angiogenesis in tumors (41–43), we postulate that tenascin-W could be a mediator of BMP activity in tumors.

Our results uncover a potential target for anticancer therapy. There are two ways ECM cancer markers can be used to combat cancer. First, they can be targeted directly. For example, decreasing the expression of tenascin-C by RNA interference was shown to inhibit metastasis of breast cancer cells in a xenograft model (19). Second, the more extensively used approach is to use cancer-specific

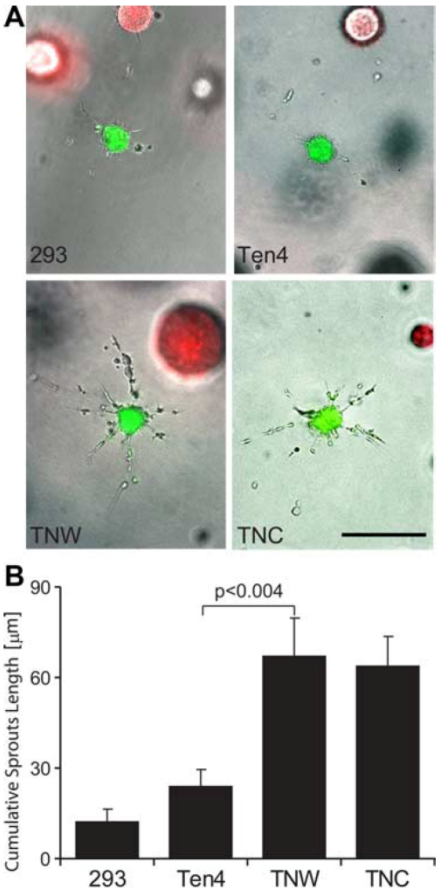


**Figure 7.** Sprouting capacity of HUVEC spheroids cocultured with HEK-293 cells secreting tenascin-W or tenascin-C in a type I collagen gel. *A*) HUVEC spheroids were combined in a type I collagen gel with HEK-293 spheroids in the presence of 10 ng/ml VEGF. HUVEC and HEK-293 spheroids were prepared with cells beforehand marked with DiO (green) and DiL (red) dyes, respectively. HEK-293 cells used in these experiments were stably transfected to express an empty plasmid (293), a teneurin-4 construct (Ten4), tenascin-W (TNW), or tenascin-C (TNC). Note that the sprouting capacity of HUVEC spheroids is increased only in the vicinity of 293 cells secreting TNW or TNC. Scale bar = 200 μm. *B*) HUVEC spheroids were added to type I collagen gels populated with dissociated HEK-293. After 48 h, pictures of 10 randomly chosen spheroids/condition were acquired. CSLs were quantified, measuring the total length of all sprouting processes originating from a single spheroid. Note that inclusion of HEK-293 cells secreting TNW and TNC significantly increased the sprouting capacity of HUVEC spheroids.

ECM proteins as "tumor flags" for the selective delivery of anticancer drugs at the site of the tumor (for review, see ref. 44). In the case of tenascin-C, such an approach has been successfully applied to brain cancer patients for many years (45, 46). The use of antibodies against the spliced isoform of tenascin-C containing extradomain C (47, 48) has led to enhanced tumor imaging and to a significant accumulation of therapeutic compounds in tumors in xenograft models. Furthermore, coupling of antibodies recognizing tenascin-C to interleukin-2 was reported to enhance the potency of chemotherapy in xenograft models of human breast cancer (49). Most important, the *in vivo* accessibility of fibronectin with extra domain B was confirmed in three lymphoma patients, in which radioimmunotherapy induced a sustained partial remission in relapsed lymphoma patients, proving the efficacy of this method (50).

On the basis of the results presented in this study, tenascin-W should be considered as a novel molecule with potential for diagnostic (imaging) or therapeutic applications since it is overexpressed in most of the gliomas, but not in healthy tissues; it is localized immediately surrounding endothelial cells and thus readily reached by the circulation; and its positive effect on angiogenesis might be neutralized by such treatments. FJ

Grant support is provided by the Schweizerische Nationalfonds (SNF), National Center for Competence in Research (C.R.), Oncosuisse OCS-01613-12-2004 (A.M.), SNF 3100A0-120235 (R.C.-E.), and Krebsliga beider Basel 20-2008 (F.B.). We thank Gregory Bieler (Division of Experimental Oncology, University of Lausanne, Lausanne, Switzerland) for kindly providing us early passages of HUVECs, Natsuko Imaizumi and Eveline Faes for their technical expertise with angiogenesis assays, Catherine Schiltz and Sandrine Bichet for their help with immunohistochemistry, Daniela Kenzelmann (FMi, Basel, Switzerland) for the teneurin-4 constructs, Laurent Gelman for his help with microscopy, and Clare Isacke (Institute of Cancer Research, London, UK) for the culture medium of pericytes. We also thank Rémi Terranova and Richard P. Tucker for critical reading of the manuscript.

## REFERENCES

1. Bhowmick, N. A., Neilson, E. G., and Moses, H. L. (2004) Stromal fibroblasts in cancer initiation and progression. *Nature* **432,** 332–337
2. Kalluri, R., and Zeisberg, M. (2006) Fibroblasts in cancer. *Nat. Rev. Cancer* **6,** 392–401
3. Lorusso, G., and Ruegg, C. (2008) The tumor microenvironment and its contribution to tumor evolution toward metastasis. *Histochem. Cell Biol.* **130,** 1091–1103
4. Kass, L., Erler, J. T., Dembo, M., and Weaver, V. M. (2007) Mammary epithelial cell: influence of extracellular matrix composition and organization during development and tumorigenesis. *Int. J. Biochem. Cell Biol.* **39,** 1987–1994
5. Plate, K. H., Breier, G., Weich, H. A., and Risau, W. (1992) Vascular endothelial growth factor is a potential tumour angiogenesis factor in human gliomas in vivo. *Nature* **359,** 845–848
6. Tuxhorn, J. A., McAlhany, S. J., Yang, F., Dang, T. D., and Rowley, D. R. (2002) Inhibition of transforming growth factor-beta activity decreases angiogenesis in a human prostate cancer-reactive stroma xenograft model. *Cancer Res.* **62,** 6021–6025
7. Kalas, W., Yu, J. L., Milsom, C., Rosenfeld, J., Benezra, R., Bornstein, P., and Rak, J. (2005) Oncogenes and Angiogenesis: down-regulation of thrombospondin-1 in normal fibroblasts exposed to factors from cancer cells harboring mutant ras. *Cancer Res.* **65,** 8878–8886
8. Brellier, F., Tucker, R. P., and Chiquet-Ehrismann, R. (2009) Tenascins and their implications in diseases and tissue mechanics. *Scand. J. Med. Sci. Sports* **19,** 511–519
9. Chiquet-Ehrismann, R., Mackie, E. J., Pearson, C. A., and Sakakura, T. (1986) Tenascin: an extracellular matrix protein involved in tissue interactions during fetal development and oncogenesis. *Cell* **47,** 131–139
10. Orend, G., and Chiquet-Ehrismann, R. (2006) Tenascin-C induced signaling in cancer. *Cancer Lett.* **244,** 143–163
11. Huang, W., Chiquet-Ehrismann, R., Moyano, J. V., Garcia-Pardo, A., and Orend, G. (2001) Interference of tenascin-C with syndecan-4 binding to fibronectin blocks cell adhesion and stimulates tumor cell proliferation. *Cancer Res.* **61,** 8586–8594
12. Herold-Mende, C., Mueller, M. M., Bonsanto, M. M., Schmitt, H. P., Kunze, S., and Steiner, H. H. (2002) Clinical impact and functional aspects of tenascin-C expression during glioma progression. *Int. J. Cancer* **98,** 362–369
13. De Wever, O., Nguyen, Q. D., Van Hoorde, L., Bracke, M., Bruyneel, E., Gespach, C., and Mareel, M. (2004) Tenascin-C and SF/HGF produced by myofibroblasts in vitro provide convergent pro-invasive signals to human colon cancer cells through RhoA and Rac. *FASEB J.* **18,** 1016–1018
14. Ishiwata, T., Takahashi, K., Shimanuki, Y., Ohashi, R., Cui, R., Takahashi, F., Shimizu, K., Miura, K., and Fukuchi, Y. (2005) Serum tenascin-C as a potential predictive marker of angiogenesis in non-small cell lung cancer. *Anticancer Res.* **25,** 489–495
15. Saito, Y., Shiota, Y., Nishisaka, M., Owaki, T., Shimamura, M., and Fukai, F. (2008) Inhibition of angiogenesis by a tenascin-c peptide which is capable of activating beta1-integrins. *Biol. Pharm. Bull.* **31,** 1003–1007
16. Tanaka, K., Hiraiwa, N., Hashimoto, H., Yamazaki, Y., and Kusakabe, M. (2004) Tenascin-C regulates angiogenesis in tumor through the regulation of vascular endothelial growth factor expression. *Int. J. Cancer.* **108,** 31–40
17. Schenk, S., Chiquet-Ehrismann, R., and Battegay, E. J. (1999) The fibrinogen globe of tenascin-C promotes basic fibroblast growth factor-induced endothelial cell elongation. *Mol. Biol. Cell* **10,** 2933–2943
18. Zagzag, D., Shiff, B., Jallo, G. I., Greco, M. A., Blanco, C., Cohen, H., Hukin, J., Allen, J. C., and Friedlander, D. R. (2002) Tenascin-C promotes microvascular cell migration and phosphorylation of focal adhesion kinase. *Cancer Res.* **62,** 2660–2668
19. Tavazoie, S. F., Alarcon, C., Oskarsson, T., Padua, D., Wang, Q., Bos, P. D., Gerald, W. L., and Massague, J. (2008) Endogenous human microRNAs that suppress breast cancer metastasis. *Nature* **451,** 147–152
20. Calvo, A., Catena, R., Noble, M. S., Carbott, D., Gil-Bazo, I., Gonzalez-Moreno, O., Huh, J. I., Sharp, R., Qiu, T. H., Anver, M. R., Merlino, G., Dickson, R. B., Johnson, M. D., and Green, J. E. (2008) Identification of VEGF-regulated genes associated with increased lung metastatic potential: functional involvement of tenascin-C in tumor growth and lung metastasis. *Oncogene* **27,** 5373–5384
21. Scherberich, A., Tucker, R. P., Samandari, E., Brown-Luedi, M., Martin, D., and Chiquet-Ehrismann, R. (2004) Murine tenascin-W: a novel mammalian tenascin expressed in kidney and at sites of bone and smooth muscle development. *J. Cell Sci.* **117,** 571–581
22. Degen, M., Brellier, F., Kain, R., Ruiz, C., Terracciano, L., Orend, G., and Chiquet-Ehrismann, R. (2007) Tenascin-W is a novel marker for activated tumor stroma in low-grade human breast cancer and influences cell behavior. *Cancer Res.* **67,** 9169–9179
23. Degen, M., Brellier, F., Schenk, S., Driscoll, R., Zaman, K., Stupp, R., Tornillo, L., Terracciano, L., Chiquet-Ehrismann, R., Ruegg, C., and Seelentag, W. (2008) Tenascin-W, a new marker of cancer stroma, is elevated in sera of colon and breast cancer patients. *Int. J. Cancer* **122,** 2454–2461
24. Lino, M., and Merlo, A. (2009) Translating biology into clinic: the case of glioblastoma. *Curr. Opin. Cell Biol.* **21,** 311–316
25. Cairncross, J. G. (1998) Cognition in survivors of high-grade glioma. *J. Clin. Oncol.* **16,** 3210–3211
26. Orend, G. (2005) Potential oncogenic action of tenascin-C in tumorigenesis. *Int. J. Biochem. Cell. Biol.* **37,** 1066–1083
27. Zamecnik, J. (2005) The extracellular space and matrix of gliomas. *Acta Neuropathol.* **110,** 435–442

28. Sivasankaran, B., Degen, M., Ghaffari, A., Hegi, M. E., Hamou, M. F., Ionescu, M. C., Zweifel, C., Tolnay, M., Wasner, M., Mergenthaler, S., Miserez, A. R., Kiss, R., Lino, M. M., Merlo, A., Chiquet-Ehrismann, R., and Boulay, J. L. (2009) Tenascin-C is a novel RBPJκ-induced target gene for Notch signaling in gliomas. *Cancer Res.* **69,** 458–465
29. Leins, A., Riva, P., Lindstedt, R., Davidoff, M. S., Mehraein, P., and Weis, S. (2003) Expression of tenascin-C in various human brain tumors and its relevance for survival in patients with astrocytoma. *Cancer* **98,** 2430–2439
30. Reardon, D. A., Zalutsky, M. R., and Bigner, D. D. (2007) Antitenascin-C monoclonal antibody radioimmunotherapy for malignant glioma patients. *Expert Rev. Anticancer Ther.* **7,** 675–687
31. Bredel, M., Bredel, C., Juric, D., Harsh, G. R., Vogel, H., Recht, L. D., and Sikic, B. I. (2005) Functional network analysis reveals extended gliomagenesis pathway maps and three novel MYC-interacting genes in human gliomas. *Cancer Res.* **65,** 8679–8689
32. Orend, G., Huang, W., Olayioye, M. A., Hynes, N. E., and Chiquet-Ehrismann, R. (2003) Tenascin-C blocks cell-cycle progression of anchorage-dependent fibroblasts on fibronectin through inhibition of syndecan-4. *Oncogene* **22,** 3917–3926
33. Fischer, D., Tucker, R. P., Chiquet-Ehrismann, R., and Adams, J. C. (1997) Cell-adhesive responses to tenascin-C splice variants involve formation of fascin microspikes. *Mol. Biol. Cell* **8,** 2055–2075
34. Korff, T., and Augustin, H. G. (1998) Integration of endothelial cells in multicellular spheroids prevents apoptosis and induces differentiation. *J. Cell Biol.* **143,** 1341–1352
35. Korff, T., and Augustin, H. G. (1999) Tensional forces in fibrillar extracellular matrices control directional capillary sprouting. *J. Cell Sci.* **112,** 3249–3258
36. Ivanov, D., Philippova, M., Tkachuk, V., Erne, P., and Resink, T. (2004) Cell adhesion molecule T-cadherin regulates vascular cell adhesion, phenotype and motility. *Exp. Cell. Res.* **293,** 207–218
37. Romer, L. H., McLean, N., Turner, C. E., and Burridge, K. (1994) Tyrosine kinase activity, cytoskeletal organization, and motility in human vascular endothelial cells. *Mol. Biol. Cell* **5,** 349–361
38. Canfield, A. E., and Schor, A. M. (1995) Evidence that tenascin and thrombospondin-1 modulate sprouting of endothelial cells. *J. Cell Sci.* **108,** 797–809
39. Giusti, B., Fibbi, G., Margheri, F., Serrati, S., Rossi, L., Poggi, F., Lapini, I., Magi, A., Del Rosso, A., Cinelli, M., Guiducci, S., Kahaleh, B., Bazzichi, L., Bombardieri, S., Matucci-Cerinic, M., Gensini, G. F., Del Rosso, M., and Abbate, R. (2006) A model of anti-angiogenesis: differential transcriptosome profiling of microvascular endothelial cells from diffuse systemic sclerosis patients. *Arthritis Res. Ther.* **8,** R115
40. Kimura, H., Akiyama, H., Nakamura, T., and de Crombrugghe, B. (2007) Tenascin-W inhibits proliferation and differentiation of preosteoblasts during endochondral bone formation. *Biochem. Biophys. Res. Commun.* **356,** 935–941
41. Langenfeld, E. M., and Langenfeld, J. (2004) Bone morphogenetic protein-2 stimulates angiogenesis in developing tumors. *Mol. Cancer. Res.* **2,** 141–149
42. Ren, R., Charles, P. C., Zhang, C., Wu, Y., Wang, H., and Patterson, C. (2007) Gene expression profiles identify a role for cyclooxygenase 2-dependent prostanoid generation in BMP6-induced angiogenic responses. *Blood* **109,** 2847–2853
43. Rothhammer, T., Bataille, F., Spruss, T., Eissner, G., and Bosserhoff, A. K. (2007) Functional implication of BMP4 expression on angiogenesis in malignant melanoma. *Oncogene* **26,** 4158–4170
44. Kaspar, M., Zardi, L., and Neri, D. (2006) Fibronectin as target for tumor therapy. *Int. J. Cancer.* **118,** 1331–1339
45. Bigner, D. D., Brown, M. T., Friedman, A. H., Coleman, R. E., Akabani, G., Friedman, H. S., Thorstad, W. L., McLendon, R. E., Bigner, S. H., Zhao, X. G., Pegram, C. N., Wikstrand, C. J., Herndon, J. E., 2nd, Vick, N. A., Paleologos, N., Cokgor, I., Provenzale, J. M., and Zalutsky, M. R. (1998) Iodine-131-labeled antitenascin monoclonal antibody 81C6 treatment of patients with recurrent malignant gliomas: phase I trial results. *J. Clin. Oncol.* **16,** 2202–2212
46. De Santis, R., Anastasi, A. M., D'Alessio, V., Pelliccia, A., Albertoni, C., Rosi, A., Leoni, B., Lindstedt, R., Petronzelli, F., Dani, M., Verdoliva, A., Ippolito, A., Campanile, N., Manfredi, V., Esposito, A., Cassani, G., Chinol, M., Paganelli, G., and Carminati, P. (2003) Novel antitenascin antibody with increased tumour localisation for pretargeted antibody-guided radioimmunotherapy (PAGRIT). *Br. J. Cancer.* **88,** 996–1003
47. Silacci, M., Brack, S. S., Spath, N., Buck, A., Hillinger, S., Arni, S., Weder, W., Zardi, L., and Neri, D. (2006) Human monoclonal antibodies to domain C of tenascin-C selectively target solid tumors in vivo. *Protein Eng. Des. Sel.* **19,** 471–478
48. Brack, S. S., Silacci, M., Birchler, M., and Neri, D. (2006) Tumor-targeting properties of novel antibodies specific to the large isoform of tenascin-C. *Clin. Cancer Res.* **12,** 3200–3208
49. Marlind, J., Kaspar, M., Trachsel, E., Sommavilla, R., Hindle, S., Bacci, C., Giovannoni, L., and Neri, D. (2008) Antibody-mediated delivery of interleukin-2 to the stroma of breast cancer strongly enhances the potency of chemotherapy. *Clin. Cancer Res.* **14,** 6515–6524
50. Sauer, S., Erba, P. A., Petrini, M., Menrad, A., Giovannoni, L., Grana, C., Hirsch, B., Zardi, L., Paganelli, G., Mariani, G., Neri, D., Durkop, H., and Menssen, H. D. (2009) Expression of the oncofetal ED-B-containing fibronectin isoform in hematologic tumors enables ED-B-targeted 131I-L19SIP radioimmunotherapy in Hodgkin lymphoma patients. *Blood* **113,** 2265–2274


*Received for publication June 26, 2009.*
*Accepted for publication October 8, 2009.*

## III.1.2 – The adhesion modulating properties of tenascin-W

Florence Brellier, Enrico Martina, Matthias Chiquet, Jacqueline Ferralli, Michael van der Heyden, Gertraud Orend, Johannes C. Schittny, Ruth Chiquet-Ehrismann and Richard P. Tucker

Int J Biol Sci. 2012;8(2):187-94

My contribution:
I performed the adhesion assays, the immunofluorescence stainings and the subsequent data analysis illustrated in the paper figure 2. I also sectioned, stained and analyzed 32 tail wounds of wild type and TNC-deficient mice. Due to the variation seen within each group of mice, we could not find a significant difference between the healing time of wounds in wild type versus TN-deficient mice and thus could not include these results in this paper.

*Int. J. Biol. Sci.* 2012, 8 187

IVYSPRING INTERNATIONAL PUBLISHER

*International Journal of Biological Sciences*

2012; 8(2):187-194

Short Research Communication

# The Adhesion Modulating Properties of Tenascin-W

**Florence Brellier[1*], Enrico Martina[1,2*], Matthias Chiquet[3], Jacqueline Ferralli[1], Michael van der Heyden[4], Gertraud Orend[4], Johannes C. Schittny[5], Ruth Chiquet-Ehrismann[1,2] and Richard P. Tucker[6,✉]**

1. Friedrich Miescher Institute for Biomedical Research, Novartis Research Foundation, CH-4058 Basel, Switzerland.
2. University of Basel, Faculty of Science, CH-4056 Basel, Switzerland.
3. Department of Orthodontics and Dentofacial Orthopedics, University of Bern, CH-3010 Bern, Switzerland.
4. Inserm, U682, Strasbourg, F-67200 France, University Strasbourg, UMR-S682, Strasbourg F-67081, France.
5. Institute of Anatomy, University of Bern, CH-3000 Bern, Switzerland.
6. Department of Cell Biology and Human Anatomy, University of California at Davis, Davis, California 95616 USA.

* These authors contributed equally to this work.

✉ Corresponding author: Department of Cell Biology and Human Anatomy, University of California at Davis, Davis, California 95616 USA. Tel: 001 530 752 0238; fax: 001 530 752 8520; E-mail: rptucker@ucdavis.edu.



Received: 2011.07.20; Accepted: 2011.12.13; Published: 2011.12.20

## Abstract

Tenascins are extracellular matrix glycoproteins associated with cell motility, proliferation and differentiation. Tenascin-C inhibits cell spreading by binding to fibronectin; tenascin-R and tenascin-X also have anti-adhesive properties in vitro. Here we have studied the adhesion modulating properties of the most recently characterized tenascin, tenascin-W. C2C12 cells, a murine myoblast cell line, will form broad lamellipodia with stress fibers and focal adhesion complexes after culture on fibronectin. In contrast, C2C12 cells cultured on tenascin-W fail to spread and form stress fibers or focal adhesion complexes, and instead acquire a multipolar shape with short, actin-tipped pseudopodia. The same stellate morphology is observed when C2C12 cells are cultured on a mixture of fibronectin and tenascin-W, or on fibronectin in the presence of soluble tenascin-W. Tenascin-W combined with fibronectin also inhibits the spreading of mouse embryo fibroblasts when compared with cells cultured on fibronectin alone. The similarity between the adhesion modulating effects of tenascin-W and tenascin-C in vitro led us to study the possibility of tenascin-W compensating for tenascin-C in tenascin-C knockout mice, especially during epidermal wound healing. Dermal fibroblasts harvested from a tenascin-C knockout mouse express tenascin-W, but dermal fibroblasts taken from a wild type mouse do not. However, there is no upregulation of tenascin-W in the dermis of tenascin-C knockout mice, or in the granulation tissue of skin wounds in tenascin-C knockout animals. Similarly, tenascin-X is not upregulated in early wound granulation tissue in the tenascin-C knockout mice. Thus, tenascin-W is able to inhibit cell spreading in vitro and it is upregulated in dermal fibroblasts taken from the tenascin-C knockout mouse, but neither it nor tenascin-X are likely to compensate for missing tenascin-C during wound healing.

Key words: tenascin, extracellular matrix, fibronectin, wound healing, C2C12.

## Introduction

Tenascins are a family of extracellular matrix glycoproteins capable of influencing cell proliferation, fate and behavior by modifying cell adhesion either directly via their cell surface receptors or indirectly through interactions with other matrix molecules (1). The first member of the family to be characterized as

'anti-adhesive' was tenascin-C. Cells cultured on substrata coated with tenascin-C fail to spread, and cells also fail to spread on substrata formed from mixtures of tenascin-C and fibronectin, or on fibronectin-coated substrata in the presence of soluble tenascin-C (2-7). The adhesion modulating properties of tenascin-R (8,9) and tenascin-X (10-12) are also well known.

Tenascin-W is the most recently discovered member of the tenascin gene family. Its expression during development is largely limited to smooth muscle, bone and the stroma of certain tumors (13-16). The addition of tenascin-W to the medium over osteoblasts cultured on fibronectin prevents them from spreading, and when these cells are cultured on tenascin-W they remain rounded (15). Moreover, in transwell assays soluble tenascin-W promotes the migration of tumor-derived cell lines (16) and osteoblasts (17) across a fibronectin-coated filter. These results suggest that tenascin-W may share some of the anti-adhesive properties of other tenascins.

The tenascin-C knockout mouse was first reported to develop normally (18), but closer examination led to the identification of a number of developmental abnormalities and well as abnormal responses to trauma (1). Tenascin-C is upregulated in the granulation tissue at the borders of skin wounds (19) where it is associated with the migration and proliferation of myofibroblasts and epidermis. However, skin wounds have been reported to heal normally in the tenascin-C knockout mouse (20). We therefore speculated that in these mice tenascin-W, if it has anti-adhesive properties, might compensate for tenascin-C in healing wounds.

Here we have cultured C2C12 cells on tenascin-W-coated substrata either alone or in combination with fibronectin and show that tenascin-W shares adhesion modulating properties with tenascin-C. We then show that tenascin-W is expressed by fibroblasts from the dermis of the tenascin-C knockout mouse, but not by fibroblasts derived from a wild type mouse. Finally, we examined the granulation tissue of healing skin wounds in the tenascin-C knockout mouse for upregulation of tenascin-W.

## Materials and methods

**Proteins and antibodies.** Fibronectin was isolated from medium conditioned by primary mouse embryonic skin fibroblasts. Medium (approximately 700 ml) from confluent 4th passage cultures was collected and concentrated 30 fold by precipitation with ammonium sulfate. The concentrated conditioned medium was dialyzed against $Ca^{++}/Mg^{++}$-free phosphate buffered saline (PBS) and applied to a 10 ml gelatin-Sepharose (Amersham/GE Health Care) column. The column was washed with 0.5 M urea in PBS, and fibronectin was eluted with 4M urea in PBS. The purified protein was dialyzed against PBS and sterilized by filtration through a 0.2 μm pore filter. Full length mouse recombinant tenascin-W was cloned, expressed and purified as described in Scherberich et al. (13). The rat anti-mouse tenascin-C monoclonal antibody (MTn-12) was characterized by Aufderheide and Ekblom (21), the rabbit polyclonal anti-mouse tenascin-W was characterized by Scherberich et al. (13), and the anti-tenascin-X rabbit polyclonal antibody was characterized by Matsumoto et al. (22). The mouse anti-vinculin monoclonal antibody was purchased from Sigma.

**Substrata and cell culture.** Tissue culture plastic dishes were coated with mouse fibronectin (5 μg/ml) or recombinant mouse tenascin-W (5 μg/ml or 10 μg/ml) diluted in serum-free Dulbecco's Modified Eagle's Medium (DMEM) for 90 min, rinsed in DMEM, blocked for 15 min with 1 mg/ml heat-inactivated bovine serum albumin (BSA), and rinsed 3X in DMEM. Control dishes were incubated in DMEM without proteins and then rinsed and blocked as described. C2C12 cells (23) (a gift from Dr. Zach Hall, National Institute of Neurological Disorders and Stroke, National Institutes of Health, Bethesda, MD) or mouse embryo fibroblasts (see below) were washed in DMEM with 10% fetal calf serum (FCS), rinsed in DMEM without serum, and a 250 μl aliquot was added to the coated substratum and the cells were incubated at 37°C. After 90 min tenascin-W diluted in warm DMEM was added to the medium of some of the cells being cultured on fibronectin-coated dishes (to a final concentration of 5 or 10 μg/ml); a similar amount of warm DMEM alone was added to the other cultures at this time as a control. After at total of 2 hr in culture the cells were fixed in 1% paraformaldehyde in DMEM for 30 min, then rinsed 3X in PBS and processed for immunocytochemistry. All experiments were conducted in triplicate.

**Immunocytochemistry, photography and image analysis.** After fixation and rinsing the cells were blocked overnight in PBS with 0.5% BSA at 4°C, permeabilized with 0.1% Triton X-100 for 5 min, and incubated in anti-vinculin (see above) and/or TRITC-labeled phalloidin (Sigma) for 1 hr. The cells were then rinsed and incubated in secondary antibody (Alexa 488-labeled goat anti-mouse; Invitrogen) for 45 min. Finally, the cells were rinsed in PBS containing DAPI (Sigma), rinsed and coverslipped. To measure cell areas, images of cells labeled with phalloidin were converted to high contrast, grayscale images and inverted. The number of black pixels was

analyzed using Adobe Photoshop CS3 and converted to cell area by similarly analyzing a black square of a known size. Statistical differences ($p < 0.05$) were determined using a two-tailed t-test.

**Fibroblast cultures and immunoblotting.** Primary embryonic skin fibroblasts were isolated from 129/Sv mouse wildtype and TN-C knockout (20) embryos at embryonic day 15.5. The dissected skin was rinsed in $Ca^{++}/Mg^{++}$-free PBS, minced and digested in 5 ml 0.05% trypsin-EDTA (Gibco/Invitrogen) for 45 min at 37°C. The digestion was stopped by adding the same volume of DMEM containing 10% FCS. Large debris was removed by centrifugation and cells were collected. Primary fibroblasts were plated in 10 cm dishes (Falcon) in 10 ml DMEM/10% FCS and grown to confluency. Cells were passaged once a week and spontaneously immortalized as described in Brellier et al. (24). To study tenascin expression, conditioned medium was collected, separated by SDS-PAGE, transferred and immunostained as described previously (12). Equal loading and transfer was confirmed with amido black. The intensities of the immunostained bands were measured with ImageQuant TL (v2005). Each tenascin value then was normalized to the intensity of an anti-vinculin immunostained band.

**Wound healing and immunohistochemistry.** Handling of the animals before and during the experiments, as well as the experiments themselves, were approved and supervised by the Swiss Agency for the Environment, Forests and Landscape and the Veterinary Service of the Canton of Bern. In addition we followed the guidelines of INSERM and the Federation of Laboratory Animal Science Associations. To study wound healing in mice we adapted an incisional tail wound model based on a previous study (25). For immunoblot analysis the tail tips of 3 SL-129 mice were cut generating 5mm long fragments that were used as controls. These were compared with 5 mm long tail fragments from tenascin-$C^{+/+}$ or tenascin-$C^{-/-}$ SL-129 mice that contained wounds that were allowed to heal for 1 day, 3 days or 10 days. All fragments were cut into small pieces with a scalpel and homogenized with a mortar and pestle in 400 µl of RIPA buffer. After 2 min of mixing, the solutions were centrifuged to remove debris. Samples were boiled in Laemmli sample buffer and stored at -20°C. For immunohistochemical analysis, wounded tail fragments like those described above were collected from tenascin-$C^{+/+}$ mice (2 male, 1 female, aged 3-7 weeks) and from tenascin-$C^{-/-}$ mice (2 male, 1 female, aged 5 weeks) and fixed overnight in 4% paraformaldehyde in PBS. The tissues were then rinsed, incubated overnight at 4°C in 20% sucrose in PBS, and embedded in O.C.T. (Sakura). Frozen sections were collected on presubbed slides (Fisher). Dried slides were then rinsed, blocked in PBS with 0.5% BSA, and incubated overnight in MTn-12 (anti-tenascin-C), anti-tenascin-X and anti-mouse tenascin-W (see above). The next day the slides were rinsed, blocked and then incubated for 2 hr in a mixture of diluted Alexa 488 labeled-goat anti-rat secondary antibody and Alexa 594 labeled-goat anti-rabbit secondary antibody (Invitrogen). Slides were rinsed in PBS with DAPI, then rinsed, coverslipped and photographed.

## Results and discussion

The mouse myoblast cell line C2C12 has the potential to transdifferentiate into osteoblasts, a cell type that we have previously shown can bind to tenascin-W (13, 17). We selected C2C12 cells for this study because we found that these cells adhere to tenascin-W, yet they do not express tenascin-W in the absence of BMP2 (13) and they were used in an earlier study illustrating the anti-adhesive properties of tenascin-C (5). C2C12 cells cultured for 2 hr in the absence of serum on tissue culture plastic blocked with BSA will attach and spread, resulting in morphologically diverse multipolar cells with many small lamellae and short phalloidin-labeled stress fibers (Fig. 1A). In contrast, when these cells are cultured for 2 hr on tissue culture plastic coated with 5 µg/ml (~25 nM) of mouse fibronectin blocked with BSA they spread and form large lamellae as well as stress fibers ending in anti-vinculin labeled focal adhesion complexes (Fig. 1B). When cultured on 10 µg/ml (~50 nM) mouse tenascin-W blocked with BSA the C2C12 cells fail to spread and form lamellae. Instead, cells on tenascin-W are typically triangular or polygonal and have numerous small, actin-rich processes (Fig. 1C). Stress fibers are not seen, and the anti-vinculin stains the cytoplasm of these cells instead of the focal adhesion complexes seen when cells are cultured on fibronectin. On mixed fibronectin/tenascin-W substrata an intermediate morphology is usually observed: the C2C12 cells do not form large lamellae, but a few anti-vinculin-positive focal adhesion complexes are typically present (Fig. 1D). There were statistically fewer ($p < 0.001$) anti-vinculin-positive focal adhesions in C2C12 cells cultured on mixed substrata (8.5 ± 9.2, n = 11) than on fibronectin alone (26.7 ± 14.5, n = 10). The adhesion modulating effects of substratum-bound tenascin-W were also observed with soluble tenascin-W. When C2C12 cells were first allowed to attach and spread on fibronectin-coated substrata for 90 min and tenascin-W was then added to the medium for an additional 30 min prior to fixation and staining, the cells typically acquired the polygonal

morphology and short actin-rich processes that were also observed with cells cultured on tenascin-W alone (Fig. 1E).

The different morphologies of C2C12 cells following culture on fibronectin, tenascin-W, mixtures of fibronectin and tenascin-W, and on fibronectin with soluble tenascin-W, are identical to the morphologies we previously described for C2C12 cells cultured under similar conditions on tenascin-C and fibronectin (5). In our previous study we observed stress fibers developing in C2C12 cells 90 min after culture on tissue culture plastic coated with 50 nM fibronectin (about twice the concentration we used here), while cells cultured on tissue culture plastic coated with 50 nM tenascin-C are polygonal with short, actin-rich processes indistinguishable from cells cultured on tenascin-W. One potentially important difference between our previous study and the current one has to do with the species of origin of the fibronectin and tenascin: Fischer et al. (5) used fibronectin purified from horse serum and recombinant chicken tenascin-C, but here we used mouse fibronectin and recombinant mouse tenascin-W. This seemed appropriate, as there may be a functional integrin-binding RGD motif found in the second fibronectin type III domain of mouse tenascin-W (13) that is missing in avian (and human) tenascin-W (26).

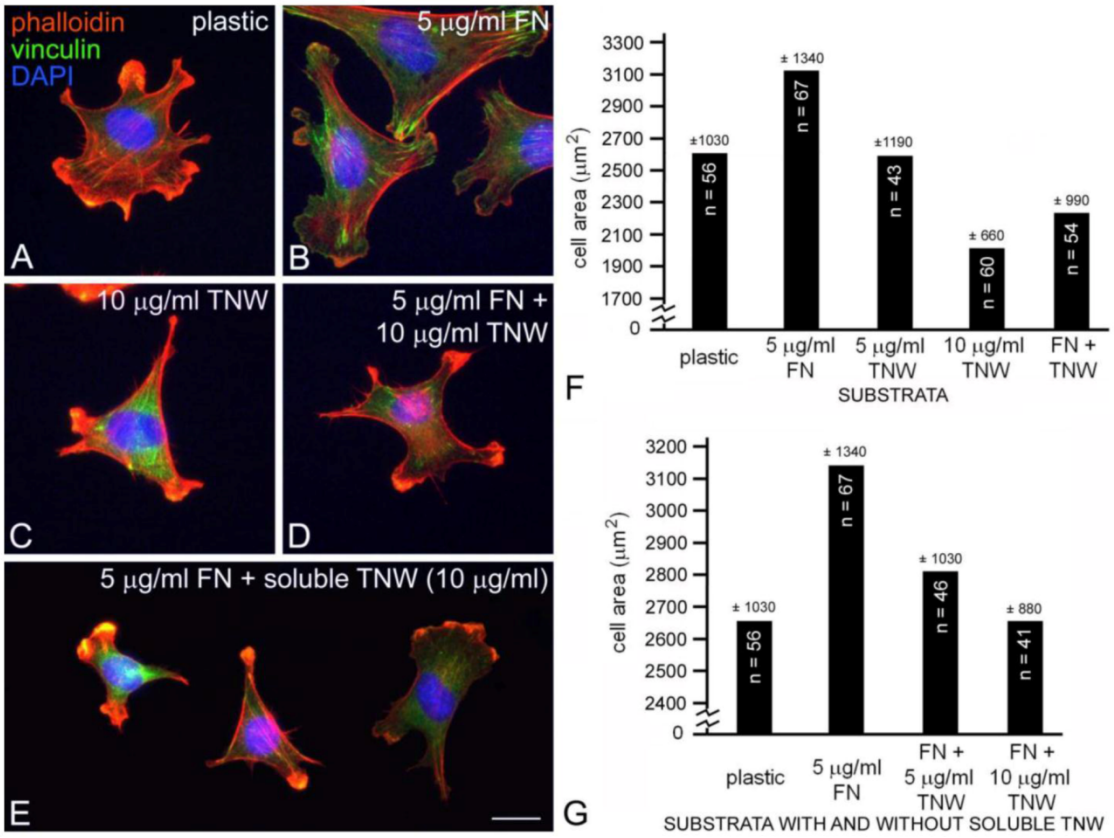


**Fig. 1.** C2C12 cells cultured on tissue culture plastic (A), fibronectin (B), tenascin-W (C), a mixture of fibronectin and tenascin-W (D) or on fibronectin with tenascin-W added to the medium (E). After 2 hr the cells were fixed and stained with TRITC-labeled phalloidin (red) to show polymerized actin, anti-vinculin (green) to show focal adhesion complexes, and the nuclear marker DAPI (blue). C2C12 cells spread and form stress fibers and numerous focal adhesion complexes on fibronectin, but are polygonal on tenascin-W and have numerous short, actin-rich processes. Cells cultured on mixtures of fibronectin and tenascin-W, or on fibronectin with tenascin-W in the medium, resemble cells cultured on tenascin-W alone. Total areas of cells cultured under the conditions indicated were measured and compared (sample size and standard deviations are indicated; F, G). C2C12 cells are significantly more spread on 5 µg/ml fibronectin than on tissue culture plastic, and are significantly less spread on 10 µg/ml tenascin-W than on tissue culture plastic alone. The C2C12 cells are also significantly less spread on the mixture of tenascin-W and fibronectin than on fibronectin alone, and on fibronectin with 10 µg/ml tenascin-W in the medium than on fibronectin alone. Scale bar = 25 µm.

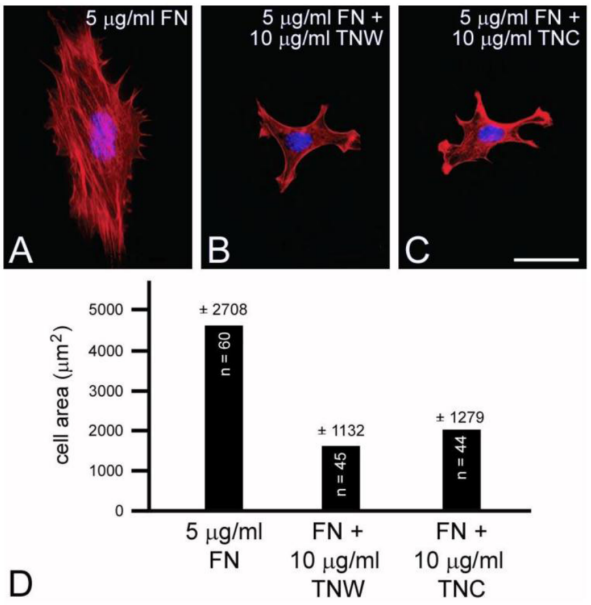


**Fig. 2.** Mouse embryo fibroblasts cultured on fibronectin (A) or combinations of fibronectin and tenascin-W (B) or fibronectin and tenascin-C (C) stained with TRITC-labeled phalloidin (red) and DAPI (blue). Mouse embryo fibroblasts cultured for 2 hr on fibronectin spread and form stress fibers; mouse embryo fibroblasts cultured on fibronectin mixed with tenascin-W or tenascin-C are stellate and fail to form lamellipodia or stress fibers. When the total cell area is measured, there is a significant decrease in the area of cells cultured on the mixed substrata when compared with fibronectin alone (D). Sample size and standard deviations are indicated. Scale bar = 100 μm.

C2C12 cells cultured on mixed fibronectin and tenascin-W substrata have fewer anti-vinculin-positive focal adhesion complexes than cells cultured on fibronectin alone, and after the addition of tenascin-W to the medium C2C12 cells cultured on fibronectin fail to elaborate lamellae and stress fibers. To quantify the effects of tenascin-W on cell morphology and to determine the effects of different concentrations of tenascin-W, the total area of C2C12 cells under different culture conditions was measured and compared (Fig. 1F, G). As expected, cells cultured on tissue culture plastic coated with 5 μg/ml fibronectin are more spread than cells cultured on tissue culture plastic alone. No effect on cell area was observed when C2C12 cells were cultured on dishes coated with 5 μg/ml tenascin-W, but on 10 μg/ml of tenascin-W the cell area is significantly less than the area of cells cultured on fibronectin or on tissue culture plastic alone. Cells cultured on mixed fibronectin/tenascin-W substrata are less spread than cells cultured on fibronectin alone, as are cells cultured on fibronectin with 10 μg/ml tenascin-W in the medium. These results show that tenascin-W has the same effects on C2C12 cell morphology as tenascin-C, and that tenascin-W shares the adhesion modulating activity of tenascin-C when cells are cultured on fibronectin. The effects of tenascin-W on cell spreading are not limited to C2C12 cells. When mouse embryo fibroblasts are cultured on 5 μg/ml fibronectin they spread and form an extensive array of stress fibers (Fig. 2A). In contrast, mouse embryo fibroblasts cultured on a combination of fibronectin and tenascin-W fail to spread and form stress fibers, and instead acquire the multipolar morphology described above for C2C12 cells cultured on tenascin-W (Fig. 2B). A similar morphology is seen when mouse embryo fibroblasts are cultured on combinations of 5 μg/ml fibronectin and 10 μg/ml of tenascin-C (Fig. 2C). When the areas of mouse embryo fibroblasts cultured under these conditions are measured and compared, they are significantly ($p < 0.001$) less on the mixed substrata containing tenascin-W and tenascin-C than on fibronectin alone (Fig. 2D).

Tenascin-C is typically expressed by cultured dermal fibroblasts (27) and is upregulated in granulation tissue at the margins of healing skin wounds (19). To determine if tenascin-W may be able to compensate for the tenascin-C missing from the granulation tissue of tenascin-C knockout mice, primary fibroblasts from the dermis of either tenascin-C $^{+/+}$ or

tenascin-C $^{-/-}$ mice were examined for tenascin-W expression by immunoblotting. Tenascin-W expression was observed in the cells from the dermis of tenascin-C $^{-/-}$ mice, but not in the control cells (Fig. 3A). The acquisition of tenascin-W expression came over time, with repeated passages (Fig. 3B). This suggests that at least some cells that normally express tenascin-C are able to upregulate tenascin-W following knockout of tenascin-C. To determine if a similar upregulation takes place in vivo during the healing of skin wounds, fragments of epidermis and dermis from unwounded tails and epidermis, dermis and early granulation tissue from wounds that had healed for 1-10 days were homogenized and studied for the expression of tenascin-C and tenascin-W by immunoblot analysis (Fig. 3C). Tenascin-C is upregulated 2.7 fold 3 days after wounding and 4.5 fold 10 days after wounding. There is no difference between tenascin-W expression in wounds of tenascin-C $^{+/+}$ versus tenascin-C $^{-/-}$ mice with a slight upreguation of tenascin-W after 2 days (average 1.5 fold) and no upregulation 10 days after wounding. This was confirmed by examining frozen sections through wounds in the tails of tenascin-C $^{+/+}$ and tenascin-C $^{-/-}$ mice 3 days following injury with anti-tenascin-C and anti-tenascin-W. As reported previously (19), tenascin-C is abundant in the early granulation tissue of the healing wounds (Fig. 4A). In contrast, tenascin-W is found in patches in the normal skin near the dermal/epidermal junction in regions corresponding to the connective tissue septae that run from the epidermis to deep connective tissue (the 'wrinkles' in the tail), but it is not present in the early granulation tissue (Fig. 4A). In the healing cutaneous wounds in the tail of the tenascin-C knockout mice, no tenascin-C immunoreactivity was seen, and the distribution of tenascin-W was identical to that seen in the control dermis (Fig. 4B). Therefore, even though tenascin-W shares the adhesion modulating properties of tenascin-C in vitro, and it can be upregulated in fibroblasts derived from the dermis of tenascin-C$^{-/-}$ mice, it is not upregulated during wound healing in the skin of the tenascin-C knockout mice and is unlikely to be compensating for the missing tenascin-C in this system. The observation made by others (20) that levels of fibronectin appear to be lower in the wounds of tenascin-C$^{-/-}$ mice may offer an explanation for the apparently normal phenotype. Moreover, tenascin-X has well documented anti-adhesive properties (12) and may play a role in compensating for the missing tenascin-C. However, antibodies to tenascin-X reveal the previously described pattern of expression in the epidermis and deep dermis (22) in sections of healing wounds from control mice (Fig. 4C), but do not show upregulation in the early granulation tissue of wounds in the tenascin-C $^{-/-}$ mice (Fig. 4D).

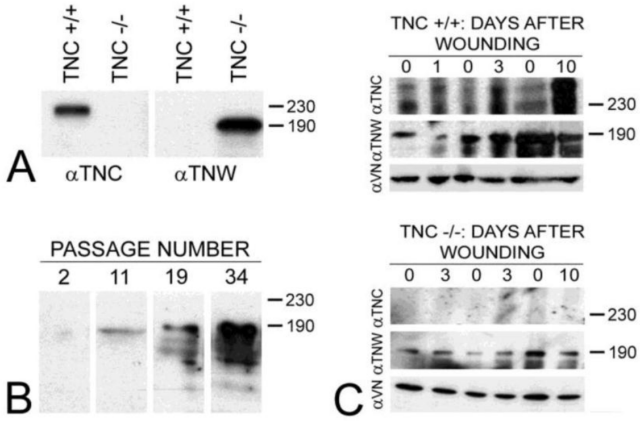


**Fig. 3.** The expression of tenascin-C (αTNC) and tenascin-W (αTNW) by primary fibroblasts from tenascin-C$^{+/+}$ and tenascin-C$^{-/-}$ dermis were compared by immunoblotting (A). Fibroblasts from normal dermis express tenascin-C, but fibroblasts derived from tenascin-C knockout skin expresses tenascin-W. Amido black was used to demonstrate equal loading (not shown). The expression of tenascin-W by the fibroblasts derived from tenascin-C$^{-/-}$ dermis increased with passaging (B). The expression of tenascins-C and -W was also examined by immunoblotting homogenates of control and wounded skin (C). There is an increase in the expression of tenascin-C 3 (2.7 fold) and 10 days (4.5 fold) following wounding. Tenascin-W expression is upregulated 1.5 fold 3 days following wounding, but is not upregulated after 10 days both in tenascin-C +/+ and tenascin-C -/- mice. Anti-vinculin (VN) was used to normalize the changes in the intensity of the anti-tenascins. In wounds from the tenascin-C-/- mice, the expression of tenascin-W remains unchanged. Apparent molecular weights are indicated by size standards (kDa).

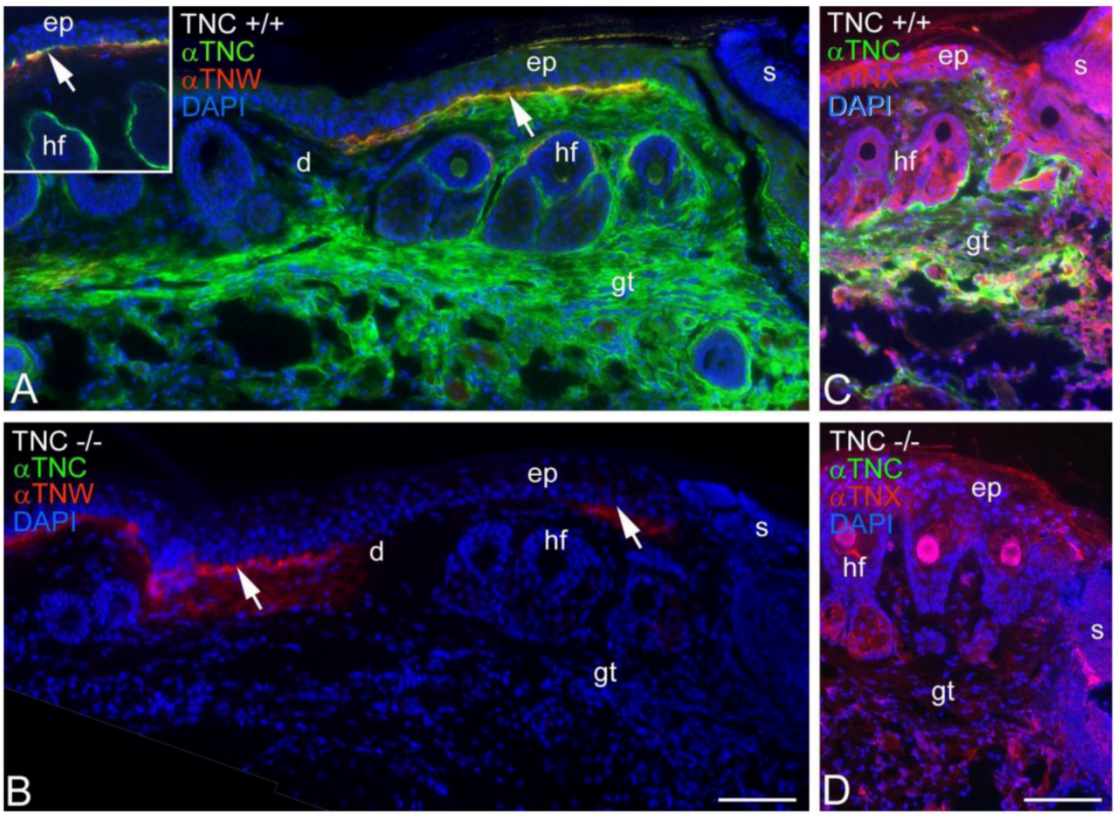


**Fig. 4.** Tenascin-C and tenascin-W expression in healing wounds was confirmed by immunohistochemistry (A, B). Three days following an incision in the skin of a tenascin-$C^{+/+}$ mouse tail, anti-tenascin-C (green) stains the early granulation tissue (gt) adjacent to the wound (A). Anti-tenascin-W (red) stains patches at the border of the epidermis (ep) and dermis (d; arrow); patchy staining was seen both near and far from the scab (s) and appears to coincide with the fibrous septum than runs from the epidermis to deeper connective tissue. In an unwounded tail, tenascin-C immunoreactivity is limited to the dermal-epidermal junction and the capsule around hair follicles (hf; inset). In a similar wound in the skin of a tenascin-$C^{-/-}$ mouse the anti-tenascin-W staining is unchanged (B). The expression of tenascin-X (red) in the tail wounds was also studied by immunohistochemistry (C, D). Tenascin-X is found in the epidermis (e), deep dermis and in structures associated with the hair follicles (hf), but it is not upregulated in the early granulation tissue (gt) of wild type or tenascin-C knockout mouse wounds. Scale bar = 100μm.

Our results show that tenascin-W shares the adhesion modulating properties of other members of the tenascin gene family. The molecular mechanisms underlying these properties remain unknown. Future studies should be directed to determining if tenascin-W can bind to fibronectin, and if it does, if it binds to the same region as tenascin-C. In addition, putative integrin binding domains have been identified in tenascin-W, and the integrins that recognize these sites and the signaling pathways mediated by these integrins need to be identified. Initial studies point to a conserved KGD motif playing a role in regulating the anti-adhesive properties of tenascin-W (17) and α8 integrins promoting tenascin-W mediated motility, at least in tenascin-W from mouse (14).

## Acknowledgements

We thank Jean-Francois Spetz for help with the skin wound models. This work was supported by the Novartis Research Foundation and Swiss National Science Foundation grants to R.C.E. and M.C. (31003A-120235/31003A-135584) and to J.C.S. (3100A0-109874/310030-125397), and by grants to G.O. from the Institut National du Cancer, Institut National de la Santé et de la Recherche Médicale, Association pour la Recherche contre le Cancer, Agence National de la recherche and the Hospital Hautepierre.

## Conflict of Interests

The authors have declared that no conflict of interest exists.

## References


1. Chiquet-Ehrismann R, Tucker RP. Tenascins and the importance of adhesion modulation. In: Hynes RO and Yamada KM, eds. Extracellular Matrix Biology. Cold Spring Harb Perspect Biol; 2012. doi: 10.1101/cshperspect.a004960
2. Chiquet-Ehrismann R, Mackie EJ, Pearson CA, Sakakura T. Tenascin: an extracellular matrix protein involved in tissue interactions during fetal development and oncogenesis. Cell 1986; 47(1): 131-139.
3. Chiquet-Ehrismann R, Kalla P, Pearson CA, Beck K, Chiquet M. Tenascin interferes with fibronectin action. Cell 1988; 53(3): 383-390.
4. Murphy-Ullrich JE, Lightner VA, Aukhil I, Yan YZ, Erickson HP, Hook M. Focal adhesion integrity is downregulated by the alternatively spliced domain of human tenascin. J Cell Biol 1991; 115(4): 1127-1136.
5. Fischer D, Tucker RP, Chiquet-Ehrismann R, Adams JC. Cell-adhesive responses to tenascin-C splice variants involve formation of fascin microspikes. Mol Biol Cell 1997; 8(10): 2055-2075.
6. Huang W, Chiquet-Ehrismann R, Moyano JV, Garcia-Pardo A, Orend G. Interference of tenascin-C with syndecan-4 binding to fibronectin blocks cell adhesion and stimulates tumor cell proliferation. Cancer Res 2001; 61(23): 8586-8594.
7. Midwood KS, Valenick LV, Hsia HC, Schwarzbauer JE. Coregulation of fibronectin signaling and matrix contraction by tenascin-C and syndecan-4. Mol Biol Cell 2004; 15(12): 5670-5677.
8. Pesheva P, Probstmeier R, Skubitz AP, McCarthy JB, Furcht LT, Schachner M. Tenascin-R (J1 160/180 inhibits fibronectin-mediated cell adhesion--functional relatedness to tenascin-C. J Cell Sci 1994; 107 (Pt 8): 2323-2333.
9. Angelov DN, Walther M, Streppel M, Guntinas-Lichius O, Neiss WF, Probstmeier R, Pesheva P. Tenascin-R is antiadhesive for activated microglia that induce downregulation of the protein after peripheral nerve injury: a new role in neuronal protection. J Neurosci 1998; 18(16): 6218-6229.
10. Tucker RP, Hagios C, Santiago A, Chiquet-Ehrismann R. Tenascin-Y is concentrated in adult nerve roots and has barrier properties in vitro. J Neurosci Res 2001; 66(3): 439-447.
11. Elefteriou F, Exposito JY, Garrone R, Lethias C. Cell adhesion to tenascin-X mapping of cell adhesion sites and identification of integrin receptors. Eur J Biochem 1999; 263(3): 840-848.
12. Fujie S, Maita H, Ariga H, Matsumoto K. Tenascin-X induces cell detachment through p38 mitogen-activated protein kinase activation. Biol Pharm Bull 2009; 32(10): 1795-1799.
13. Scherberich A, Tucker RP, Samandari E, Brown-Luedi M, Martin D, Chiquet-Ehrismann R. Murine tenascin-W: a novel mammalian tenascin expressed in kidney and at sites of bone and smooth muscle development. J Cell Sci 2004; 117(Pt 4): 571-581.
14. Scherberich A, Tucker RP, Degen M, Brown-Luedi M, Andres AC, Chiquet-Ehrismann R. Tenascin-W is found in malignant mammary tumors, promotes alpha8 integrin-dependent motility and requires p38MAPK activity for BMP-2 and TNF-alpha induced expression in vitro. Oncogene 2005; 24(9): 1525-1532.
15. Meloty-Kapella CV, Degen M, Chiquet-Ehrismann R, Tucker RP. Avian tenascin-W: expression in smooth muscle and bone, and effects on calvarial cell spreading and adhesion in vitro. Dev Dyn 2006; 235(6): 1532-1542.
16. Degen M, Brellier F, Kain R, Ruiz C, Terracciano L, Orend G, Chiquet-Ehrismann R. Tenascin-W is a novel marker for activated tumor stroma in low-grade human breast cancer and influences cell behavior. Cancer Res 2007; 67(19): 9169-9179.
17. Meloty-Kapella CV, Degen M, Chiquet-Ehrismann R, Tucker RP. Effects of tenascin-W on osteoblasts in vitro. Cell Tissue Res 2008; 334(3): 445-455.
18. Saga Y, Yagi T, Ikawa Y, Sakakura T, Aizawa S. Mice develop normally without tenascin. Genes Dev 1992; 6(10): 1821-1831.
19. Mackie EJ, Halfter W, Liverani D. Induction of tenascin in healing wounds. J Cell Biol 1988; 107(6 Pt 2): 2757-2767.
20. Forsberg E, Hirsch E, Frohlich L, Meyer M, Ekblom P, Aszodi A, Werner S, Fassler R. Skin wounds and severed nerves heal normally in mice lacking tenascin-C. Proc Natl Acad Sci U S A 1996; 93(13): 6594-6599.
21. Aufderheide E, Ekblom P. Tenascin during gut development: appearance in the mesenchyme, shift in molecular forms, and dependence on epithelial-mesenchymal interactions. J Cell Biol 1988;107(6 Pt 1): 2341-2349.
22. Matsumoto K, Saga Y, Ikemura T, Sakakura T, Chiquet-Ehrismann R. The distribution of tenascin-X is distinct and often reciprocal to that of tenascin-C. J Cell Biol 1994; 125(2):483-493.
23. Gordon H, Hall ZW. Glycosaminoglycan variants in the C2 muscle cell line. Dev Biol 1989; 135(1): 1-11.
24. Brellier F, Hostettler K, Hotz HR, Ozcakir C, Çöloğlu SA, Togbe D, Ryffel B, Roth M, Chiquet-Ehrismann R. Tenascin-C triggers fibrin accumulation by downregulation of tissue plasminogen activator. FEBS Lett 2011; 585(6): 913-920.
25. Kretz M, Euwens C, Hombach S, Eckardt D, Teubner B, Traub O, Willecke K, Ott T. Altered connexin expression and wound healing in the epidermis of connexin-deficient mice. J Cell Sci 2003; 116(Pt 16): 3443-3452.
26. Tucker RP, Drabikowski K, Hess JF, Ferralli J, Chiquet-Ehrismann R, Adams JC. Phylogenetic analysis of the tenascin gene family: evidence of origin early in the chordate lineage. BMC Evol Biol 2006; 6: 60.
27. Pearson CA, Pearson D, Shibahara S, Hofsteenge J, Chiquet-Ehrismann R. Tenascin: cDNA cloning and induction by TGF-beta. EMBO J 1988; 7(10): 2977-2982.

# III.2 Submitted manuscript

## III.2.1 – Tenascin-W is a better cancer biomarker than tenascin-C for most human solid tumors

Florence Brellier[1,*], Enrico Martina[1,2,*], Martin Degen[1,2,#], Nathalie Heuzé-Vourc'h[3], Agnès Petit[3], Thomas Kryza[3], Yves Courty[3], Luigi Terracciano[4], Christian Ruiz[4] and Ruth Chiquet-Ehrismann[1,2]

[1]Friedrich Miescher Institute for Biomedical Research, Novartis Research Foundation, Basel, Switzerland

[2]University of Basel, Faculty of Sciences, Basel, Switzerland

[3]INSERM, Unit 618, Proteases and Pulmonary Vectorization, Université François Rabelais, Tours, France

[4]University Hospital Basel, Institute of Pathology, Basel, Switzerland

[*] Equal contribution

[#] Present address: Department of Dermatology, Brigham and Women's Hospital, Harvard Skin Disease Research Center, Harvard Medical School, Boston, MA, USA

My contribution:
I have developed the image analysis protocol adopted in the present work, and I used it in the quantitation of the tenascin-W and tenascin-C staining in the samples. I also performed the experiments of double immunofluorescence staining that confirmed the co-localization of tenascin-W and blood vessels in samples from different tumor types. Finally, I prepared the figures for the manuscript.

Submitted to *Molecular Cancer*

## Abstract

### *Background*

Tenascins are large glycoproteins found in the extracellular matrix of many embryonic and adult tissues. Tenascin-C is a well-studied biomarker known for its high overexpression in the stroma of most solid cancers. Tenascin-W, the least described member of the family, is highly expressed in the stroma of colon and breast tumors and in gliomas, but not in the corresponding normal tissues. Other solid tumors have not been analyzed. The present study was undertaken to determine whether tenascin-W could serve as a general cancer-specific extracellular matrix protein in a broad range of solid tumors.

### *Methods*

We analyzed the expression of tenascin-W and tenascin-C by immunoblotting and by immunohistochemistry on multiple frozen tissue microarrays of carcinomas of the pancreas, kidney, lung as well as melanomas and compared it to healthy tissues.

### *Results*

From all healthy adult organs tested, only liver and spleen showed detectable levels of tenascin-W, suggesting that tenascin-W is absent from most human adult organs in normal, non-pathological conditions. In contrast, tenascin-W was detectable in the majority of melanomas and their metastases, as well as in pancreas, kidney, and lung carcinomas. Comparing lung tumor samples and matching control tissues for each patient revealed a clear overexpression of tenascin-W in tumor tissues. Although the number of samples examined is too small to draw statistically significant conclusions, there seems to be a tendency for increased tenascin-W expression in higher grade tumors. Interestingly, in most tumor types, tenascin-W is also expressed in close proximity to blood vessels, as shown by CD31 co-staining of the samples.

### *Conclusions*

The present study extends the tumor biomarker potential of tenascin-W to most solid tumors and shows its accessibility from the blood stream for potential therapeutic strategies.

## Background

During recent years increasing evidence has emerged showing that the microenvironment plays a prominent role in determining tumor behavior [1-4]. Tumor progression is influenced and controlled by activation of nearby stromal cells, including fibroblasts, endothelial cells and macrophages. In their activated states, these cells modulate and reorganize the extracellular matrix and create a congenial microenvironment for the tumor cells. Accepting an active role of the microenvironment for tumor progression, it will be important to consider how the activated tumor stroma can be harnessed for clinical benefit. Extracellular matrix proteins specifically expressed in tumor stroma could thus represent promising predictive/diagnostic biomarkers or target molecules for therapeutics.

Tenascin-C and tenascin-W are two members of the tenascin family of large extracellular matrix glycoproteins whose functions are associated with cellular mechanisms such as adhesion modulation, motility, proliferation and differentiation [5]. Both proteins share highest expression during embryonic development and reduced and very restricted expression in the adult organism [6]. Tenascin-C, the best-described family member, reappears during pathological conditions such as cancer, inflammation or wounds [7,8]. Soon after its initial identification, tenascin-C was proposed as a stromal marker in breast cancer [9]. Since then, many more studies have been performed and tenascin-C expression shows predictive value for local tumor recurrence and metastatic dissemination in many aggressive cancers (for reviews see [2,10,11]. Its cancer-specific expression has been exploited to make tenascin-C a promising target for different anti-cancer therapies, including the delivery of cytokines or radionuclides to the tumor using tenascin-C-specific monoclonal antibodies [12-14] or aptamers [15,16].

Similar physiological expression patterns as well as shared functions of tenascin-W with tenascin-C prompted us to investigate the presence of the newest tenascin family member, tenascin-W in different human cancers. Tenascin-W expression was detected in a large majority of human breast tumors, showing enrichment in low-grade compared to high-grade tumors [17]. In colorectal cancer, tenascin-W expression was restricted to the tumor-associated microenvironment, while the protein was not detectable in the corresponding healthy tissue [18]. In brain tumors, all glioma subtypes tested (oligodendroglioma, astrocytoma and glioblastoma) were

enriched in tenascin-W in comparison to healthy control brain tissues [19]. Noticeably, in all glioblastoma samples analyzed the localization of tenascin-W was perivascular [19].

Encouraged by the highly tumor-specific expression of tenascin-W in breast, colon, and brain tumors, we now extended our expression study to many more types of solid tumors. We show here, that tenascin-W expression displays an even higher specificity for cancer-related microenvironments than tenascin-C. Hence, tenascin-W represents a novel attractive cancer biomarker of broad potential for tumor detection, prediction and targeting approaches.

## Results

### *Tenascin-W is not detectable in most adult organs*

To compare tenascin-W and tenascin-C protein expression in normal healthy adult humans, we analyzed tissue extracts from ten different organs and analyzed their protein content on western-blots (Fig. 1A). Only in spleen and liver very faint bands for tenascin-W were observed. In agreement with our recent observations, we did not detect any tenascin-W in healthy human breast, colon and brain tissues [17-19]. Furthermore, normal uterus, lung, heart, pancreas and kidney appeared devoid of tenascin-W, too. In contrast, tenascin-C was detectable in all organs tested, except for normal breast and heart tissues. As has been described earlier [17-20], we detected different tenascin-C isoforms in our immunoblot analysis of normal human tissues, although in pancreas, kidney, and colon only the lower tenascin-C isoform was observed.

Our earlier studies showed tenascin-W overexpression in human breast, colon, as well as brain tumors [17-19]. To obtain a more complete neoplasia-associated expression profile of tenascin-W, we tested here whether tenascin-W enrichment also can be found in solid tumors originating from other organs.

### *Tenascin-W is overexpressed in pancreas carcinomas*

Pancreas carcinoma extracts from nine different patients were analyzed by western-blotting for their expression of tenascin-W and tenascin-C (Fig. 1B). In contrast to healthy pancreas tissue (Fig. 1A), most pancreas carcinomas (7/9) did express detectable amounts of tenascin-W. Among the seven tenascin-W positive tumors,

four contained very high levels of tenascin-W (patients # 1, 2, 5, and 6) and three samples displayed moderate levels (patients # 7-9). Tenascin-C was observed in most of the samples varying from barely detectable (patients # 1, 7-9) to intermediate (patients # 4, 5) and to high levels (patient # 2, 6). The levels of tenascin-W and tenascin-C did not correlate and in the sample from patient #1 with the highest tenascin-W level tenascin-C was barely detectable (Fig. 1B). While in normal pancreas tissue only a low molecular-weight isoform of tenascin-C was detectable (Fig. 1A), pancreas tumor tissues expressed additional high isoforms (Fig. 1B). So far we do not have any evidence for the existence of tenascin-W splice-variants (Fig.1)

***Tenascin-W is overexpressed in kidney tumors***

Tenascin-W and tenascin-C expression was analyzed by western-blotting in kidney carcinoma samples (Fig. 1C). Tenascin-W was detected in most cases (6/9): 2 out of 9 expressed very high levels of tenascin-W, 4 moderate levels and in 3 samples tenascin-W was not detectable. Tenascin-C was also observed in most samples (7/9), but again could not be correlated with tenascin-W expression.

In parallel, a frozen kidney tumor TMA (n=84) was stained by immunohistochemistry for expression of tenascin-W and tenascin-C. For each tumor sample, we quantified expression levels of both tenascins and classified them into the following 4 categories with respect to their tenascin expression: absent, low, moderate and high, as described in Materials and Methods (Fig. 2A,B). Although we could not detect tenascin-W by western-blot in healthy kidney tissue (Fig. 1A), immunohistochemical analysis revealed slight, but clearly visible expression of tenascin-W in most of the control kidney samples (see representative image in Fig. 2C). As can be seen in the pie chart more than half of the tumors (56%) expressed easily detectable expression of tenascin-W (*i.e.* moderate or high) while for tenascin-C this was the case for 92% of all kidney tumors on the TMA (Fig. 3A). Interestingly, tenascin-W was never in a higher expression category than tenascin-C as no number appears in the upper right “triangle” of the table in Fig. 2B. Using a numerical score for each category (see Materials and methods) the average scores for each tumor type was calculated. The average scores for the levels of tenascin-W and tenascin-C of the 70 clear cell carcinomas were 1.7±0.10 and 2.69±0.07

respectively, for the 6 papillary carcinomas 1.33±0.33 and 2.67±0.33, for the 6 chromophobe carcinomas 1.17±0.31 and 2±0.26 and for the 2 oncocytoma 1 and 1. This suggests that the tenascin levels may correlate with the tumor type. However, more samples would be necessary to strictly proof such a correlation.

***Tenascin-W is overexpressed in melanomas***

A frozen TMA containing 34 melanoma samples including primary tumors and metastases was stained by immunohistochemistry for tenascin-W and tenascin-C. Each individual tumor staining was quantified and categorized as described above (Fig. 3). Representative pictures for each tenascin-W group for each type of sample are shown in parallel to the matching tenascin-C stainings of the same tumor patient. Fig.3A shows stainings of primary tumors (PT), Fig. 3B metastases (MET) and Fig. 3C lymph node metastases (LN-MET). These tumor samples can be compared to the healthy skin tissue shown in Fig. 3E. Tenascin-W was not detectable in any normal skin sample whereas tenascin-C was observed in the dermis of three out of six samples (Fig. 3D), just below the basement membrane underlying the basal epidermal cell layer, as has been described previously [21]. A summary of all stainings is presented in a table (Fig. 3D). It shows that 60% (3 out of 5) of primary melanomas (PT) had moderate or high expression of tenascin-W, while tenascin-C was detectable in all of the primary tumor samples with a staining classified at least as moderate. In samples obtained from metastasis from diverse locations (i.e. spleen, lung, skin), tenascin-W had moderate staining in 25% (2 out of 8) of the samples, while tenascin-C is strongly expressed in 87% (7 out of 8) of samples. Similar proportions were observed in samples of lymph node metastasis: 38% of samples (8 out of 21) showed moderate or high tenascin-W, while 71% (15 out of 21) of the samples displayed at least moderate tenascin-C staining. Similar to the kidney TMA analysis, tenascin-W expression was never found in a higher expression category than tenascin-C. It is noteworthy that the only two samples in which tenascin-W is classified in the highest category of expression are both lymph node metastases.

***Tenascin-W is overexpressed in lung tumors***

In our analysis of lung tumors we stained a total of 95 tumor samples for the presence of tenascin-W and tenascin-C. Immunohistochemical analysis showed that tenascin-W was detectable in all 95 tumor samples (Fig. 4). For 21 of these samples we were able to analyze matching adjacent normal lung parenchyma that had been biopsied at least 3cm away from the edge of the tumor. These corresponding healthy tissues did not display any detectable tenascin-W expression demonstrating that tenascin-W expression was restricted to tumor associated stroma. In contrast, tenascin-C was also present in the normal lung tissue adjacent to the tumors. In many of the lung tumor samples, we could observe a very typical pattern of tenascin-W expression: a fibrous staining (parallel lines forming bundles) surrounding nests of tumor cells (Fig. 4C, #9297). This suggests that tenascin-W is mainly expressed by stromal cells surrounding the carcinoma cells. Quantification of the stained area of tumors from an extended cohort of patients (n=95) revealed that tenascin-W expression was never completely absent in any of the tumors, a feature shared by tenascin-C (Fig. 4A,B). 65% of the tumor samples had at least moderate tenascin-W expression while for tenascin-C this was the case for 92% of the samples. With the exception of 5 cases, tenascin-C was in the same or higher expression category as tenascin-W (Fig. 4B). However, since tenascin-C expression levels in control lung tissues have been much higher than tenascin-W levels, tenascin-W seems to be much more tumor-specific than tenascin-C in the case of the lung. Information about the stage of the tumor was available for 69 of the 95 samples included in the present study. Interestingly, the average level of tenascin-W seems to correlate with tumor grade: the two grade I tumors both have a tenascin-W score of 1 (tenascin-C score is 2); grade II tumors (n=19) have an average tenascin-W score of 1.74±0.15 (tenascin-C: 2.47±0.18); tumors with grade intermediate between II and III (n=6) have an average score of 1.83±0.30 (tenascin-C: 2.33±0.33); grade III tumors (n=27) have average score of 2.18±0.17 (tenascin-C: 2.55±0.11); finally, the average tenascin-W score of grade IV tumors (n=15) is 2.07±0.23 (tenascin-C: 2.6±0.16). Although the number of samples examined is too small to draw statistically significant conclusions, there seems to be a tendency for increased tenascin-W expression in higher grade tumors.

***Tenascin-W is expressed around blood vessels***

Our previous study on tenascin-W expression in brain tumors showed for the first time that tenascin-W is expressed around blood vessels of gliomas [19]. Here, we investigated whether this observation holds true as well for tumors originating from other organs. For this purpose, we co-stained lung and kidney tumors for tenascin-W and CD-31, an established blood vessel marker (Fig. 5). In most of the tumor samples a prominent co-localization between tenascin-W and blood vessels (CD31 positive) was observed. These results confirmed our earlier study in brain tumors and suggest that tenascin-W is often expressed adjacent to blood vessels, independently of vessel size. Tenascin-W co-localization with blood vessels was also observed in additional analyses of colon, breast, ovarian and prostate tumors (data not shown). Thus, the presence of tenascin-W around tumor blood vessels seems to be widespread.

## Discussion

Recent studies on tenascin-W have identified this protein as a candidate biomarker for breast tumors [17], colorectal tumors [18] as well as gliomas [19]. In addition to these tumor sites, we report in the present study that tenascin-W is also prominently expressed in melanomas, pancreas, kidney and lung carcinoma samples. Importantly, we were not able to detect it in the normal corresponding organs, except for a slight presence in normal kidney. The tumor-specific expression was especially striking for the lung for which we had clinical material available to compare 21 tumors with matching healthy tissue fragments of the same patient. All of these 21 tumor/non-tumor pairs revealed a specific tumor-restricted tenascin-W staining, whereas the non-tumor samples were all negative. Therefore, tenascin-W might be a diagnostic marker for lung cancer and its expression seems to increase with tumor grade. Tenascin-W was also expressed in the majority of kidney tumors tested. Although western-blot analysis did not reveal the presence of tenascin-W in a kidney control tissue extract, we could observe a slight tenascin-W staining by immunohistochemistry in all 10 control kidney tissues analyzed. This result is in agreement with our previous observation that tenascin-W can be found in the kidney of adult mice [22]. Tenascin-W and tenascin-C levels appeared in average to be higher in clear cell carcinomas than in papillary or chromophobe renal cell

carcinomas and lowest in oncocytoma, suggesting a correlation with severity of the disease. In addition, we could also observe overexpression of tenascin-W in ovarian cancer samples and in prostate tumors (data not shown). Our general observation that tenascin-W is overexpressed in the stroma surrounding many tumors, but absent in most corresponding control tissues, qualifies tenascin-W as a tumor biomarker. This is less the case for tenascin-C, as tenascin-C overexpression has been correlated with various conditions other than cancers, such as inflammation, infection, asthma, fibrosis and wound healing (for reviews see [7,8]).

So far, tenascin-W overexpression has been exclusively described in the context of tumorigenesis and osteogenesis [6], which suggests that it might be a more specific tumor marker than tenascin-C. In the case of tenascin-C there remains the possibility that certain splice variants could be more tumor-specific than others and thereby provide a good target as well [23,24]. This is also the case for another ubiquitous extracellular matrix protein, namely fibronectin, which was shown to have cancer-specific splice variants which can be used as targets for antibody-mediated therapy in human patients [25,26]. It remains to be seen whether tenascin-W is elevated in sera of patients suffering from solid tumors other than breast and colon, where elevated tenascin-W serum levels have been described [18]. The same might be the case for pancreas, kidney or lung tumor patients as these tumors show strong tenascin-W staining *in situ*.

Here we have found that tenascin-W is expressed in close vicinity of blood vessels in a wide range of tumors including kidney, colon, breast, ovary and prostate tumors. In another study we have found that tenascin-W acts as a pro-angiogenic factor *in vitro* [19]. Therefore, we can speculate that *in vivo* tenascin-W could act on tumor endothelial cells, influencing their migration and thus contributing to the expansion of the endothelial network. What triggers tenascin-W expression in the tumor stroma and more particularly next to the blood vessels remains to be established, but it likely involves complex tumor-microenvironment interactions.

In several tumors, there is now compelling evidence that the capacity for a tumor to grow and proliferate lies in a small fraction of cells, called cancer stem cells (CSC) or cancer initiating cells. Similar to normal stem cells, CSC have the ability to self-renew and to differentiate into a variety of proliferating cells that make up the tumor mass. It can be speculated that maintenance of CSCs depends upon a specific

stem cell niche microenvironment that protects CSCs from therapeutics. Therefore, targeting these microenvironments might result in more effective treatments of cancers. Interestingly, tenascin-C has been reported to maintain an ABCB5+ subpopulations of melanoma-initiating cells thereby promoting melanoma progression [27]. Moreover, for several cancers, cancer stem cell populations reside in perivascular niches as their preferred microenvironment [28-31]. Given the tumor-specific overexpression of tenascin-W and its perivascular staining pattern, one can speculate about a role for tenascin-W in maintaining CSC's and offering them a congenial niche.

The present study extends the potential of tenascin-W as biomarker to a large variety of solid tumors. Given both its specific expression in tumors compared to corresponding healthy tissues and its proximity to tumor blood vessels (making it easily accessible *via* the bloodstream) we propose tenascin-W as a good candidate for selective delivery of anticancer medicine.

## Methods

### *Tissue samples*

Protein extracts from uterus, spleen, liver, lung, cerebrum and heart control tissues were from autoptic material obtained from the Institute of Pathology from the University Hospital of Basel, Switzerland. Pancreas, kidney and colon control whole tissue homogenates were purchased from BioCat GmbH (Heidelberg, Germany). Protein extracts from breast, pancreas and kidney tumors were obtained from the Institute of Pathology of the University Hospital of Basel, Switzerland. All extracts were prepared as described before [17].

Melanomas, kidney and lung tumors used for immunohistochemistry were part of frozen tissue microarrays (TMA) obtained from the Institute of Pathology of the University Hospital of Basel, Switzerland. References for their construction can be found elsewhere [17]. The melanoma TMA was constructed from frozen tissue samples of 34 malignant melanomas (5 primary tumors, 8 metastases from different organs and 21 lymph node metastases) and 6 control healthy cutaneous tissue samples. The kidney TMA was constructed from frozen tissue samples of 84 kidney tumors (70 clear cell renal carcinomas, 6 papillary renal carcinomas, 6 chromophobe renal cell carcinomas and 2 oncocytoma) and 10 healthy control

kidney tissues. The lung TMA was constructed from frozen tissue samples of 74 lung tumors (40 squamous carcinomas, 19 adenocarcinomas and 15 undifferentiated carcinomas). Additional lung tumor samples were obtained from the University Hospital of Tours, France. The latter collection contained frozen tissues from matched samples of tumor and adjacent non-tumor tissue. They were obtained from 21 patients who had undergone lung cancer resection as their primary therapy without preoperative radiation or chemotherapy. These non-small cell lung cancers consisted of 10 adenocarcinomas, 10 squamous carcinomas and 1 undifferentiated carcinoma. The non-malignant tissue samples were taken from sites at least 3 cm away from the edge of the tumor. The histological diagnosis was determined by two pathologists.

Studies were performed in compliance with the Declaration of Helsinki and in accordance with the guidelines of the ethical committee of the University of Basel, Switzerland or with French bioethical regulations.

***Western blot analysis***

Tissue samples were thawed on ice, minced and homogenized in RIPA lysis buffer. After determination of protein concentration by a Bio-Rad Protein assay, samples were separated by SDS-PAGE (6%) and electroblotted to polyvinylidene difluoride membranes. Equal loading and transfer of protein was confirmed by staining the membranes with amidoblack. After a blocking step in 5% milk powder in Tris-buffered saline (TBS), membranes were incubated overnight with the rabbit polyclonal antiserum pAb (3F/4) raised against human tenascin-W (1:750), the mouse monoclonal antibody B28-13 raised against human tenascin-C (1:100), the V-9131 mouse monoclonal antibody against vinculin (1:2000; Sigma). After incubation for 1 hour with anti-mouse IgG or anti-rabbit IgG coupled to horseradish peroxidase, blots were developed using Super Signal (Pierce) for tenascin-C and tenascin-W and ECL reagent (GE Healthcare) for vinculin followed by exposure to Kodak BioMax MR Films.

***Immunostaining and quantification***

Chromogenic and fluorescent detections were performed on 9 µm-thick cryosections using the Discovery XT automated stainer (Ventana Medical Systems) with standard

and customized procedures, respectively. Frozen tissue slides were dried for 1 hr at room temperature, fixed for 10 min at 4°C in cold acetone and then introduced into the automate. For chromogenic stainings, slides were incubated for 1 hr at 37°C with the mouse monoclonal 56O antibody raised against human tenascin-W (1:1000) [18] or the B28-13 anti-tenascin-C antibody (1:1000). They were then treated for 32 min at 37°C with a biotinylated anti-mouse secondary antibody (1:200; Jackson Immunoresearch laboratories 715-065-150) and developed with DAB Map detection kit (Ventana). Counterstainings were obtained with hematoxylin and bluing reagent (Ventana). For immunofluorescent stainings, slides were incubated for 1 hour at 37°C with anti-tenascin-W mAb 56O (1:50), anti-tenascin-C mAb B28-13 (1:50) or anti-CD31 (1:200; M0823, DAKO). They were then treated for 32 min at 37°C with Alexa Fluor 647 donkey anti-mouse IgG and Alexa Fluor 488 goat anti-rabbit IgG secondary antibodies (1:200; Invitrogen A31571 and A11029, respectively), carefully rinsed by hand and mounted with prolong Gold reagent (Invitrogen). Pictures were either acquired with a Mirax Slidescanner (Zeiss AG, Zurich, Switzerland) using a 20×/0.5 lens (0.2 µm/pixel) and converted into standard TIFF format or with a Nikon Eclipse 80i microscope equipped with a Leica DFC420 color camera. For quantification, the area of the section stained by tenascin-W or tenascin-C was measured using ImageJ by setting the color threshold as follows: hue 0-40, saturation 50-255, luminosity 0-200. The resulting area was divided by the total area of the section to obtain a percentage. The samples were then classified in four categories according to the amount of staining: 0%, no staining; 1%-10%, low; 11%-40%, moderate; >40%, high. In order to compare tumor type or grade with the tenascin stainings a numerical score was assigned to each category (no staining=0, low=1, moderate=2, and high=3) and the average scores for each tumor type/grade was calculated.

**Competing interests**

The authors declare that they have no competing interests.

**Authors' contributions**

FB performed immunostainings of kidney, lung and melanoma TMAs and drafted the manuscript. EM performed the immunofluorescence stainings, quantified all

immunostainings, performed the statistical analyses and made the figures. MD performed the immunoblots and contributed to the writing. NHV, AP, TK, YC collected, classified and stained the lung cancer tissues and the normal control tissues of the same patients. CR and LT provided the kidney, lung and melanoma frozen TMAs and classified the tumor and patient data. RCE conceived of the study and participated in its design and coordination and helped to write the manuscript.

**Acknowledgments**

We would like to thank Sandrine Bichet from the Histology Facility of the FMI for her help with immunohistochemistry. This work was funded by the Institut National de la Santé et de la Recherche Médicale, Institut National du Cancer (grant MatriGo, France) and the Région Centre (KalliCaP) as well as by the Krebsliga beider Basel and the Swiss National Science Foundation (3100A0-120235 and 31003A-135584 to R.C.E.)

**References**

[1] Friedl P, Alexander S: Cancer invasion and the microenvironment: plasticity and reciprocity. *Cell* 2011, 147:992-1009.
[2] Brellier F, Chiquet-Ehrismann R: How do tenascins influence the birth and life of a malignant cell? *J Cell Mol Med* 2012, 16:32-40.
[3] Hanahan D, Weinberg RA: Hallmarks of cancer: the next generation. *Cell* 2011, 144:646-674.
[4] Bissell mj, Hines WC: Why don't we get more cancer? A proposed role of the microenvironment in restraining cancer progression. *Nat Med* 2011, 17: 320-329.
[5] Chiquet-Ehrismann R, Tucker RP: Tenascins and the importance of adhesion modulation. *Cold Spring Harb Perspect Biol* 2011, 3:a004960.
[6] Martina e, Chiquet-Ehrismann R, Brellier F: Tenascin-W: an extracellular matrix protein associated with osteogenesis and cancer. *Int J Biochem Cell Biol* 2010, 42: 1412-1415.
[7] Chiquet-Ehrismann R, Chiquet M: Tenascins: regulation and putative functions during pathological stress. *J Pathol* 2003, 200:488-499.
[8] Midwood KS, Orend G: The role of tenascin-C in tissue injury and tumorigenesis. *J Cell Commun Signal* 2009, 3:287-310.
[9] Mackie EJ, Chiquet-Ehrismann R, Pearson CA, Inaguma Y, Taya K, Kawarada Y, Sakakura T: Tenascin is a stromal marker for epithelial malignancy in the mammary gland. *Proc Natl Acad Sci U S A* 1987, 84:4621-4625.
[10] Orend G, Chiquet-Ehrismann R: Tenascin-C induced signaling in cancer. *Cancer Lett* 2006, 244:143-163.
[11] Midwood KS, Hussenet T, Langlois B, Orend G: Advances in tenascin-C biology. Cellular and molecular life sciences. *CMLS* 2011, 68:3175-3199.

[12] Schliemann S, Wiedmer A, Pedretti M, Szczepanowski M, Klapper W, Neri D: Three clinical-stage tumor targeting antibodies reveal differential expression of oncofetal fibronectin and tenascin-C isoforms in human lymphoma. *Leuk Res* 2009, 33:1718-1722.
[13] Steiner M, Neri D: Antibody-radionuclide conjugates for cancer therapy: historical considerations and new trends. *Clin Cancer Res* 2011, 17:6406-6416.
[14] Reardon DA, Zalutsky MR, Bigner DD: Anti-tenascin-C monoclonal antibody radioimmunotherapy for malignant glioma patients. *Expert Rev Anticancer Ther* 2007, 7:675-687.
[15] H.Y. Ko, K.J. Choi, C.H. Lee, S. Kim, A multimodal nanoparticle-based cancer imaging probe simultaneously targeting nucleolin, integrin alphavbeta3 and tenascin-C proteins. *Biomaterials* 2011, 32:1130-1138.
[16] Hicke BJ, Stephens AW, Gould T, Chang YF, Lynott CK, Heil J, Borkowski S, Hilger CS, Cook G, Warren S, Schmidt PG: Tumor targeting by an aptamer. *J Nuclear Med* 2006, 47:668-678.
[17] Degen M, Brellier F, Kain R, Ruiz C, Terracciano L, Orend G, Chiquet-Ehrismann R: Tenascin-W is a novel marker for activated tumor stroma in low-grade human breast cancer and influences cell behavior. *Cancer Res* 2007, 67:9169-9179.
[18] Degen M, Brellier F, Schenk S, Driscoll R, Zaman K, Stupp R, Tornillo L, Terracciano L, Chiquet-Ehrismann R, Ruegg C, Seelentag W: Tenascin-W, a new marker of cancer stroma, is elevated in sera of colon and breast cancer patients. *Int J Cancer* 2008, 122:2454-2461.
[19] Martina E, Degen M, Ruegg C, Merlo A, Lino MM, Chiquet-Ehrismann R, Brellier F: Tenascin-W is a specific marker of glioma-associated blood vessels and stimulates angiogenesis in vitro. *FASEB J* 2010, 24:778-787.
[20] Leprini A, Querze G, Zardi L: Tenascin isoforms: possible targets for diagnosis and therapy of cancer and mechanisms regulating their expression. *Perspect Dev Neurobiol* 1994, 2:117-123.
[21] Schenk S, Bruckner-Tuderman L, Chiquet-Ehrismann R: Dermo-epidermal separation is associated with induced tenascin expression in human skin. *Br J Dermatol* 1995, 133:13-22.
[22] Scherberich A, Tucker RP, Samandari E, Brown-Luedi M, Martin D, Chiquet-Ehrismann R: Murine tenascin-W: a novel mammalian tenascin expressed in kidney and at sites of bone and smooth muscle development. *J Cell Sci* 2004, 117:571-581.
[23] Guttery DS, Shaw JA, Lloyd K, Pringle JH, Walker RA: Expression of tenascin-C and its isoforms in the breast. *Cancer Metastasis Rev* (2010) 29:595-606.
[24] Brack SS, Silacci M, Birchler M, Neri D: Tumor-targeting properties of novel antibodies specific to the large isoform of tenascin-C. *Clin Cancer Res* 2006, 12:3200-3208.
[25] Eigentler TK, Weide B, de Braud F, Spitaleri G, Romanini A, Pflugfelder A, Gonzalez-Iglesias R, Tasciotti A, Giovannoni L, Schwager K, Lovato V, Kaspar M, Trachsel E, Menssen HD, Neri D, Garbe C: A Dose-Escalation and Signal-Generating Study of the Immunocytokine L19-IL2 in Combination with Dacarbazine for the Therapy of Patients with Metastatic Melanoma. *Clin Cancer Res* 2011, 17:7732-7742.

[26] Johannsen M, Spitaleri G, Curigliano G, Roigas J, Weikert S, Kempkensteffen C, Roemer A, Kloeters C, Rogalla P, Pecher G, Miller K, Berndt A, Kosmehl H, Trachsel E, Kaspar M, Lovato V, Gonzalez-Iglesias R, Giovannoni L, Menssen HD, Neri D, de Braud F: The tumour-targeting human L19-IL2 immunocytokine: preclinical safety studies, phase I clinical trial in patients with solid tumours and expansion into patients with advanced renal cell carcinoma. *Eur J Cancer* 2010, 46:2926-2935.

[27] Fukunaga-Kalabis M, Martinez G, Nguyen TK, Kim D, Santiago-Walker A, Roesch A, Herlyn M: Tenascin-C promotes melanoma progression by maintaining the ABCB5-positive side population. *Oncogene* 2010, 29:6115-6124.

[28] Hjelmeland AB, Lathia JD, Sathornsumetee S, Rich JN: Twisted tango: brain tumor neurovascular interactions. *Nat Neurosci* (2011) 14:1375-1381.

[29] Beck B, Driessens G, Goossens S, Youssef KK, Kuchnio A, Caauwe A, Sotiropoulou PA, Loges S, Lapouge G, Candi A, Mascre G, Drogat B, Dekoninck S, Haigh JJ, Carmeliet P, Blanpain C: A vascular niche and a VEGF-Nrp1 loop regulate the initiation and stemness of skin tumours. *Nature* 2011, 478:399-403.

[30] Calabrese C, Poppleton H, Kocak M, Hogg TL, Fuller C, Hamner B, Oh EY, Gaber MW, Finklestein D, Allen M, Frank A, Bayazitov IT, Zakharenko SS, Gajjar A, Davidoff A, Gilbertson RJ: A perivascular niche for brain tumor stem cells. *Cancer Cell* 2007, 11:69-82.

[31] Charles N, Holland EC: The perivascular niche microenvironment in brain tumor progression. *Cell Cycle* 2010, 9:3012-3021.

## Figure legends

***Figure 1***

Immunoblot analysis of tenascin-W and tenascin-C protein expression in various healthy human adult organs (A), in pancreas carcinomas (B) and in kidney carcinomas (C). Blots were also probed for vinculin (VCL) to check equal loadings of protein samples. A: Note the presence of tenascin-C in all but one organ tested, whereas tenascin-W is undetectable in the majority of organs. The last two lanes contain 25ng of purified tenascin-C (TNC) or tenascin-W (TNW), respectively. B: Extracts from nine pancreas carcinomas were tested for their tenascin-W and tenascin-C levels. Note that tenascin-W is expressed in most of the pancreas carcinomas tested. C: Extracts of nine kidney carcinomas were tested for their tenascin-W and tenascin-C expression. Tenascin-W was observed in most of the kidney carcinomas tested.

***Figure 2***

Immunohistochemical analysis of kidney tumor samples. Eighty-four kidney tumor samples, spotted on a frozen TMA were stained for of tenascin-W and tenascin-C. The area of the section stained for tenascin-W or tenascin-C was quantified and the samples were classified in four categories (absent, low, moderate and high) as described in Materials and Methods. The percentage of tumors classified in each category for tenascin-W and tenascin-C is shown as pie charts (A). A double-entry table details how many tumors show each combination of tenascin-W/tenascin-C expression (B). Top panel in C shows normal kidney tissues stained for tenascin-W (left) and tenascin-C (right). Representative pictures of tumors of each category are shown for tenascin-W (C, left panel) with the corresponding tumor area stained for tenascin-C in parallel (C, right panel). Scale bars = 200 μm.

***Figure 3***

Immunohistochemical analysis of malignant melanoma samples. Thirty-four melanoma tissues from a frozen TMA were stained for their expression of tenascin-W and tenascin-C. The area of the section stained for tenascin-W or tenascin-C was quantified and the samples were classified as in Figure 2. Representative pictures of each tumor type are grouped in different panels: A) primary tumors (PT), B)

metastases (MET), C) lymph node metastases (LN-MET). From top to bottom, pictures in the left column of each panel represent increasing scores of tenascin-W from absent, low, moderate to high (only in panel C) with the corresponding tumor stained for tenascin-C in the right column of each panel. Panel E shows normal skin tissue stained for tenascin-W (left) and tenascin-C (right). Scale bars = 200 μm. Table D summarizes the distribution of the scores for each tenascin in the different groups.

***Figure 4***

Immunohistochemical analysis of lung tumor samples. Ninety-five lung tumor sections were stained for their expression of tenascin-C and tenascin-W and classified as described in Figure 2. The percentage of tumors classified in each category for tenascin-C and tenascin-W is shown as pie charts (A). A double-entry table details how many tumors show each combination of tenascin-W/tenascin-C expression (B). Twenty-one pairs of matching lung tumor/control lung tissue samples were stained for their expression of tenascin-W and tenascin-C. Representative stainings are shown: sample #5162 is from an adenocarcinoma, #9297 is from a squamous carcinoma and #4713 is from an undifferentiated carcinoma (C). Scale bars = 200 μm.

***Figure 5***

Double immunofluorescence staining of tenascin-W and CD31 in kidney tumors (upper panel) and lung tumors (lower panels). Tumor cryosections were used for fluorescent detection of tenascin-W (red), CD31 (green) and DAPI (blue). Each row represents a different tumor sample. Scale bars = 50 μm.

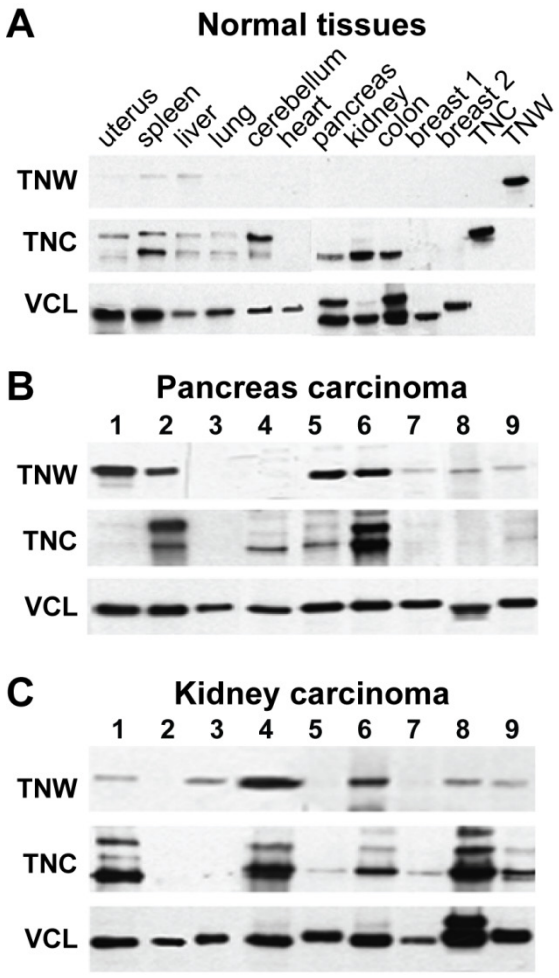
A
Normal tissues
uterus
spleen
liver
lung
cerebellum
heart
pancreas
kidney
colon
breast 1
breast 2
TNC
TNW
TNW
TNC
VCL
B
Pancreas carcinoma
1 2 3 4 5 6 7 8 9
TNW
TNC
VCL
C
Kidney carcinoma
1 2 3 4 5 6 7 8 9
TNW
TNC
VCL

**Figure 1**

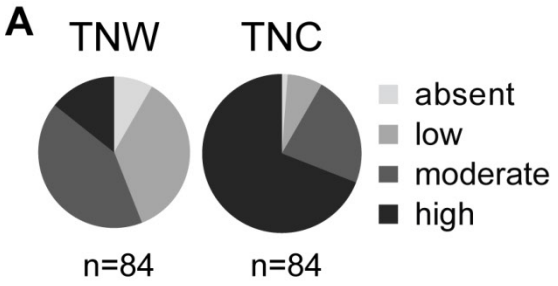


B

| TNC \ TNW (n=84) | absent | low | moderate | high | |
|---|---|---|---|---|---|
| absent | 1 | 0 | 0 | 0 | 1 |
| low | 2 | 4 | 0 | 0 | 6 |
| moderate | 3 | 9 | 7 | 0 | 19 |
| high | 1 | 17 | 28 | 12 | 58 |
| | 7 | 30 | 35 | 12 | |

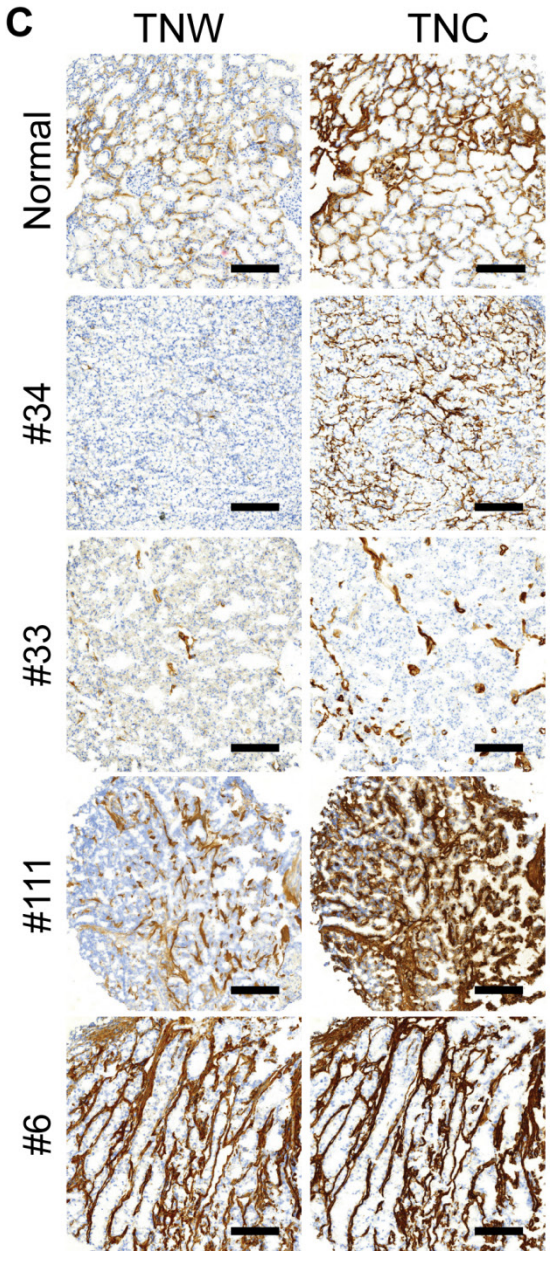


**Figure 2**

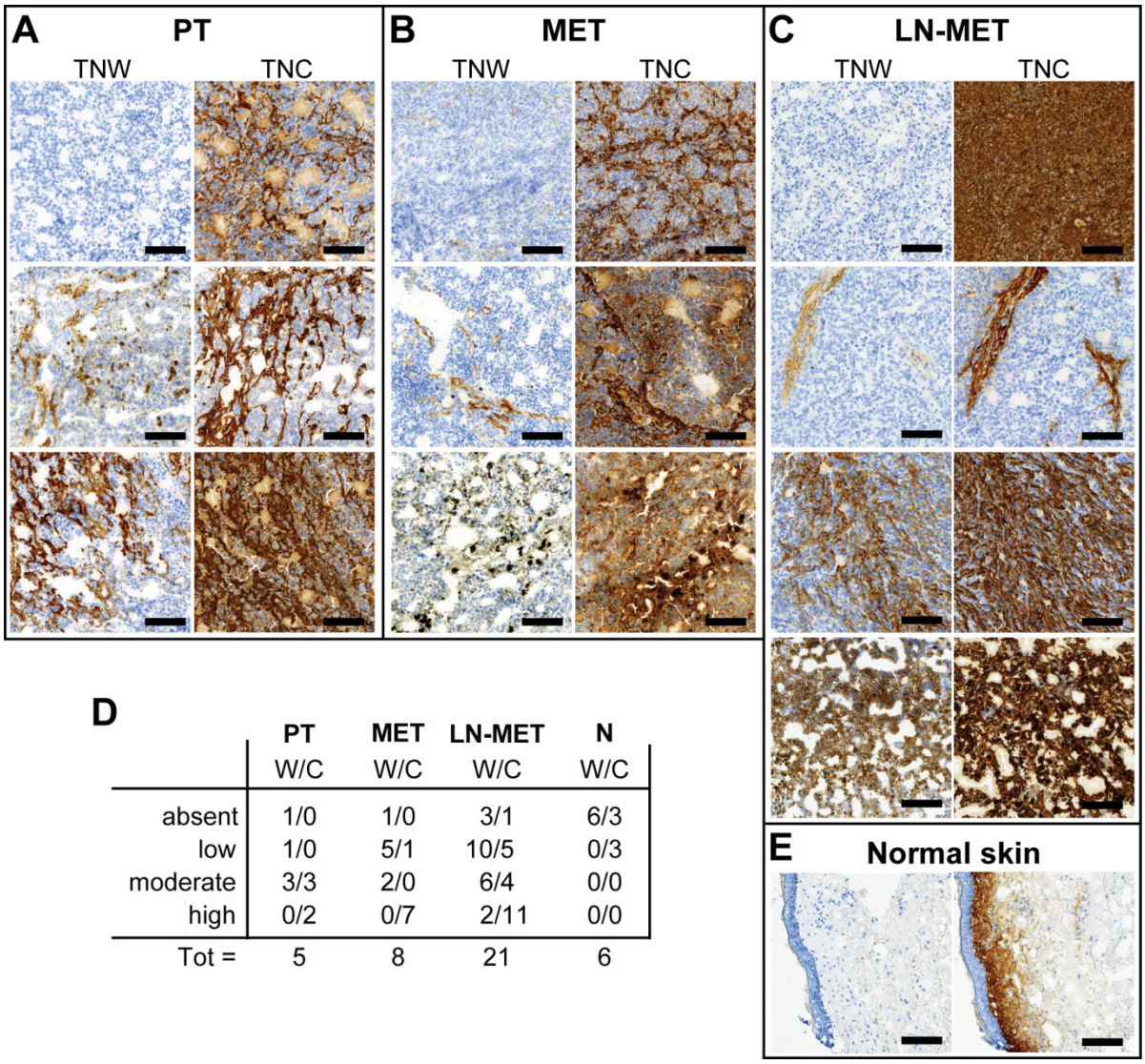


D

| | PT W/C | MET W/C | LN-MET W/C | N W/C |
|---|---|---|---|---|
| absent | 1/0 | 1/0 | 3/1 | 6/3 |
| low | 1/0 | 5/1 | 10/5 | 0/3 |
| moderate | 3/3 | 2/0 | 6/4 | 0/0 |
| high | 0/2 | 0/7 | 2/11 | 0/0 |
| Tot = | 5 | 8 | 21 | 6 |

**Figure 3**

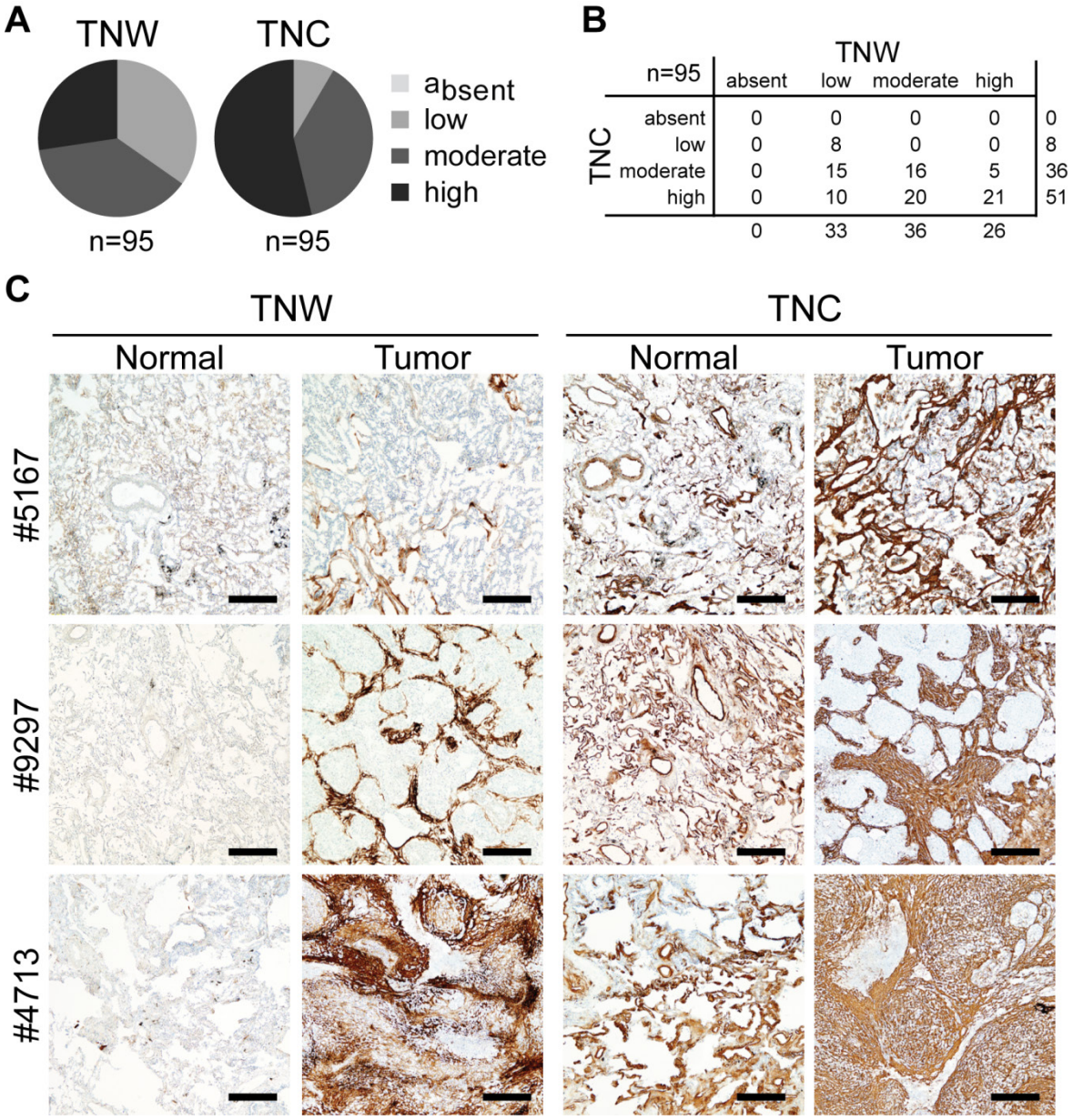
A
TNW
TNC
absent
low
moderate
high
n=95
n=95
B
TNW
n=95
absent
low
moderate
high
TNC
absent 0 0 0 0 0
low 0 8 0 0 8
moderate 0 15 16 5 36
high 0 10 20 21 51
0 33 36 26
C
TNW
TNC
Normal
Tumor
Normal
Tumor
#5167
#9297
#4713

**Figure 4**

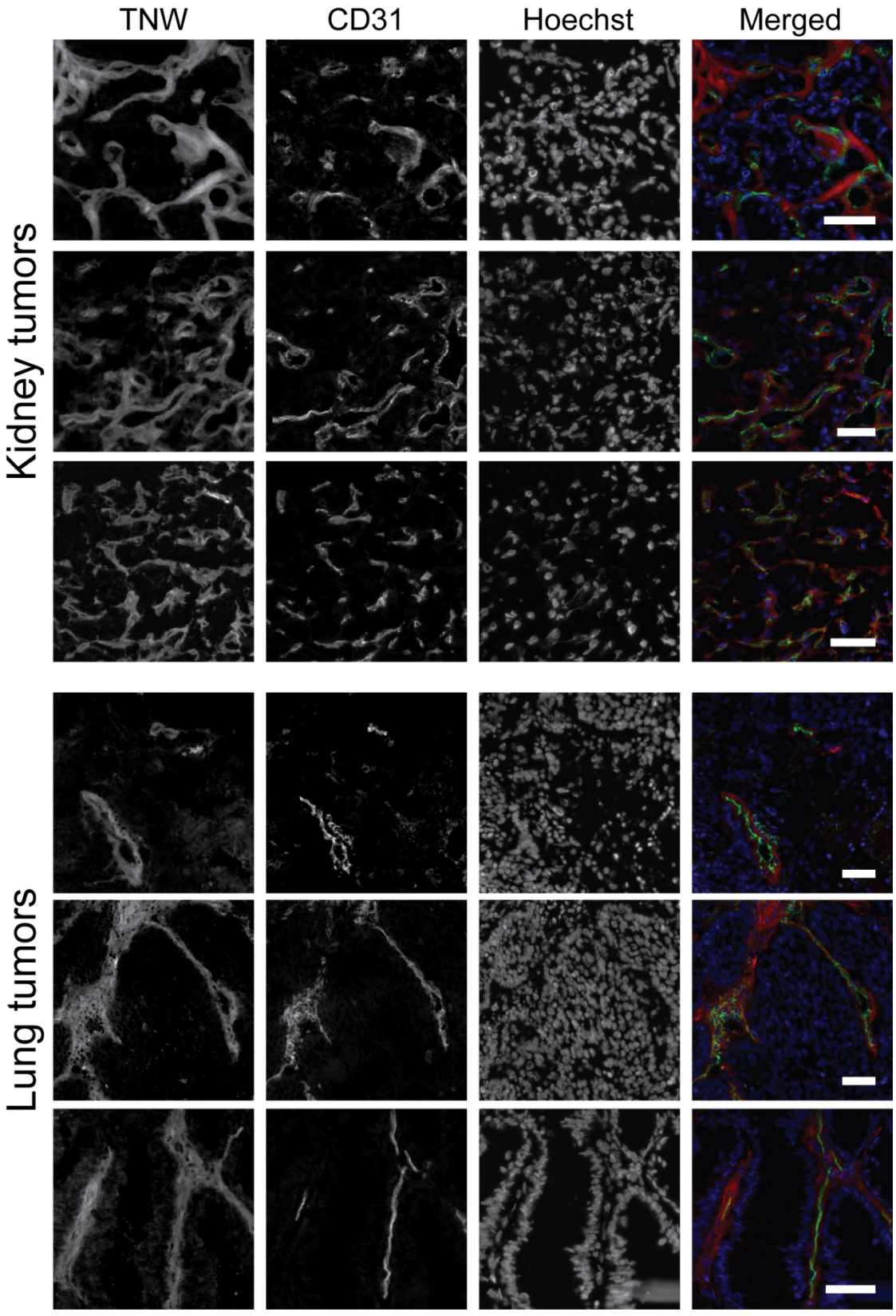


**Figure 5**

# III.3 Unpublished results

## III.3.1 – Tenascin-W gene is repressed by the NuRD complex

### III.3.1.1 – The genomic location of the human tenascin-W gene

The human tenascin-W gene is located on chromosome 1 (chr1:175,036,994-175,117,202) and consists of 19 exons. The first 76bp-long untranslated exon is followed by a second exon that contains the start codon (Fig.III.1A). Figure 1B represents the genomic location of the 5' region of the tenascin-W gene encompassing the region around the first exon and including the entire first intron and the second exon, as it can be seen on the UCSC genome browser (http://genome.ucsc.edu/). To locate potential cis-regulatory elements in this region we took advantage of the different bioinformatic tools implemented in the browser. Both PhyloP and PhastCons *(24)* tracks show 4 non-coding regions that are conserved among 46 vertebrate species, represented as positive peaks. The first peak (-319/+82) corresponds to exon 1 and upstream region; the other three peaks (+1500/+1900, +3100/+3450, +4700/+5200) are located in the intron between exon 1 and 2. All of these four sequences have positive scores in the GERP track. Positive scores represent a substitution deficit (i.e. fewer substitutions than the average neutral site) and thus indicate that these sites are under evolutionary constraint. This evolutionary conservation suggests the possibility of regulatory functions. Further indications for regulatory potential come from areas of DNaseI hypersensitivity, an indication of accessible chromatin. The corresponding track shows, among others, a weak cluster (obtained from 2 experiments with H1-hESC) localized to the region of the transcription start and one very strong one (result from 114 experiments with various cell lines) present at the +4700/+5200 conserved region. Finally, the last track on the bottom shows the repeating elements mapped to this region.

In the present study, we focused on the conserved region immediately upstream of the transcription start site, assuming that this corresponds to the promoter of the gene, while the conserved regions inside the first intron may be distal regulatory elements.

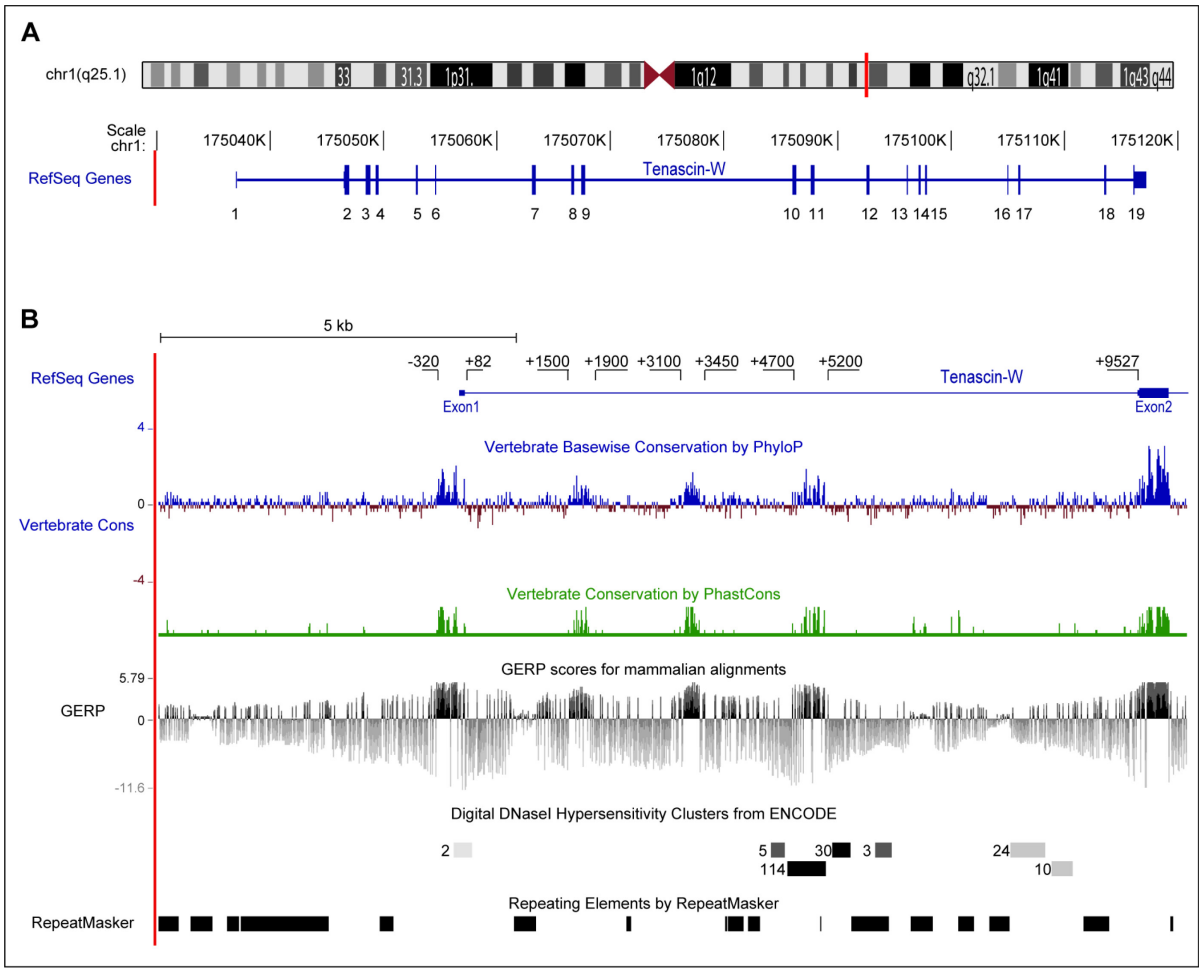


***Figure III.1*** *– **A**) Genomic localization of the human tenascin-W gene. The position of tenascin-W gene is indicated by a red line on the chromosome 1 ideogram. A schematic representation of the gene structure shows the distribution of tenascin-W 19 exons. Absolute chromosome coordinates are indicated above the scheme. **B**) UCSC browser display of the 5' and upstream region of human tenascin-W gene. The uppermost track shows the gene structure, with coordinates relative to the transcription start. The second and third tracks show the basewise conservation among vertebrates as calculated by PhyloP (blue/red histogram) and PhastCons (green histogram). The fourth track displays the GERP score (grey histogram). Conserved regions are revealed by positive peaks in these histograms. The lower tracks represent with grey and black boxes DNaseI hypersentivity clusters and region of repetitive DNA, respectively.*

### III.3.1.2 – Characterization of the human tenascin-W promoter

In order to identify regulatory elements in the conserved region upstream of the TNW gene, a 501bp fragment of genomic DNA spanning a region of TNW that is 423 bases 5' and 78 bases 3' of the start site of transcription, and thus includes the entire exon1, was inserted into a promoterless pSEAP2-basic vector to control the expression of the secreted embryonic alkaline phosphatase reporter. This reporter plasmid, *pSEAP-TNW(-423)*, was cotransfected with a plasmid expressing a

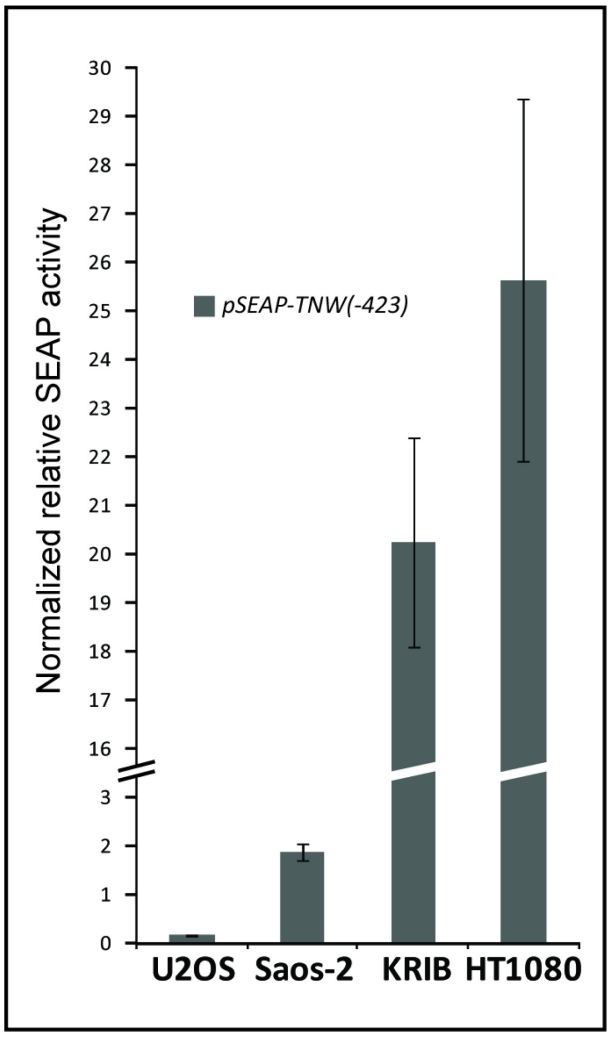


***Figure III.2*** *– Osteosarcoma (USO2, Saos-2 and KRIB) and fibrosarcoma (HT1080) cell lines were transiently transfected with a secreted alkaline phosphatase (SEAP) reporter under the control of the -423/+78 region of the TNW gene. Reporter activity in the culture medium was normalized against a co-transfected secreted luciferase expressing vector used to control for transfection efficiency. Error bars represent standard error of the means of a single experiment done in triplicate.*

secreted luciferase (*pMetLuc-Control*) to control for transfection efficiency into three osteosarcoma cell lines, U2OS, Saos-2, KRIB, and into one fibrosarcoma cell line, HT1080. None of these cell lines express detectable levels of endogenous tenascin-W protein in standard cell culture conditions. However, since tenascin-W is known to be involved in bone development and is expressed in the periosteum in the adult, we decided to use these easily transfectable cell lines for our promoter study. The relative activity of the -423/+78 TNW region was compared between the cell lines by measuring the secreted alkaline phosphatase activity in the culture media, normalized to the level cells showed the highest reporter gene activation and were thus selected for further studies. To further characterize the TNW promoter, SEAP reporter plasmids containing up to 1800bp and progressively shorter fragments 5' of the TNW gene were transiently transfected in HT1080 cells (Fig.III.3A). No significant reduction in reporter activity was observed when the region spanning nucleotides -1800 to -319 was progressively deleted and the activity of the tested constructs remained 30-fold higher than the promoterless pSEAP2-basic background activity. By contrast, plasmids *pSEAP-TNW(-252)* and *pSEAP-TNW(-148)* displayed significantly lower reporter activity, 2.38 fold and 3.36 fold lower than *pSEAP-TNW(-319)*, respectively.

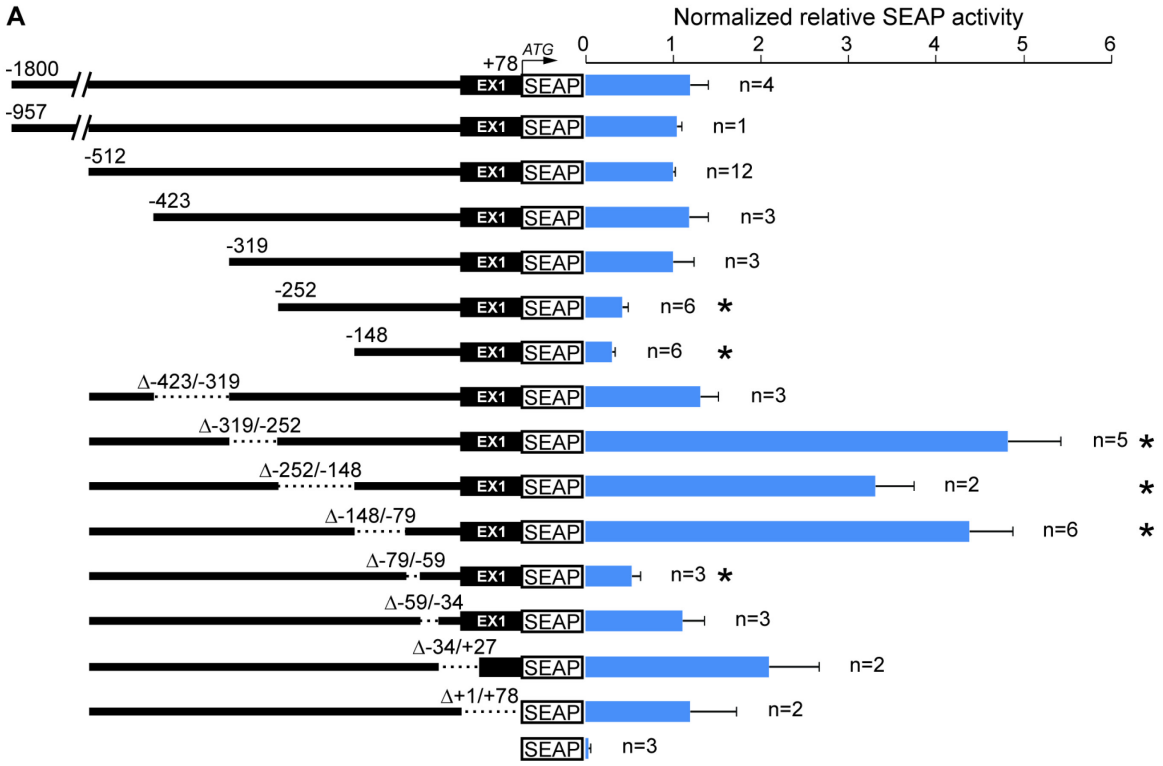


C

| | Complexes | Normalized SEAP activity |
|---|---|---|
| *pSEAP-TNW(-512)* | #1, (#2), #3 | 0.99 ±0.02 |
| *pSEAP-TNW(-423)* | #1, #3 | 1.18 ±0.21 |
| *pSEAP-TNW(-319)* | #1, #3 | 1.00 ±0.23 |
| *pSEAP-TNW(-252)* | #1 | 0.42 ±0.06 |
| *pSEAP-TNW(-148)* | #1 | 0.30 ±0.04 |
| *pSEAP-TNW(-512)Δ-79/-59* | (#2), #3 | 0.52 ±0.10 |
| *pSEAP-TNW(-512)Δ-319/-252* | #1, #2 | 4.82 ±0.60 |
| *pSEAP-TNW(-512)Δ-252/-148* | #1, #2 | 3.30 ±0.45 |
| *pSEAP-TNW(-512)Δ-148/-79* | #1, #2 | 4.38 ±0.49 |

***Figure III.3 (previous page) – A****) Fibrosarcoma cells HT1080 were transiently transfected with reporter constructs expressing SEAP under control of various deletion mutants of the genomic sequence upstream the TNW gene. Dotted lines represent nucleotides deleted in the construct. Co-transfected secreted luciferase vector was use as control for transfection efficiency and for the normalization. The figure represents a summary of multiple experiments in which different combination of constructs were transfected in triplicate. Results from different experiment were calibrated using the -512/+78 construct as reference, as it was transfected in every experiment. The number of experiments in which a construct was used it is indicated beside its bar in the graph. Error bars represents standard error of the mean. Asterisks indicate a p<0.001 in a Mann-Whitney U test against the -512/+78 construct.* ***B****) A speculative model that explains the observed results. Three cis-regulatory elements, -512/-423, -319/-79, and -79/-59, are recognized by three putative transcription regulator complexes, identified by #2, #3 and #1 respectively. When the sequence is intact (on the left), regulatory complex #2 it is inhibited by complex #3: The transcription is mildly activated by complex #3 and #1; when part of the sequence from -319 to -79 is absent (on the right; in this case -148/-79), complex #3 do not inhibit complex #2 anymore: The transcription is strongly activated by complex #2 and #1.* ***C****) The table summarizes the three-complexes interpretation in case of all the relevant construct tested. For each plasmid, the putative complexes that can bind and the observed normalized SEAP activity are indicated. Complex #2 is indicated between brackets when it is repressed by complex #3.*

Thus, the TNW minimal promoter is most likely located within nucleotides -319 to +78. Interestingly, the very same nucleotides correspond to the highly evolutionary conserved nucleotides 5' of TNW exon1 (cf. Fig.III.1). To further characterize this region, we made internal deletions within the *pSEAP-TNW(-512)* plasmid. All together, the eight deletion mutants cover the genomic region from -423 to +78 (Fig.III.3A). No significant variation in reporter activity was observed when the plasmids carrying the deletions *-423/-319*, *-59/-34*, and *+1/+78* (exon1) were transiently transfected in HT1080 cells. Deletion of nucleotides -79 to -59 resulted in a significant 2-fold reduction of reporter activity, suggesting the importance of these 20bp for gene activation.

However, the most striking results were observed when deletions *-319/-252*, *-252/-148*, and *-148/-79* were tested. All three of this deletion mutants showed a significant increase in reporter activity when compared to the original *pSEAP-TNW(-512)* of 4.82-, 3.30-, and 4.37-fold, respectively. Similar results were observed when plasmids *pSEAP-TNW(-512)* and *pSEAP-TNW(-512)Δ-148/-79* were transfected in U2OS, Saos-2, and KRIB cells to confirming the inhibitory effect of this region on reporter activity in several cell lines (Fig.III.4).

A hypothetical model to explain the results obtained is presented in Fig.III.3B. This model encompasses at least three regulatory factors/complexes that bind the

identified cis-elements on the DNA sequence acting together in the regulation of the transcription of TNW (Fig.III.3C). Nucleotides -79 to -59 are recognized by complex *#1*, a weak transcriptional activator. Nucleotides -512 to -423 are required for the binding of complex *#2*, a stronger activator of transcription, which in turn is inhibited by complex *#3* requiring the complete sequence from nucleotide -319 to -79 to exert its inhibition on complex #2. On the intact construct *pSEAP-TNW(-512)* the three complex bind the promoter, #2 is inhibited by #3 and #3 and #1 together weakly activate the transcription. The level of transcription is similar in constructs *pSEAP-TNW(-423)* and *pSEAP-TNW(-319)* where only complex #3 and #1 can bind. In constructs *pSEAP-TNW(-252)* and *pSEAP-TNW(-148)* only complex #1 binds and the level of transcription in reduced. Similar reduction is observed when complex #1 binding region is lost, in *pSEAP-TNW(-512)Δ-79/-59*, and the only activation is from #3, since #2 is inhibited by #3. Finally, in constructs *pSEAP-TNW(-512)Δ-319/-252*, *pSEAP-TNW(-512)Δ-252/-148*, and *pSEAP-TNW(-512)Δ-148/-79,* the complex #2 is no longer repressed by #3 and the transcription level is strongly increased (Fig.III.3B,C).

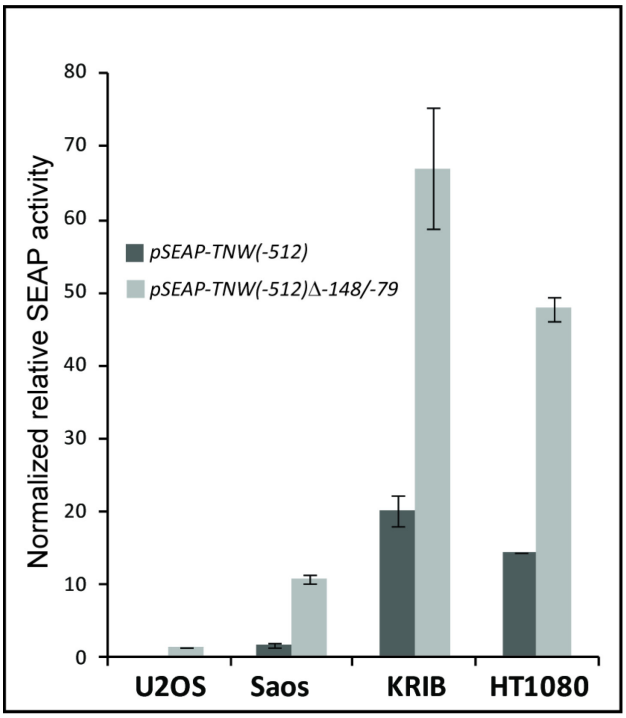


***Figure III.4 –*** *U2OS, Saos-2, KRIB and HT1080 cells were transfected with SEAP reporter constructs under the control of the -512/+78 region of the TNW gene, intact (dark grey) or missing nucleotides from -148 to -79 (light grey). The graph shows the reporter activity in the medium, normalized against secreted luciferase activity. Error bars indicate standard error of the mean of a single experiment done in triplicate.*

Although speculative and oversimplified, this interpretation of the data fits with the observations and the model of transcriptional repression as depicted here offers an explanation why TNW is not expressed in cultured cells.

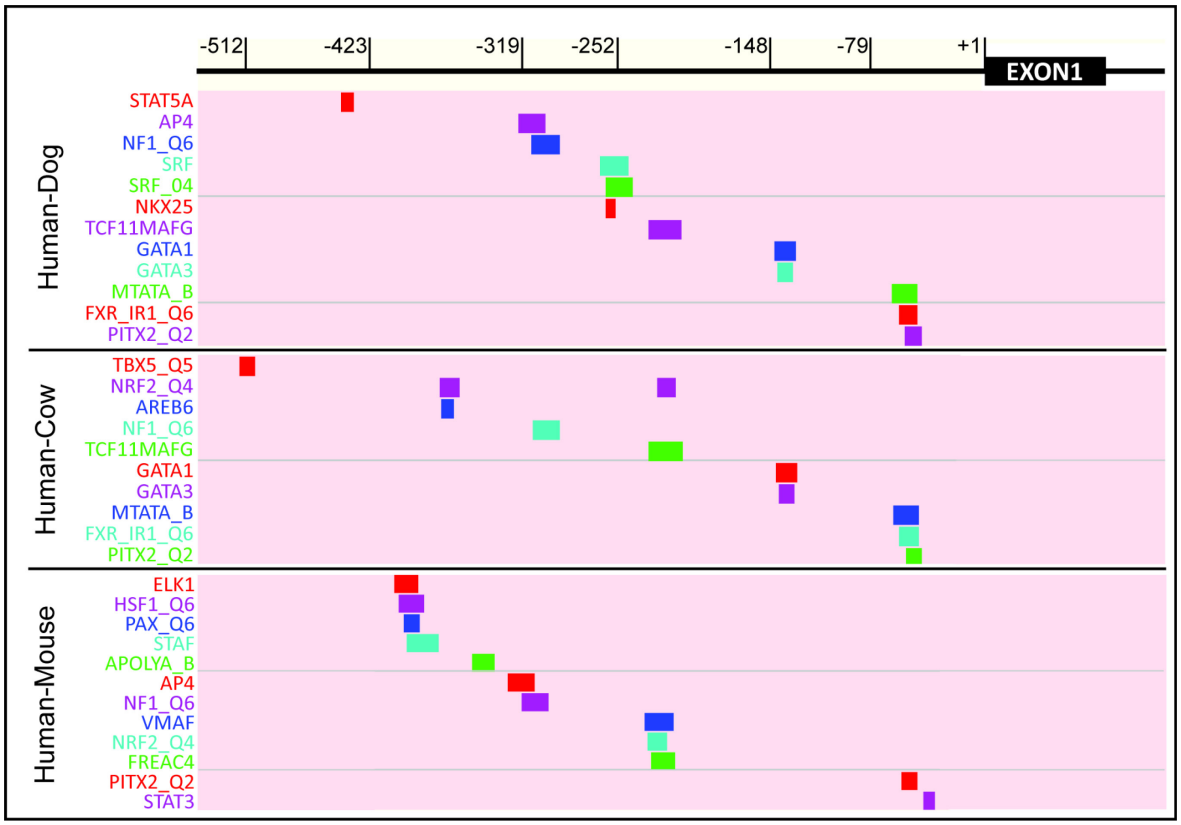


***Figure III.5*** *– Predicted transcription factor binding sites in the evolutionary conserved region immediately upstream the tenascin-W gene. Conserved binding sites between human and dog (upper panel), between human and cow (middle panel) and between human and mouse (lower panel) are shown as obtained by running the rVISTA 2.0 algorithm.*

### III.3.1.3 – In silico prediction of transcription factor binding sites

An examination of the genomic sequence used for the reporter gene assays was conducted using MatInspector (www.genomatix.de), and several potential binding sites for transcription factors were found (data not shown). A similar search of binding sites for transcription factors that in addition considers the evolutionary conservation of the analyzed sequence was performed using rVISTA 2.0 *(25)*, comparing the human genomic sequence with the orthologous sequences of dog, cow and mouse (Fig.III.5). Using this method, a smaller set of putative conserved binding sites were found; among them, the GATA binding site (5'-aaaaGATAatgag-3'; on the minus strand) between nucleotides -137/-125 caught our interest. Recent work reported GATA-6 as a transcriptional repressor of tenascin-C in fibroblasts *(26)*.

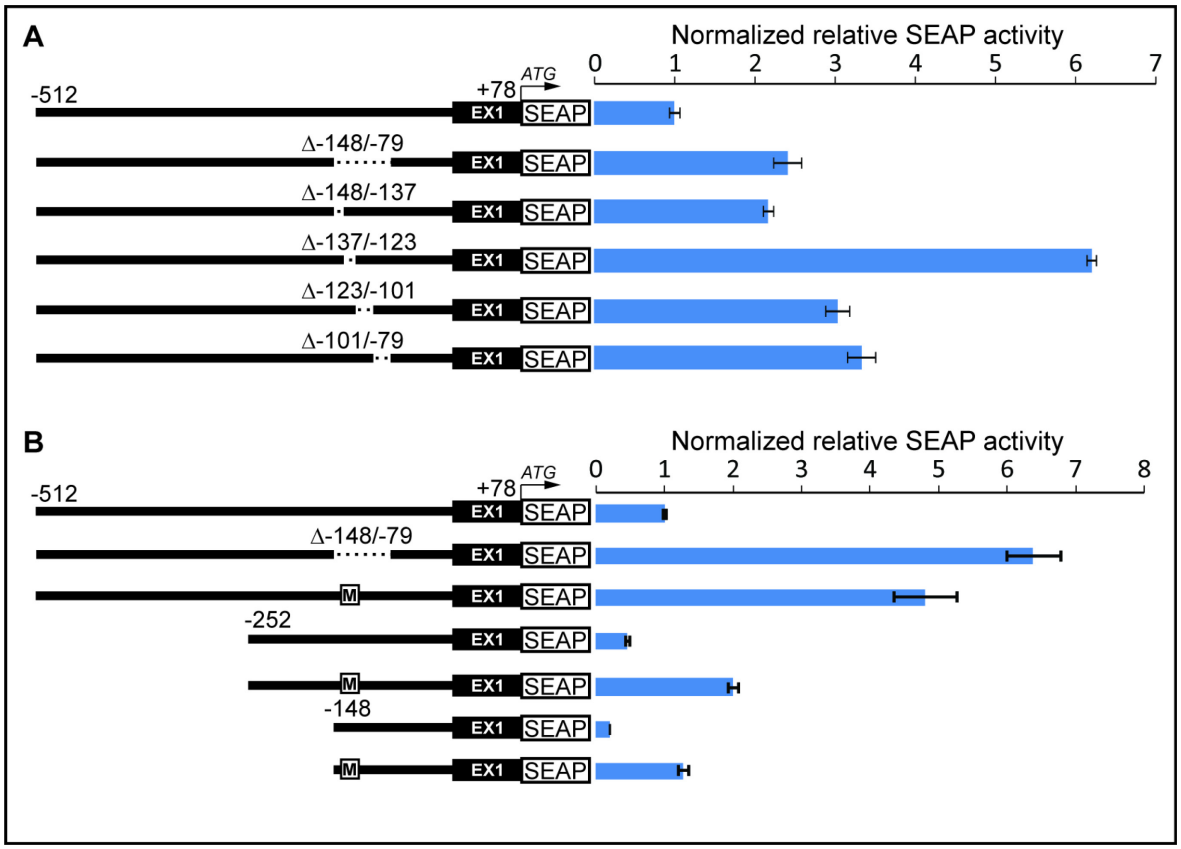


***Fig III.6 – A**) HT1080 cells were transfected with reporter constructs expressing SEAP under the control of the -512/+78 region of the TNW gene, intact or missing the indicated nucleotides. The graph shows the reporter activity in the medium, normalized against secreted luciferase activity. Error bars indicate standard error of the mean of two experiments done in triplicate. **B**) HT1080 cells were transfected with SEAP reporter under control of region -512/+78 intact, with nucleotides -148/-79 deleted, or with a 4-nucleotides mutation in the putative GATA binding (the mutation is indicated by an "M"); region -252/+78, intact or with the GATA site mutation; region -148/+78, intact or with the GATA site mutation. The graph shows the reporter activity in the medium, normalized against secreted luciferase activity. Error bars indicate standard error of the mean of a single experiment done in triplicate.*

Furthermore, the conserved GATA site is located in one of the regions that increase the reporter gene expression upon deletion and according to our model is binding a repressor complex. Interestingly, the GATA binding site is not conserved in mouse. To evaluate the importance of this GATA site the promoter region corresponding to nucleotides -148 to -79 was divided in four sub regions, *-148/-137*, *-137/-123*, *-123/-101*, and *-101/-79*, and four new SEAP plasmids based on *pSEAP-TNW(-512)* carrying each deletion were transfected in HT1080 cells (Fig.III.6A). Interestingly, *pSEAP-TNW(-512)Δ-137/-123*, the construct in which the deletion overlaps with the conserved putative GATA binding site, displayed the highest reporter activity. To confirm the importance of the GATA binding site with an alternative approach, we

mutated the four nucleotides of the core of the binding site (*-131/-128*) from TATC to CTCG in three constructs of different lengths. When transfected in HT1080 cells (Fig.III.6B), we observed that in *pSEAP-TNW(-512)* the mutation induced the reporter gene expression at a level comparable with the full *-148/-79* deletion. Also in *pSEAP-TNW(-252 and pSEAP-TNW(-148)*, the mutation increases the reporter activity. Thus, the GATA-binding region is an important element for the observed transcriptional repression of the TNW constructs. Although the regulatory mechanism may be more complicated than the one postulated, taken together, these last experiments suggest that a complex that acts as transcriptional repressor requires the intact *-131/-128* sequence to exert its effect.

### III.3.1.4 – DNA pull-down of complexes binding to the repressor region

We decided to use a proteomic approach to identify the protein complexes that bind the identified repressive element in the tenascin-W promoter. Biotinylated double strand DNA probes corresponding to nucleotides -149 to -119, either wild-type (WT) or containing the -131/-128 mutation (MUT), were incubated with nuclear extract of

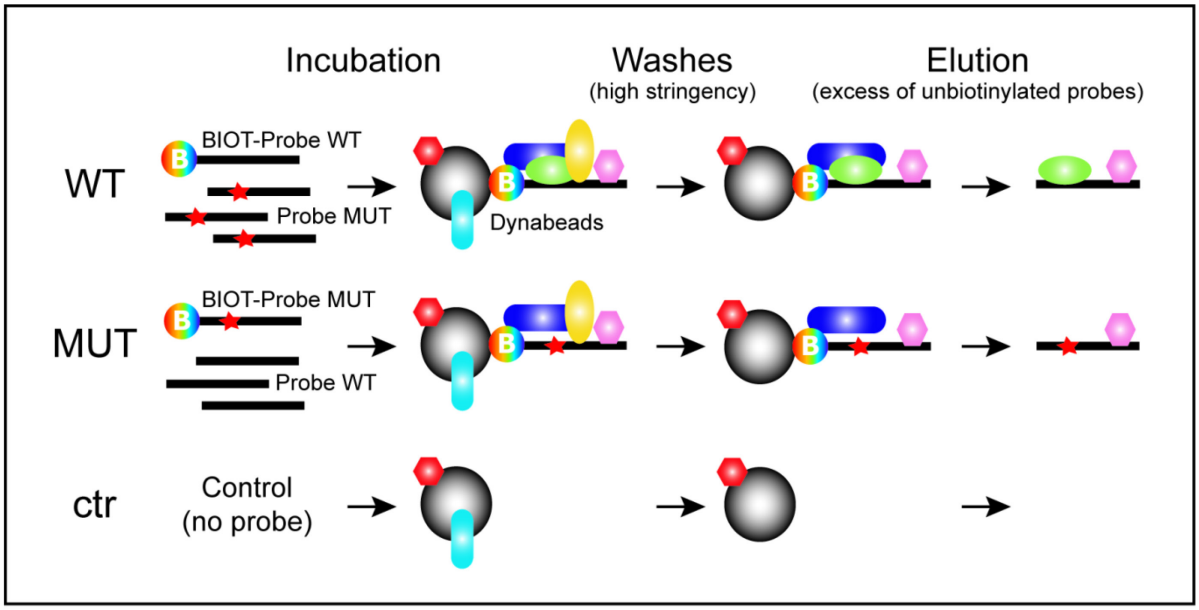


***Figure III.7 –*** *Schematic of the pull-down assay. Wild-type (WT) and mutated (MUT) -149/-119 double strand DNA probes were incubated with nuclear extracts from HT1080 cells, in presence of an excess of unlabeled MUT or WT probe respectively (the red star represents the -131/-128 mutation). A control without probe was also included in the experiment. The mixtures were coupled to streptavidin-conjugated paramagnetic beads and subjected to extensive washing. The nucleoprotein complexes were eluted with an excess of unlabeled probe and subjected to MS analysis.*

HT1080 cells. To increase the specificity of binding, an excess of unbiotinylated MUT probe was added to the nuclear extract incubated with the biotinylated WT probe; similarly, an excess of unbiotinylated WT probe was included in the MUT sample. The resulting nucleoprotein complexes were pulled down using streptavidin-conjugated paramagnetic particles and washed extensively. To estimate the background noise due to unspecific binding to the beads, a negative control in which paramagnetic particles were incubated with nuclear extract in absence of any probe was included in the experiment. Specific elution was performed by incubation with an excess of the appropriate unlabeled probe (for the negative control an equimolar mixture of WT and MUT unlabeled probe was used). Eluted proteins were then identified by mass spectrometry (MS). A schematic summary of the whole procedure is depicted in Fig.III.7. The output of the MS analysis consisted in a list of identified proteins and their average normalized abundance in each sample (WT, MUT and CTR). The list was first examined according to the GO terms associated with each entry: cytosolic, mitochondrial, and transmembrane proteins were purged from the list, as obvious contaminants of the nuclear extract. Ratios between the average normalized abundance in eluates of WT, MUT and CTR were calculated for each protein in the list. Only proteins that were at least twice as abundant in WT or in MUT in comparison with CTR were kept in the list. This operation aimed at filtering out most of the noise due to unspecific binding to the paramagnetic particles. Since our aim was to identify proteins that are part of the postulated repressor complex that recognizes the original *-131/-128* sequence, we were interested in proteins that are more abundant in the WT sample than in the MUT one. We therefore calculated the ratio between the average normalized abundance in WT and in MUT eluates for each protein, and assembled a list of proteins with a ratio higher than 1. The filtered list of results from one typical experiment containing 61 proteins is presented in Table III.1, ranked according the WT/MUT ratio.

Although at least GATA-2, GATA-3, GATA-4 and GATA-6 transcripts are present in HT1080, as assessed by RT-PCR (data not shown), the pull down experiment gave no indication of an interaction of any member of the GATA family with the conserved GATA binding site present in the WT probe. Interestingly though, two proteins that contain a GATA-type zinc finger domain, GATAD2B and GATAD2A, are in the list,

in position #37 and #49 respectively. Also known as transcriptional repressor P66β and -α, these proteins can interact with each other and are often part of the Mi-2/NuRD complex *(27)*. Two other members of Mi-2/NuRD are also found in the list: the core member of the complex, CHD4, in position #8, and RBBP4, in position #45. The Mi-2/NuRD is a well studied transcriptional repressor complex, which acts through chromatin remodeling and histone modifications: it represents a promising candidate for the role of a repressor of TNW gene transcription.

Another protein in the list, SUZ12 (position #50) is also linked to transcriptional repression as an essential component of the Polycomb repressive complex 2 (PRC2). Although SUZ12 relative abundance is low and the protein is only slightly more abundant in WT sample than in MUT, it might be worthy of further investigation.

### III.3.1.5 – Chromatin immunoprecipitation

To further strengthen the hypothesis that Mi2/NuRD and PRC2 complexes bind the endogenous human tenascin-W promoter *in vivo*, we performed chromatin immunoprecipitation (ChIP) assay. The chromatin extracted from HT1080 cells was immunoprecipitated using antibody against CHD4, against SUZ12, or non targeting IgG, and the enrichment of tenascin-W promoter (position -428 to -215) was analyzed by quantitative real-time PCR (Fig.III.8). Two genomic regions were used as negative controls for CHD4 and SUZ12 binding, a long interspersed nuclear element (LINE) located 1800 bp upstream the transcription start site, and tenascin-W exons 10 and 11 and the non conserved intron in between. We observed enrichment relative to the input of the promoter region three times higher when the anti-CHD4 antibody is used compared to non-targeting IgG. By contrast, the two control region display a negligible enrichment. Our results, therefore suggest that indeed the Mi2/NuRD complex occupy the promoter of human tenascin-W.

In case of SUZ12, although enrichment was observed on the promoter region, the two control regions resulted enriched as well, suggesting that the binding of PRC2 may be not specific to tenascin-W promoter.

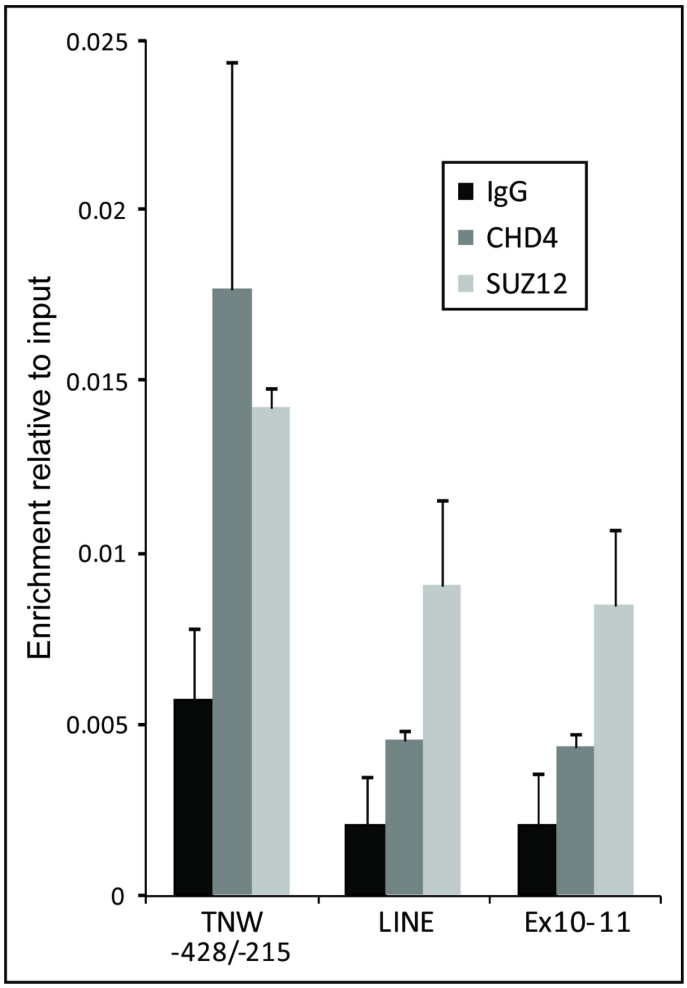


***Figure III.8 –*** *ChIP assay. HT1080 chromatin was extracted, immunoprecipitated with anti CHD4, anti SUZ12 antibody, and non specific IgG. Primers designed on tenascin-W promoter (TNW-428/-215), on a repetitive DNA sequence upstream tenascin-W gene (LINE), or on the sequence between exon 10 and 11 (Ex10-11) were used for quantitative real-time PCR analysis. Results are plotted relative to input DNA. Error bars indicate standard error of the mean of two independent experiments.*

| Rank # | Gene name | Protein names | Average Normalized Abundances | | | WT/MUT (>1) | MIN diff CTR (>2) |
|---|---|---|---|---|---|---|---|
| | | | WT | MUT | ctr | | |
| **1** | **PHF6** | **PHD finger protein 6** | **19400** | **2293.03** | **10.64** | **8.46** | **215.51** |
| 2 | EXOSC7 | Exosome complex exonuclease RRP42 | 7942.48 | 1943.52 | 368.33 | 4.09 | 5.28 |
| **3** | **SMARCE1** | **SWI/SNF-related matrix-associated actin-dependent regulator of chromatin subfamily E member 1** | **118000** | **50000** | **16700** | **2.36** | **2.99** |
| 4 | PARP1 | Poly [ADP-ribose] polymerase 1 | 1370000 | 589000 | 251000 | 2.33 | 2.35 |
| 5 | PDCD11 | Protein RRP5 homolog | 33600 | 16400 | 4174.6 | 2.05 | 3.93 |
| 6 | UHRF1 | E3 ubiquitin-protein ligase UHRF1 | 64700 | 32200 | 12600 | 2.01 | 2.56 |
| 7 | EXOSC1 | 3'-5' exoribonuclease CSL4 homolog | 22100 | 11000 | 1125.7 | 2.01 | 9.77 |
| **8** | **CHD4** | **Chromodomain-helicase-DNA-binding protein 4** | **6513.1** | **3399.19** | **95.71** | **1.92** | **35.52** |
| **9** | **HMGN1** | **Non-histone chromosomal protein HMG-14** | **10400** | **5753.01** | **2853.7** | **1.81** | **2.02** |
| **10** | **FAU** | **40S ribosomal protein S30** | **35400** | **19700** | **6743.3** | **1.8** | **2.92** |
| 11 | RPL22 | 60S ribosomal protein L22 | 52000 | 29100 | 14100 | 1.79 | 2.06 |
| 12 | MAP4 | Microtubule-associated protein 4 | 39300 | 22000 | 8328.2 | 1.79 | 2.64 |
| **13** | **THOC4** | **THO complex subunit 4** | **1360000** | **762000** | **280000** | **1.78** | **2.72** |
| **14** | **MYBBP1A** | **Myb-binding protein 1A** | **13900** | **7840.2** | **3375.5** | **1.77** | **2.32** |
| 15 | C12orf43 | Uncharacterized protein | 3023.93 | 1730.42 | 163.69 | 1.75 | 10.57 |
| 16 | RPS25 | 40S ribosomal protein S25 | 63500 | 38200 | 13200 | 1.66 | 2.89 |
| 17 | KIFC1 | Kinesin-like protein KIFC1 | 1570.7 | 958.92 | 59.3 | 1.64 | 16.17 |
| 18 | ATF1 | Cyclic AMP-dependent transcription factor ATF-1 | 907.02 | 561.26 | 73.14 | 1.62 | 7.67 |
| 19 | SNRPD1 | Small nuclear ribonucleoprotein Sm D1 | 43500 | 27400 | 9690.5 | 1.59 | 2.83 |
| 20 | TPX2 | Targeting protein for Xklp2 | 9457.58 | 6014.92 | 488.02 | 1.57 | 12.33 |
| **21** | **HMGA1** | **High mobility group protein HMG-I/HMG-Y** | **12000** | **7908.54** | **2553.3** | **1.52** | **3.1** |
| 22 | EIF2S1 | Eukaryotic translation initiation factor 2 subunit 1 | 6958.14 | 4692.83 | 307.89 | 1.48 | 15.24 |
| 23 | KPNA3 | Importin subunit alpha-3 | 889.05 | 602.24 | 169.62 | 1.48 | 3.55 |
| 24 | HNRNPU | Heterogeneous nuclear ribonucleoprotein U | 2900000 | 1990000 | 388000 | 1.46 | 5.13 |
| 25 | RPS7 | 40S ribosomal protein S7 | 455000 | 314000 | 43800 | 1.45 | 7.17 |
| 26 | EXOSC10 | Exosome component 10 | 241000 | 169000 | 63500 | 1.43 | 2.66 |
| 27 | SNRPF | Small nuclear ribonucleoprotein F | 1008.8 | 721.99 | 9.74 | 1.4 | 74.13 |
| 28 | FMR1 | Fragile X mental retardation 1 protein | 7228.75 | 5190.93 | 1782.6 | 1.39 | 2.91 |

| | | | | | | | |
|---|---|---|---|---|---|---|---|
| 29 | EXOSC4 | Exosome complex exonuclease RRP41 | 1858.33 | 1336.77 | 149.58 | 1.39 | 8.94 |
| 30 | LYAR | Cell growth-regulating nucleolar protein | 4628.72 | 3331.49 | 947.39 | 1.39 | 3.52 |
| 31 | DDX56 | Probable ATP-dependent RNA helicase DDX56 | 2948.08 | 2152.85 | 188.32 | 1.37 | 11.43 |
| 32 | PRKDC | DNA-dependent protein kinase catalytic subunit | 11400 | 8853.29 | 4309 | 1.29 | 2.05 |
| 33 | TMPO | Lamina-associated polypeptide 2, isoform alpha | 50800 | 39500 | 14600 | 1.29 | 2.71 |
| 34 | SART1 | U4/U6.U5 tri-snRNP-associated protein 1 | 9946.74 | 7741.77 | 792.15 | 1.28 | 9.77 |
| 35 | DDX47 | Probable ATP-dependent RNA helicase DDX47 | 14900 | 11700 | 890.73 | 1.27 | 13.14 |
| 36 | RBM27 | RNA-binding protein 27 | 31000 | 24400 | 2206.2 | 1.27 | 11.06 |
| **37** | **GATAD2B** | **Transcriptional repressor p66-beta (GATA zinc finger domain-containing protein 2B)** | **3771.25** | **2970.59** | **910.29** | **1.27** | **3.26** |
| 38 | RPL23 | 60S ribosomal protein L23 | 226000 | 180000 | 78900 | 1.26 | 2.28 |
| **39** | **WDR5** | **WD repeat-containing protein 5** | **1748.16** | **1393.19** | **566.61** | **1.25** | **2.46** |
| 40 | PRPF19 | Pre-mRNA-processing factor 19 | 280000 | 224000 | 109000 | 1.25 | 2.06 |
| 41 | NOLC1 | Nucleolar and coiled-body phosphoprotein 1 | 166000 | 133000 | 48800 | 1.25 | 2.73 |
| 42 | RSL1D1 | Ribosomal L1 domain-containing protein 1 | 115000 | 92500 | 40200 | 1.24 | 2.3 |
| 43 | RPS2 | 40S ribosomal protein S2 | 24800 | 20000 | 2000.4 | 1.24 | 10 |
| 44 | HMGN4 | High mobility group nucleosome-binding domain-containing protein 4 | 11500 | 9374.38 | 4638.1 | 1.23 | 2.02 |
| **45** | **RBBP4** | **Histone-binding protein RBBP4** | **29500** | **24200** | **10200** | **1.22** | **2.37** |
| 46 | POLDIP3 | Polymerase delta-interacting protein 3 | 135000 | 111000 | 19600 | 1.22 | 5.66 |
| **47** | **SMARCA2** | **Probable global transcription activator SNF2L2** | **1615.87** | **1339.49** | **364.21** | **1.21** | **3.68** |
| **48** | **RBM14** | **RNA-binding protein 14** | **99000** | **83500** | **20200** | **1.19** | **4.13** |
| **49** | **GATAD2A** | **Transcriptional repressor p66-alpha (GATA zinc finger domain-containing protein 2A)** | **4134.73** | **3518.76** | **276.88** | **1.18** | **12.71** |
| **50** | **SUZ12** | **Polycomb protein SUZ12 (Chromatin precipitated E2F target 9 protein)** | **550.09** | **469.5** | **190.44** | **1.17** | **2.47** |
| 51 | RPS16 | 40S ribosomal protein S16 | 39200 | 34300 | 1572.8 | 1.14 | 21.81 |
| 52 | HNRNPR | Heterogeneous nuclear ribonucleoprotein R | 465000 | 408000 | 152000 | 1.14 | 2.68 |
| **53** | **HIST1H2BC** | **Histone H2B type 1-C/E/F/G/I** | **157000** | **139000** | **43500** | **1.13** | **3.2** |
| 54 | RPS27L | 40S ribosomal protein S27-like | 873.1 | 777.51 | 86.63 | 1.12 | 8.98 |
| 55 | RPL35 | 60S ribosomal protein L35 | 10900 | 9773.8 | 927.35 | 1.12 | 10.54 |
| 56 | PSIP1 | PC4 and SFRS1-interacting protein | 6109.45 | 5488.09 | 1434.2 | 1.11 | 3.83 |

| | | | | | | | |
|---|---|---|---|---|---|---|---|
| 57 | POLR2E | DNA-directed RNA polymerases I, II, and III subunit RPABC1 | 823.99 | 760.95 | 159.1 | 1.08 | 4.78 |
| 58 | EXOSC3 | Exosome complex exonuclease RRP40 | 34400 | 31800 | 12000 | 1.08 | 2.65 |
| 59 | ACIN1 | Apoptotic chromatin condensation inducer in the nucleus | 11900 | 11300 | 563.1 | 1.05 | 20.07 |
| 60 | NOM1 | Nucleolar MIF4G domain-containing protein 1 | 820.23 | 786.45 | 144.38 | 1.04 | 5.45 |
| 61 | TOP1 | DNA topoisomerase 1 | 196000 | 188000 | 78900 | 1.04 | 2.38 |

***Table III.1*** *– List of the proteins identified by MS on the eluates of the DNA pulldown experiment. The average normalized abundance of each protein in the three conditions (WT, MUT and ctr) is indicated. The proteins are ranked according WT/MUT ratio. Proteins of potential interest are in bold font.*

## III.3.2 – Bone marrow-derived stem cells differentiated to osteoblasts express tenascin-W *in vitro*

*In collaboration with Arnaud Scherberich, Department of Biomedicine, University Hospital Basel, Basel, Switzerland*

While tenascin-W can be induced by BMP-2 stimulation in a variety of murine cells (i.e. C2C12 *(28)*, MEF*(29)*, HC11 *(29)*), we were not able to detect tenascin-W expression in any human cell line tested so far, kept in standard culture condition, stimulated or not with a panel of growing factors (i.e. FGF2, BMP2, TNF$\alpha$) (data not shown).

Since tenascin-W is prominently expressed during embryonic bone development *(30)* we decided to test its expression in a *in vitro* model of endochondral bone formation *(31)*. The model consists in a 3D culture of bone marrow-derived, adult mesenchymal stem cells (BMSC) kept first in chondrogenic medium (with TGF$\beta$1) for 3 weeks, followed by 2 weeks in hypertrophic medium (without TGFβ1 and with beta-glycerophosphate and thyroxin). Under these conditions, the BMSC undergo differentiation and display clear cartilaginous features at the core of the structure surrounded by a mineralized rim. In order to look for tenascin-W expression, cryosections obtained from the above described 3D cultures were stained with anti-tenascin-W monoclonal antibodies (Fig.III.9A). The result showed a strong positive signal in the mineralized periphery of the culture. The staining is strongly reduced when the primary antibody is pre-incubated with purified tenascin-W, confirming the specificity of the observed signal (data not shown).

We decided to test if BMSC undergoing osteogenic differentiation express tenascin-W also in standard 2D cultures. At that purpose, we cultured BMSC derived from three different patients either in osteogenic medium (containing dexamethasone, beta-glycerophosphate and ascorbic acid-2-P) or in control medium (growth medium). After three days in osteogenic medium, cells start to express the osteoblasts marker alkaline phosphatase (ALP), and the expression reaches the maximum at the end of the first week (Fig.III.9B). As expected, cells in control medium remain undifferentiated and do not express ALP. The expression of tenascin-W follows a similar kinetic, increasing during the first week of culture in

osteogenic medium and remaining low in control cells (Fig.III.9C). The expression of tenascin-W was confirmed at protein level by immunofluorescence staining of cells kept in osteogenic medium for one week, using anti-tenascin-W antibody (Fig.III.9D, lower panels). Tenascin-W appears as a mesh of extracellular fibers that surrounds the differentiated cells, and is completely absent in the cells cultured in control medium. Similar results were obtained with BMSC derived from the other two patients. In our knowledge, this is the first report of human cells that express endogenous tenascin-W in culture.

***Figure III.9 (next page) –*** *Bone marrow-derived stem cells (BMSCs) differentiated to osteoblasts express tenascin-W.* ***A****) BMSC were cultured as 3D pellet for three weeks in chondrogenic medium, followed by two weeks in hypertrophic medium. The disc-shaped pellets were harvested, frozen and 9 μm tick cryosections were prepared. The picture shows the immunostaining of a section using anti-tenascin-W monoclonal antibody. The specific tenascin-W signal is localized in correspondence of the mineralized border. Scale bar = 200 μm.* ***B****) In BMSC cultured in osteogenic medium the expression of the marker for osteogenic differentiation alkaline phosphatase (AP) increases after 3 days, while in cells maintained in growth medium its level remains low. Results of a typical experiment are shown.* ***C****) Expression of tenascin-W mRNA steadily increases during the first days of osteogenic differentiation of BMSCs, reaching the peak after one week. In control cells, tenascin-W level remains negligible. Error bars represent standard error of the mean of two experiments.* ***D****) BMSCs cultured for one week in osteogenic medium or growth medium were stained for AP to demonstrate osteogenic differentiation (upper pictures), or immunostained with anti-tenascin-W monoclonal antibody and a secondary antibody conjugated with Alexa-488 (lower pictures). Only differentiated cells display specific tenascin-W staining (scale bars=200 μm).*

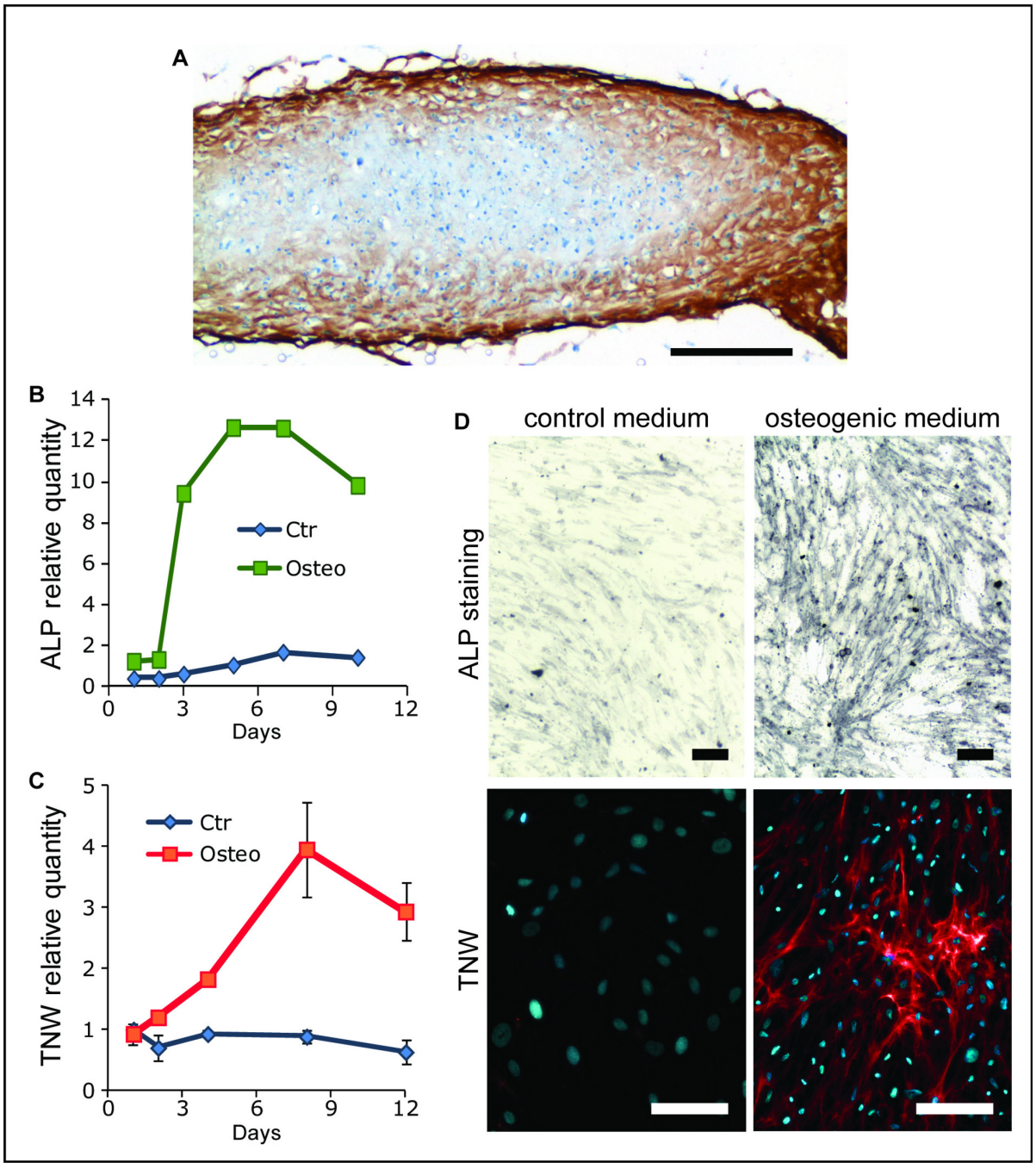
A
B
ALP relative quantity
14
12
10
8
6
4
2
0
0
3
6
9
12
Days
Ctr
Osteo
C
TNW relative quantity
5
4
3
2
1
0
0
3
6
9
12
Days
Ctr
Osteo
D
control medium
osteogenic medium
ALP staining
TNW

# DISCUSSION

# IV. DISCUSSION

## IV.1 – Tenascin-W in the context of tumors

Since its discovery as antigen present in glioma-associated stroma *(32)*, tenascin-C has been found to be strongly expressed in the extracellular matrix of various types of cancer *(17, 33)*. Due to the structural analogy and the partially overlapping pattern of expression with tenascin-C, it was natural to study the expression and the functions of tenascin-W in the tumor context. The first observation of tenascin-W in the tumor stroma was made in mouse models for mammary carcinogenesis, where its presence around primary tumors was linked with the likelihood to develop metastasis *(29)*. The association with tumor stroma was confirmed in human by a study that found tenascin-W expression in the large majority of breast cancer lysates subjected to immunoblotting *(34)*. Immunohistochemistry showed that tenascin-W staining was localized in the stromal compartment that surrounds the transformed epithelial cells. In contrast, tenascin-C was in some cases observed to be expressed by the tumor cells themselves. Notably, neither tenascin-W nor tenascin-C was detected in the healthy breast tissue. A following study extended the observations to colorectal cancer *(35)*. Also in this case, tenascin-W was detected in the majority of the samples examined, localized in the stroma around the tumors. Interestingly, whereas the healthy colon tissue is devoid of tenascin-W, strong staining was observed for tenascin-C in the normal colon mucosa.

Here, we have presented new studies that investigated tenascin-W in brain tumors (see III.1.1) and in melanomas, pancreas, kidney and lung carcinomas (see III.2.1). We were not able to detect tenascin-W expression in any of the corresponding normal tissues, with the exception of a relatively low amount in kidney. This is the most remarkable difference with tenascin-C, since we detected the latter in every normal organ examined, except for breast and heart tissue. Considering that tenascin-C overexpression has been associated with other pathological conditions than cancer, namely inflammation, infection, asthma, fibrosis and wound healing *(17, 33)*, tenascin-W seems to be a more specific marker for cancer. However, since tenascin-C is expressed in numerous splice variants, there remains the possibility

that certain isoforms could be more tumor-specific than others and provide a good target as well *(36, 37)*. For instance in normal kidney, pancreas and colon samples, we observed only a low molecular weight tenascin-C isoform, while in tumors a number of larger variants are visible in the immunoblots.

Our observations on glioblastoma samples revealed an obvious coincidence between tenascin-W staining and the tumor microvasculature. Double immunofluorescence staining together with the blood vessel marker von Willebrand factor confirmed the colocalization of tenascin-W and endothelial cells. Prompted by this finding, we looked for the same pattern of expression in other types of solid tumors. By using the same double immunofluorescence approach, this time using CD31 as endothelial cell marker, we confirmed tenascin-W association with blood vessels also in the case of lung and kidney carcinomas. Additional observations (not shown) on a limited number of ovarian and prostate cancer samples gave similar results. In breast tumors, tenascin-W overexpression is in general higher and not limited to the close proximity of blood vessels, but distributed in the whole stromal compartment, making the colocalization less obvious. In general, we can conclude that the presence of the protein around tumor blood vessels seems to be a common feature for tenascin-W-expressing tumors.

We demonstrated that tenascin-W has a pro-migratory effect on endothelial cells. As assessed by our *in vitro* experiments using HUVEC, cell motility increased in presence of tenascin-W. Additionally, HUVEC spheroids embedded in a collagen-type I gel sprouted when tenascin-W was present in the surrounding matrix. Since proangiogenic activities have also been described for tenascin-C in several studies *(38, 39)*, our results suggested a common proangiogenic role for tenascin-C and tenascin-W. A very recent study compared tumor angiogenesis with physiological angiogenesis using a proteomic approach *(40)*. By comparing the protein expression profile of proliferating vessels in glioblastoma with the one of those in endometrium, a tissues in which physiological angiogenesis takes place, the authors identified tenascin-C among the protein aberrantly expressed only in tumor blood vessel. In contrast with our results, said study did not report tenascin-W among the tumor blood vessel-specific proteins. An explanation for this discrepancy may be that unlike us, the authors of the mentioned study did not specifically look for

tenascin-W and tenascin-W, although there, did not pass the strict filtering process applied on the mass spec data or was not expressed at high enough levels to be detected by their method.

The amount of tenascin-W and tenascin-C varies significantly among tumor samples, in all divers solid tumors examined. Therefore, we searched for correlations between tenascin-W overexpression and clinicopathological features of the tumors. A previous study *(41)* reported that the mean level of tenascin-W in low-grade breast tumors (G1/G2) is significantly higher than in high-grade tumors (G3), although the values within each group are so spread that there are high-grade samples with high level of tenascin-W and *vice versa*.
By contrast, the study conducted on lung tumor patients presented here suggests a direct correlation between tenascin-W level and the grade of the tumor; high-grade tumors (G3/G4) have a statistically significant higher mean level of tenascin-W compared to normal lung tissue, and there seems to be a tendency for tenascin-W to increase with tumor grade (Supplementary figure V.2.1). In the same set of samples, tenascin-C levels appear consistently elevated regardless of the tumor grade and are not significantly higher than in the normal lung tissue of the same patient. Although we are aware that the number of samples examined is too small to draw definitive conclusions, there seems to be a tendency for increased tenascin-W expression in higher grade lung tumors.

Many studies over the years revealed the utility of tenascin-C as biomarker for many aggressive cancers, with predictive value for local recurrences and metastatic dissemination *(42–44)*. Moreover, tenascin-C has been a target of different anti-cancer therapies, including the delivery of cytokines or radionuclides to the tumor using tenascin-C-specific monoclonal antibodies *(45–47)* or aptamers *(48, 49)*. We think that in the future tenascin-W might have the better potential to serve as tumor biomarker, due to its cancer-specific expression, its proximity to blood vessels that suggests accessibility from the blood stream, and finally its positive influence on tumor angiogenesis that could be disrupted by such treatments.

## IV.2 – Regulation of tenascin-W

Our observations in immunohistochemical stainings of tumor sections presented here and previous immunoblot studies *(34, 35)* revealed that tenascin-W and tenascin-C relative ratios differ greatly from sample to sample. This implies the existence of independent regulatory mechanisms specific for each tenascin, but at the same time it does not exclude that the two genes also share conserved mechanism of regulation.

Several publications are available on the structure of the tenascin-C promoter and its cis-regulatory elements *(26, 50–54)*. By contrast, nothing has been published to date about the promoter of tenascin-W. To our knowledge, the results presented in section III.3.1 of this thesis represent the first experiments to characterize the promoter of the human tenascin-W gene. It is our ambition that through the study of the tenascin-W promoter and the identification of its regulatory elements, it might be possible to link the expression of the gene to particular transcription factors and specific signaling pathways. The outcome of such studies might clarify how the strict spatio-temporal regulation of tenascin-W expression is achieved during development and will possibly give an indication of why the gene is so prominently expressed in cancer.

Very little is known about the regulation of tenascin-W. It has been reported previously that TNF$\alpha$ and BMP2 can induce tenascin-W expression in cultured murine cells, such as MEFs, C2C12 and 4T1 cells *(28, 29)*. This seems to be different in human cells. Indeed, we were not able to detect endogenous tenascin-W expression in any of the numerous cell lines of human origin tested and neither TNF$\alpha$ nor BMP2 or any other growth factors tested induced tenascin-W expression in the human cells. We therefore concluded that certain regulatory mechanism must be very different between the two species, and caution is advised before extending what has been learned in mouse to human. Based on this, two main approaches to the study of tenascin-W regulation by reporter gene assay seemed reasonable: (i) adopting murine cell line models in which tenascin-W can be induced, in order to identify the mechanism of induction and the pathways involved, or (ii) making use of cell lines of human origin, to identify the mechanisms responsible for gene repression. We chose the latter option, since the results may be of broader interest.

We first examined the *homo sapiens* genomic region that contains the tenascin-W gene, looking for conserved non coding regions that may harbor regulatory elements *(55)*. We found four regions highly conserved among vertebrates: three situated in the first intron and one immediately upstream of the putative untranslated tenascin-W first exon. The regions of high conservation located in the first intron may represent regulatory elements which often can be found in the first introns of genes *(56)*. They are also compatible with the presence of an alternative promoter. Since the ATG codon is located in the second exon, this hypothetical transcript would result in the same protein, the only difference being in the 5' UTR sequence and in the regulatory mechanism, which could be tissue-specific. After performing 5'RACE on RNA extracted from few human cell lines (data not shown), and examining human EST collections, we have no evidence of any alternative tenascin-W transcript, but its existence could not be ruled out yet and further investigations are needed.

The study presented here focuses on the conserved region immediately upstream of the first untranslated exon, assuming that it corresponds to the promoter of the main tenascin-W transcript. The promoter activity was confirmed using SEAP reporter assays. Progressively shortened constructs were transfected into human fibrosarcoma cells (HT1080) resulting in a drop in reporter gene activity when the sequence was shorter than 319 bp upstream of the putative transcription starting site (TSS). Interestingly, 320 bp is precisely the length of the conserved region upstream the first exon.

Adopting an approach of using internal deletion constructs, we were surprised to observe significant increases in reporter activity when constructs with deletions encompassing nucleotide -319 to -79 were transfected. An obvious explanation is that the deleted sequence harbors a cis-regulatory element involved in gene repression. A more detailed interpretation is presented in section III.3.1.2 (Fig. III.3B), where a speculative model that takes in accounts of all the observations is illustrated.

Further examination of the *-319/-79* region with a software that predicts putative binding sites for transcription factors revealed a conserved GATA binding site located between nucleotides -137 and -125. Considering that a recent report identified GATA-6 as a novel repressor of the tenascin-C gene *(26)*, we investigated

the region that contains the GATA binding site in more detail. The importance of the putative GATA binding site was further supported by transfection of constructs in which the binding site was specifically inactivated, either by a short 13bp deletion or by a 4bp mutation, resulting in both cases in increased reporter activity. The same result was observed in three different osteosarcoma cell lines in which the experiment was repeated. Taken together, our experiments suggest that a repressor complex acts on the tenascin-W promoter, and the putative GATA site is involved in its recruitment to the promoter.

In an effort to identify the repressor complex, we used a probe designed to match the sequence containing the GATA site in a DNA-pulldown assay in order to isolate proteins from nuclear extracts that specifically bind to this sequence. While a similar approach is commonly used to confirm the binding of a known protein to DNA, by following the pull down by western blot (for an example see *(57)*), DNA-pulldown followed by mass spectrometry identification of unknown binding complexes is far less common *(58)*. In our protocol, two types of probes were employed, one corresponding to the native sequence and the other one carrying a mutated GATA site. The list of proteins enriched in the eluate corresponding to the wild type probe contained several interesting proteins.

The protein that displayed the greatest specificity for the wild type sequence is PHD finger protein 6 (PHF6). It was more than 8-fold enriched using the wild type probe versus the mutated one. PHF6 is a protein that has been linked to Börjeson-Forssman-Lehmann syndrome *(59)*, a form of X-linked mental retardation, and to acute myeloid leukemia *(60)*. It contains two PHD finger motifs and has probably a role in transcriptional regulation. PHD finger motifs recognize trimethylated histone 3 on lysine 4 *(61)*, thus it is not clear why PHF6 would bind to our oligo and why the 4-nucleotide mutation would affect its recruitment.

The most abundant protein retrieved in the eluates was THO complex subunit 4 (THOC4). It was 1.8-fold enriched in wild type probe eluates versus the one with the mutated probe. THOC4 is a molecular chaperone, thought to regulate dimerization, DNA binding, and transcriptional activity of basic region-leucine zipper proteins *(62)*.

The most interesting finding however was the presence of four members of the nucleosome remodeling and histone deacetylase (NuRD, aka Mi-2) complex *(27,*

*63, 64)*. The NuRD complex regulates gene expression through chromatin remodeling and is a well studied transcriptional repressor. Among the core components of the NuRD complex, our pulldown experiment identified the enzymatic subunit chromodomain-helicase-DNA-binding protein 4 (CHD4, aka Mi2β), the structural component retinoblastoma-binding protein 4 (RBBP4, aka RBAP48), and the two GATA zinc finger domain-containing proteins GATAD2A (aka P66α) and GATAD2B (aka P66β). The last two proteins contain a DNA-binding zinc finger domain very similar to the one shared by the GATA family of transcription factors. It is not implausible to think that the previously identified conserved GATA binding site in the promoter sequence is recognized by one or both of the proteins and that, in turn, GATAD2A and/or GATAD2B recruit the rest of the repression complex by protein/protein interactions *(65)*.

Another protein found, although in low quantity, in the pulldown eluted fractions was the polycomb protein SUZ12, part of the polycomb repressor complex 2 (PCR2) *(66)*. None of the other components of this complex were found in our experiments, but at least in ES cells it has been reported that NuRD and PCR2 can act together at specific loci *(67)*. Further experiments are necessary to confirm the specific binding before drawing any conclusion.

We tested if NuRD complex and PCR2 complex associate to the human tenascin-W promoter also in vivo, through chromatin immunoprecitation with antibody against CHD4 and SUZ12, respectively. Our preliminary results indicate that indeed NuRD complex is recruited to tenascin-W promoter. In contrast, we could not see an enrichment of the tenascin-W promoter in the SUZ12 enriched precipitate speaking against an association of the PCR2 complex with the tenascin-W promoter in vivo.

From our experiments a picture emerges suggesting that tenascin-W gene is kept silenced in cultured cells by the presence of the NuRD complex on its promoter due to recognition of the nucleotides *-131/-128* by GATAD2A or GATAD2B, and subsequent remodeling of the chromatin in a packed, non accessible form for transcription.

It would be interesting to test the association of the NuRD complex and tenascin-W promoter in murine cells. The GATA site we deem responsible for NuRD complex recruitment is not conserved in the murine sequence. For this reason, if our hypothesis is correct, the NuRD complex is not expected to associate with the

mouse tenascin-W promoter which remains accessible for transcription. This may explain why BMP-2 and TNF$\alpha$ can induce tenascin-W expression only in mouse cells and not in cells of human origin.

## IV.3 – Tenascin-W and bone marrow-derived mesenchymal stem cells

The main site of tenascin-W expression is the extracellular matrix of developing bones *(28, 68, 69)*. Various pre-osteoblastic cell lines can be differentiated to osteoblasts by BMP-2 stimulation *(70)*. Additionally, BMP-2 can stimulate tenascin-W expression in various murine cell lines *(28, 29)*. We presented here results that show that human mesenchymal stem cells induced to differentiate to osteoblasts by culture in standard osteogenic medium express endogenous tenascin-W (Figure III-9). Remarkably, this is the first observation of tenascin-W being expressed by cultured human cells.

To our knowledge, there are only two previous studies that measured tenascin-W transcript levels throughout osteogenic differentiation, both conducted on murine osteoprogenitor cell lines, and with contradictory results. Mikura et al., monitoring tenascin-W level in Kusa-A1 cells cultured in osteogenic medium for six days, observed a steady increase of tenascin-W transcript starting as soon as the differentiation was initiated *(71)*. In the second and more recent study, Morgan et al. followed tenascin-W level in MC3T3-E1 cells during three weeks of osteogenic culture and reported a marked reduction in the expression with differentiation, that was reduced to one half during the first week *(72)*. Our results from human MSC cultured in osteogenic medium for twelve days were consistent with Mikura's observations of a significant increase in tenascin-W expression, with differentiation and are at least in partial contrast with Morgan's observations, since we didn't follow tenascin-W in the subsequent weeks. Morgan et al. commented on Mikura et al. that the opposite results are due to the less mature nature of Kusa-A1 cells compared to MC3T3-E1 cells, claiming that their cell model is more representative of the in vivo process. Although for the reasons previously exposed, one has to be careful to compared results obtained in human with ones obtained in mouse when speaking about tenascin-W, our models, the 3D culture model of endochondral bone

formation and the MSC-derived osteoblasts, show how tenascin-W is expressed in correlation with early mineralization.

Mesenchymal stem cells have the potential to differentiate in a variety of cells like osteoblasts, chondrocytes, adipocytes, fibroblasts and muscle cells *(73)*. We showed that MSC cultured in osteogenic medium start expressing tenascin-W, indicating that these cells have the ability to release the repression that keeps the gene silenced. What about tenascin-W expression when MSC are differentiated in other directions? When we cultured the MSC in adipogenic medium we did not detect any tenascin-W expression in the derived adipocytes (data not shown). Thus, this in vitro model resembles the tenascin-W expression in vivo, which was restricted to differentiating bone.

The major source of MSC is bone marrow; MSC are traveling in the blood stream and are able to home at sites of inflammation and tissue repair *(74)*. It has recently been shown that MSC are normally also recruited to tumor sites *(75, 76)*, where they differentiate to tumor-associated fibroblasts and become part of the tumor microenvironment *(15)*.

We previously reported our observation of tenascin-W to be localized in the proximity of blood vessels in a variety of solid tumors. We want to propose here a speculation to explain this. MSC may be attracted from tumors by chemokines and factors secreted by tumor cells and are induced to differentiate as soon as they emerge from the blood stream. As they differentiate, they start expressing and secreting tenascin-W into the surrounding tissue. Tenascin-W in turn will influence the behavior of surrounding cells, for instance by enhancing the motility of endothelial cells and thus contribute to the extension of the tumor blood vessel network.

As hypothetical this interpretation is at the moment, it could prompt and guide future investigations, as it remains to be established whether MSC differentiation other than to osteoblasts triggers tenascin-W expression.

# APPENDIX

# V. APPENDIX

# V.1 Experimental procedures (unpublished results)

**SEAP constructs**

Plasmids *pGL3-TNW-2000bp*, *pGL3-TNW-1000bp*, *pGL3-TNW-500bp*, *pGL3-TNW-350bp*, and *pGL3-TNW-250bp*, containing various lengths of the human tenascin-W promoter inserted in the pGL3-basic vector (Promega) were obtained from Dr. Martin Degen. The inserts were excised by digestion with NheI and XhoI and directionally cloned in the MCS of pSEAP2-basic (Clontech), generating the plasmids *pSEAP-TNW(-1800)*, *pSEAP-TNW(-957)*, *pSEAP-TNW(-512)*, *pSEAP-TNW(-252)*, and *pSEAP-TNW(-148)*.

All successive PCR reactions were performed using the Expand High Fidelity PCR System (Roche) and plasmid *pSEAP-TNW(-512)* as template. Reverse primer 5'-AGAAGTCCGGGTTCTCCTCCTCA-3' was used together with forward primer 5'-TTTGCTAGCGCTCATTTCTTTCTGTGCTAAAGG-3' or forward primer 5'-TTTGCTAGCCACTTTTGAACCCCGAGACCCAG-3'; the resulting amplicons were digested with NheI and XhoI and cloned in pSEAP2-basic to obtain *pSEAP-TNW(-319)* and *pSEAP-TNW(-252)* respectively.

The plasmids with internal deletions were obtained as follows. In the first set of PCR reactions, the forward primer listed in Table 1 (upper section) was used together with the common reverse primer mentioned above, while the common forward primer 5'-GGTACCGAGCTCTTACGCGT-3' was used with the appropriate reverse primer listed in Table 1. The corresponding partially overlapping PCR products were gel purified, mixed at equimolar ratio and annealed by slowly cooling from 95°C to 55°C in 10 min. The second set of PCR used the common forward primer and the common reverse primer to amplify the partially overlapping amplicons annealed in the previous step. The PCR products were digested with NheI and XhoI and cloned in pSEAP2-basic to obtain the plasmid listed in Table 1. The construct *pSEAP-TNW(-512)MUT* was obtained by site directed mutagenesis using the following

primers: forward primer 5'-GCTCATCTCGTTTTAGCAGAGTCCCTG-3'; reverse primer 5'- CTAAAACGAGATGAGCAATTCCTTC-3' (mutated bases are underlined).

| ***Cloning*** | *Forward primer (5'-3')* | *Reverse primer (5'-3')* |
|---|---|---|
| **pSEAP-TNW(-512)Δ-423/-319** | TGAGGGTCTCTCACTTTTGAACCCCGAGA | TTCAAAAGTGAGAGACCCTCAGGGACAGAA |
| **pSEAP-TNW(-512)Δ-319/-252** | CTTTATAAATGGGATTCACTTAAATGGAAAC | TAAGTGAATCCCATTTATAAAGTTTCTTTCTCTT |
| **pSEAP-TNW(-512)Δ-252/-148** | CCTTATTCTGAGAAGGAATTGCTCATTATC | ATTCCTTCTCAGAATAAGGATATTAAAAG |
| **pSEAP-TNW(-512)Δ-148/-79** | GTTAGAATAATTTGCTCCTCCTCTGGCCTAG | AGGAGCAAATTATTCTAACTAGGAAAGAAA |
| **pSEAP-TNW(-512)Δ-79/-59** | AGGAGTCTCCAGACAGGATTTAAACCCAGGA | AAATCCTGTCTGGAGACTCCTGGTGTTTTCC |
| **pSEAP-TNW(-512)Δ-59/-34** | GGCCTAGACAAAGCCAAGGAGAGACGAGAAC | TCCTTGGCTTTGTCTAGGCCAGAGGAGGAGC |
| **pSEAP-TNW(-512)Δ-34/+27** | CCAGGAAGGGACCGGCTCACAGGAGCAGCAG | GTGAGCCGGTCCCTTCCTGGGTTTAAATCC |
| **pSEAP-TNW(-512)Δ+1/+78** | GACGACCAGCCTCGAGATCTGCGATCTAAG | CAGATCTCGAGGCTGGTCGTCCCTGGTTCT |
| **pSEAP-TNW(-512)Δ-148/-136** | AGTTAGAATAACTCATTATCTTTTAGCAGAGT | AGATAATGAGTTATTCTAACTAGGAAAGAAAAA |
| **pSEAP-TNW(-512)Δ-136/-122** | GAGAAGGAATTGGCAGAGTCCCTGCTAGGAAGGG | AGGGACTCTGCCAATTCCTTCTCTTATTCTAACTA |
| **pSEAP-TNW(-512)Δ-122/-100** | TATCTTTTAAGGAAAACACCAGGAGTCT | TGTTTTCCTTAAAAGATAATGAGCAATTC |
| **pSEAP-TNW(-512)Δ-100/-79** | TAGGAAGGGTTTGCTCCTCCTCTGGCCT | AGGAGCAAACCCTTCCTAGCAGGGACTCTGCTA |
| ***qPCR*** | | |
| **TNW** | ATGCCCTCACAGAAATTGACAG | TCTCTGGTCTCTTGGTCGTC |
| **ALPL** | GCTGGCAGTGGTCAGATGTT | CTATCCTGGCTCCGTGCTC |
| **TBP** | TGCACAGGAGCCAAGAGTGAA | CACATCACAGCTCCCCACCA |
| ***ChIP*** | | |
| **TNW -425/-215** | CTCTGCTCATTTCTTTCTGTGCTA | GCTAAAAATACTGGAGGCTGTTTC |
| **TNW Ex10-11** | CTCTTCCTCCAGGGGCTTAC | GACATGGTCTCTGCTCACCA |
| **LINE** | TTCCAGGCAAGAATCAACAA | CTTGGACCACTTGGTTAGGG |

***Table V.1*** *– Primers used in this study*

### Cell culture and transfection

HT1080 (ATCC #CCL-121), Saos-2 (ATCC #HTB-85), KRIB ( ) and U2OS (ATCC #HTB-96) cells were cultured in Dulbecco's Modified Eagle Medium (DMEM) supplemented with 10% FCS, 2mM/l glutamine and antibiotics (100 U/ml penicillin; 100 µg/ml streptomycin). Cells were plated in 12-well plates at a density of 50000 cells/well, in growth medium. The next day, at cell confluence of about 60-70%, the medium was exchanged with DMEM 0.3% FCS and the cells were transfected by JetPEI (Polyplus) with 0.6 µg/well of total DNA (pSEAP reporter construct and pMetLuc for normalization mixed at 1:20 molar ratio). After 48h in cultures, an

aliquot of conditioned medium was collected, centrifuged max speed for 1 min and used directly for SEAP or MetLuc assays.

**Reporter gene assay**

The measurement of the amount of alkaline phosphatase in the culture medium was performed using the SEAP Reporter Gene Assay kit (Roche), following the protocol of the manufacturer. Ready-To-Glow secreted luciferase reporter system (Clontech) was used for the luciferase quantification in the culture medium, according to the instructions of the manufacturer. Chemiluminescence levels were read with a luminometer Mithras LB940 (Berthold technologies). SEAP luminescence values of each sample were divided by the corresponding luciferase luminescence values, to obtain the normalized SEAP luminescence. Although different combinations of SEAP constructs were transfected in triplicate in different experiments, the plasmid *pSEAP-TNW(-512)* was included in all experiment and was thus used as a calibrator to compare different experiments. Normalized SEAP luminescence of each sample of each experiment was divided by the *pSEAP-TNW(-512)* normalized SEAP luminescence of the same experiment, to obtain the normalized relative SEAP activity. The geometric mean of the normalized relative SEAP activities among all the experiments is displayed in the graphs. Error bars are standard error of the mean among all the replicates considered. Mann-Whitney U test was performed to test the statistical significance of the results when indicated.

**In silico analysis for conserved sequences and transcription factor binding sites**

The genomic location of the human tenascin-W gene was examined using the UCSC genome browser (http://genome.ucsc.edu/) and the ECR browser (http://ecrbrowser.dcode.org/). To look for predicted transcription factor binding sites in the genomic sequence, we used MatInspector (http://www.genomatix.de) and rVISTA 2.0 (http://rvista.dcode.org/).

**DNA pull-down**

Approximately 8 x $10^7$ HT1080 cells were harvested in cold PBS by scraping the culture dishes with a rubber policeman. Cells were spun at 400 x g for 5 min at 4°C and the pellet was resuspended in lysis buffer (10 mM HEPES; 15 mM KCl; 2 mM EDTA; 0.5 mM spermidine; 0.15 mM spermine; 0.5% NP-40; 1 mM DTT, 0.4 mM Pefabloc SC [Roche]; complete protease inhibitors cocktail [Roche]). After 5 min incubation on ice, cells were vortexed (complete cell lysis was confirmed at the microscope after staining a drop of lysate with Tripan-blue). To separate the intact nuclei from cytoplasm and membrane debris, the suspension was spun at 1900 x g for 20 min at 4 °C through a sucrose cushion (lysis buffer with addition of 0.88 M sucrose). The nuclei pellet was resuspended in nuclear lysis buffer (10 mM HEPES; 550 mM KCl; 0.1 mM EDTA; 10% glycerol; 3 mM $MgCl_2$; 1 mM DTT; 0.4 mM Pefabloc SC; complete protease inhibitors cocktail) and incubated under rotation for 30 min at 4 °C. After 20 min centrifugation at 5000 x g at 4 °C, the supernatant was collected and stored at -80 °C. The 5'-biotinylated forward oligo 5'-AGAGAAGGAATTGCTCATTATCTTTTAGCAG-3' and the unlabeled reverse 5'-CTGCTAAAAGATAATGAGCAATTCCTTCTCT-3' were annealed to obtain the biotinylated probe WT; 5'-biotinylated forward oligo 5'-AGAGAAGGAATTGCTCATCTCGTTTTAGCAG-3' and the unlabeled reverse 5'-CTGCTAAAACGAGATGAGCAATTCCTTCTCT-3' were annealed to obtain the biotinylated probe MUT, containing the underlined mutation. Corresponding unlabeled probes were obtained by annealing unlabeled oligos.

Nuclear extract was diluted in 2.6 volumes of nuclear dilution buffer (27.7 mM Tris-HCl pH 8; 1.35 mM EDTA; 16.9% glycerol; 0.07% NP-40; 1 mM DTT; 0.4 mM Pefabloc SC; complete protease inhibitors cocktail) and 600 ng were incubated with approximately 10 μg of biotinylated probe (WT or MUT), 50 μg of competitor unlabeled probe (MUT or WT, respectively), 100 μg of poly[d(I-C)] (Roche) in binding buffer (20 mM Tris-HCl pH 8; 150 mM KCl; 1 mM EDTA; 15% glycerol; 0.05% NP-40; 1 mM DTT; 0.4 mM Pefabloc SC; complete protease inhibitors cocktail). A control sample was incubated with a 1:1 mixture of unlabeled probe and omitting the biotinylated probe (ctr). After 1 hour of rotation at 4 °C, 30 μL of previously washed Streptavidin Magnespheres paramagnetic particles (Promega)

equilibrated in binding buffer were added to the suspension, and the mixture was further incubated for 1 hour. The paramagnetic particles were then washed four times for 5 min in binding buffer at room temperature. The elution step consisted in 1 hour incubation at room temperature in presence of 100 μg of the corresponding unlabeled probe in binding buffer. The supernatant was collected, subjected to TCA precipitation and submitted to mass spectrometry analysis.

**Mass spectrometry**

The eluted proteins were precipitated with TCA followed by acetone washing of the protein pellets. The proteins were reduced with TCEP, alkylated with iodoacetamide and cleaved with trypsin. Peptides were injected onto a reversed phase column for liquid chromatography-tandem mass spectrometry (LC-MSMS) analysis in the information-dependent acquisition mode. Electrospray ionization LC-MSMS was performed using a Magic C18 HPLC column (75 µm × 10 cm; Swiss BioAnalytics) with a 1200 Nano-HPLC system (Agilent Technologies) connected to a LTQ Orbitrap Velos (Thermo Scientific). The peptides were loaded onto a peptide captrap (Michrom BioResources) at a flow rate of 10 µl/min for 5 minutes in buffer A (H2O/acetonitrile/formic acid/trifluoroacetic acid, 98/2/0.1/0.005, v/v/v/v). They were eluted at a flow rate of 400 nl/min with a linear gradient of B (acetonitrile/H2O/formic acid/trifluoroacetic acid, 80/20/0.1/0.005, v/v/v/v) in A as follows: 0–10% in 3 min, 10-40% in 80 min, 40-55% in 10 min, 55%-100% in 2 min followed by a 2 min flush of 100% B. Information-dependent acquisition analyses were done according to the manufacturer's recommendations, i.e. 1 survey scan at 60K resolution in the Orbitrap cell was followed by 20 product ion scans in the linear ion trap, and precursors were excluded for 15 second after their second occurrence. Individual MSMS spectra, containing sequence information were compared with the program Mascot against the protein sequence database Swiss-Prot 2010_09 (Perkins et al 1999). Carboxyamidomethylation of cystein (+57.0245) was set as a fixed modification and oxidation of methionine (+15.9949 Da), acetylation of the protein N-terminus (+42.0106), deamidation of asparagine and glutamine (-0.9840) and glutamine to pyroglutamic acid (-17.0265) were selected as variable modifications.

Parent tolerance was 5 PPM and fragment tolerance 0.6 Da. Quantitative analyses of the peptides were done with the program ProgenesisLC (Nonlinear).

### qPCR

Total RNA or mRNA was extracted using the RNeasy kit (QIAGEN) or Dynabeads mRNA Direct kit (Invitrogen), respectively. 0.2-1 μg of RNA was reverse transcribed to cDNA using High Capacity cDNA Reverse Transcription kit (Applied Biosystem), and the cDNA was diluted 1:6. The PCR reactions were performed using a StepOne Plus qPCR system (Applied Biosystems) in 20 μL total volume on 5 μL of diluted cDNA, using Platinum SYBR Green qPCR SuperMix-UDG (Invitrogen) and the gene specific primers listed in Table V.1 (middle section). The raw fluorescence data were exported and analyzed using Miner (http://www.ewindup.info/miner/version2/). Tata-BOX binding protein (TBP) was considered as housekeeping gene for normalization purposes.

### Antibodies

Anti-tenascin-W mAb 56O *(35)* was used for immunofluorescence at 1:50 dilution.
The antibodies employed in ChIP are rabbit anti-CHD4 pAb (cat #ab72418, Abcam), rabbit anti-SUZ12 mAb (cat #D39F6, Cell Signalling), anti-mouse-IgG rabbit serum (Lot No. 0111-0082, cat #29204, Cappel Organon Teknika).

### Chromatin immunoprecipitation

A total of 4 x $10^7$ HT1080 cells were harvested for each experiment. One volume of formaldehyde buffer (50 mM HEPES pH=8.0, 1 mM EDTA, 0.5 mM EGTA, 100 mM NaCl, 11% formaldehyde) was added to ten volumes of culture medium, and the cells were incubated at room temperature for 10 min. To stop the cross-linking, 0.125 M glycine was added, and the incubation was continued on ice for 10 min. All procedures were carried out at 0 to 4°C unless specifically stated otherwise. Cells were rinsed twice with PBS, then collected using a rubber policeman and resuspended in PBS containing protease inhibitors (complete mini, EDTA-free protease inhibitors cocktail tablets, Roche). The cells were washed once in wash

buffer 1 (10 mM Tris pH=8.0, 10 mM EDTA, 0.5 mM EGTA, 0.25% Triton X-100), washed twice in wash buffer 2 (10 mM Tris pH=8.0, 1 mM EDTA, 0.5 mM EGTA, 200 mM NaCl), and resuspended in lysis buffer (50 mM HEPES/KOH pH=7.5, 500 mM NaCl, 1 mM EDTA, 1% Triton X-100, 0.1% deoxycholic acid, 0.1% SDS, and protease inhibitors) and incubated 10 min. After shearing the DNA by sonication, the lysate was clarified by centrifugation (at 14000 x g for 10 min) and then pre-incubated with a mixture of protein-A (75%) and protein-G (25%) magnetic beads (Dynabeads, Invitrogen), previously blocked with 1 mg/mL BSA and 500 μg/mL of tRNA. The clarified chromatin was divided in 70 μg aliquots (ca 500 μL) for immunoprecipitation (IP). After the addition of 1 to 10 μg of antibody and overnight incubation, 20 μl of protein-A/protein-G blocked magnetic beads were added to the lysate and mixed by rotation for an additional 3 h. the beads were washed twice with 1 mL of Lysis buffer without protease inhibitors with rotation for 5 min, once with DOC buffer (10 mM Tris pH=8.0, 0.25 LiCl, 0.5% NP-40, 0.5% deoxycholic acid, 1 mM EDTA), and then once with TE buffer. Protein-DNA cross-linked material was then eluted by vortexing in 150 μl of elution buffer (100 mM $NaHCO_3$, 1% SDS) at room temperature for 15 min. After the beads were pelleted by centrifugation (14000 x g for 2 min at room temperature) a second elution was performed and eluates were pooled.

The procedure to reverse cross-linking consisted in a preliminary incubation for 30 min at 37°C with 0.2 mg/mL RNase A, followed by addition of 10 mM EDTA, 40 mM Tris pH=6.5, 50 μg/mL Proteinase K to the IP fraction, or 1% SDS, 100 mM NaCl, 200 μg/mL Proteinase K to the Input fraction, and incubated 3 h at 55°C and overnight at 65°C. The DNA was purified using a QIAquick PCR purification kit (Qiagen) and then subjected to real-time quantitative PCR assay with SYBR green.

PCR assays were performed in triplicate from two independent immunoprecipitations. The abundance of specifically immunoprecipitated DNA relative to input was calculated from the $C_T$ values for the samples, and the amplification efficiency was determined using Miner. The PCR primers used are shown in Table V.1 (lower section).

**Primary BMSC culture and differentiation**

Bone marrow-derived mesenchymal stem cells (BMSC), isolated from three patients (#169, #184 and #199), expanded to P3 and frozen, were obtained from Dr. Arnaud Scherberich (University Hospital of Basel). Cells were cultured in α-MEM containing 10% FCS, 1% HEPES, 1% sodium pyruvate, 10 mM glutamine (control medium), supplemented with 5 ng/mL FGF2. Osteogenic differentiation medium consisted of control medium supplemented with 100 nM dexamethasone (cat #D-2915, Sigma), 10 mM β-glycerophosphate (cat #G-9891, Sigma), and 100 μM ascorbic acid 2-phosphate (cat #A-8960, Sigma). Medium was exchanged every second day. To test for osteogenic differentiation, cells were washed with PBS, fixed for 10 min with Formal-fixx (Thermo-Scientific) at RT, and washed twice with PBS. Cells were then incubated 2 min at RT in alkaline phosphatase activity staining solution (one SIGMAFAST BCIP/NBT tablet [cat #B5655, Sigma] dissolved in 10 mL $H_2O$). After three washes in PBS, pictures of stained cells were acquired with a Nikon Eclipse 80i microscope equipped with a Leica DFC420 color camera.

**Immunofluorescence**

Cells were cultured on 8-chambers slide (cat #354108, BD Falcon) either in control or in osteogenic medium, for the indicated amount of time. Cells were then fixed for 10 min in Formal-fixx (Thermo-Scientific) at RT, rinsed with PBS and additionally fixed for 10 min in methanol at -20°C. After 30 min blocking at RT in blocking buffer (PBS/0.01%Tween, 1% BSA), cells were incubated O/N at 4°C in blocking buffer containing the primary antibody. After three washes in PBS, cells were incubated for one hour at RT in PBS/0.01%Tween containing the Alexa-488-conjugated secondary antibody (1:200) and Hoechst (1:2000). Cells were then washed three times with PBS and mounted in ProLong Gold Antifade reagent (Invitrogen). Pictures were acquired using a Zeiss Axioimager Z1 connected to an AxioCam MRm and processed with ImageJ.

# V.2 Supplementary data

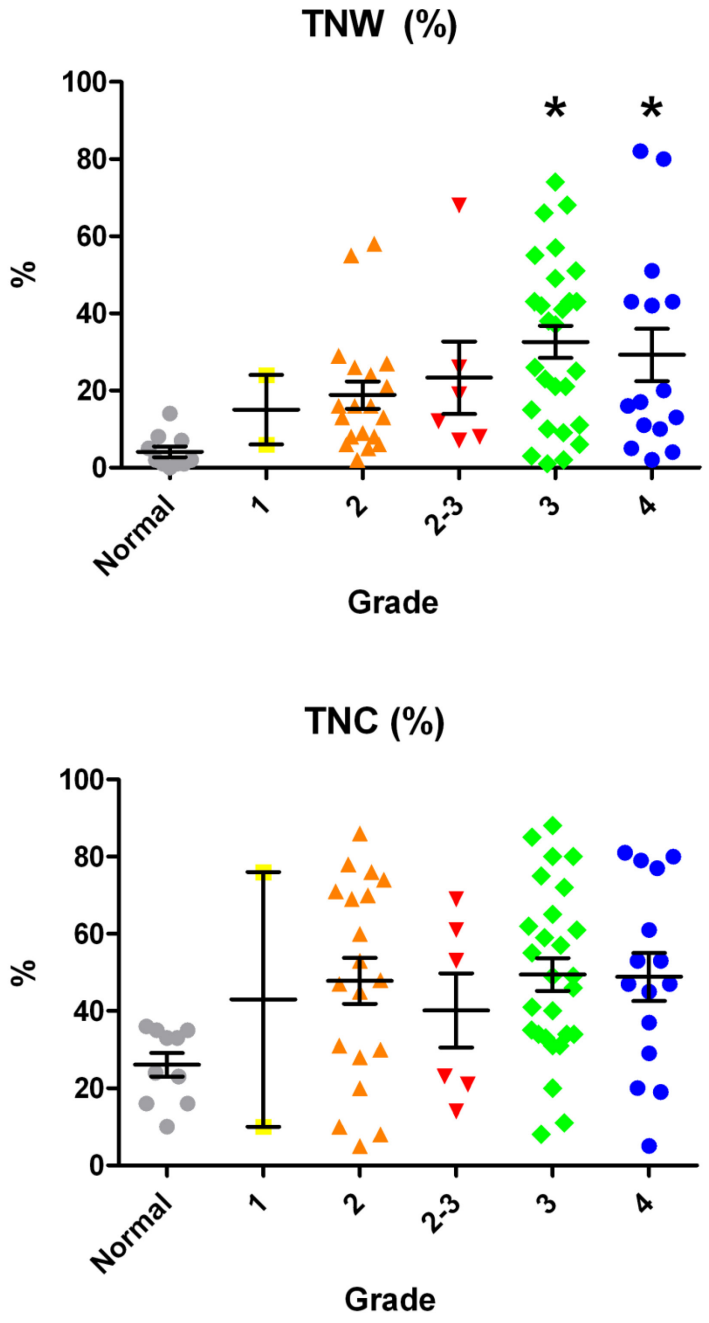


***Figure V.2.1*** *– Correlation between tenascin-W and tenascin-C and tumor grade in lung cancer samples. Sixty-nine kidney tumor samples, spotted on a frozen TMA were stained for of tenascin-W and tenascin-C. The area of the section stained for tenascin-W or tenascin-C was quantified as described in Section III.2.1 - Materials and Methods. Samples were grouped according with the tumor grade and the percentage of staining for each sample was plotted as a spot. Asterisks indicate* $p < 0.05$ *in a non parametric group test.*

# V.3 References


1. D. Hanahan, R. a Weinberg, Hallmarks of cancer: the next generation., *Cell* 144, 646-74 (2011).

2. M. Greaves, C. C. Maley, Clonal evolution in cancer., *Nature* 481, 306-13 (2012).

3. J. P. Sleeman et al., Concepts of metastasis in flux: The stromal progression model., *Seminars in cancer biology* (2012).

4. A. Lujambio, S. W. Lowe, The microcosmos of cancer., *Nature* 482, 347-55 (2012).

5. D. Hanahan, R. a Weinberg, The hallmarks of cancer, *cell* 100, 57-70 (2000).

6. J. E. Dancey, P. L. Bedard, N. Onetto, T. J. Hudson, The genetic basis for cancer treatment decisions., *Cell* 148, 409-20 (2012).

7. G. Lorusso, C. Rüegg, The tumor microenvironment and its contribution to tumor evolution toward metastasis., *Histochemistry and cell biology* 130, 1091-103 (2008).

8. D. Hanahan, L. M. Coussens, Accessories to the Crime: Functions of Cells Recruited to the Tumor Microenvironment, *Cancer Cell* 21, 309-322 (2012).

9. M. J. Bissell, D. Radisky, Putting tumours in context., *Nature reviews. Cancer* 1, 46-54 (2001).

10. Y. Kim, M. a Stolarska, H. G. Othmer, The role of the microenvironment in tumor growth and invasion., *Progress in biophysics and molecular biology* 106, 353-79 (2011).

11. L. M. Coussens, Z. Werb, Inflammation and cancer., *Nature* 420, 860-7 (2002).

12. B. Ruffell, N. I. Affara, L. M. Coussens, Differential macrophage programming in the tumor microenvironment., *Trends in immunology* 33, 119-26 (2012).

13. D. Neri, R. Bicknell, Tumour vascular targeting., *Nature reviews. Cancer* 5, 436-46 (2005).

14. A. Aboussekhra, Role of cancer-associated fibroblasts in breast cancer development and prognosis., *The International journal of developmental biology* 55, 841-9 (2011).

15. E. L. Spaeth et al., Mesenchymal stem cell transition to tumor-associated fibroblasts contributes to fibrovascular network expansion and tumor progression., *PloS one* 4, e4992 (2009).

16. M. Allen, J. Louise Jones, Jekyll and Hyde: the role of the microenvironment on the progression of cancer., *The Journal of pathology* 223, 162-76 (2011).

17. K. S. Midwood, G. Orend, The role of tenascin-C in tissue injury and tumorigenesis., *Journal of cell communication and signaling* 3, 287-310 (2009).

18. B. Carnemolla et al., A Tumor-associated Fibronectin Isoform Generated by Alternative Splicing of Messenger RNA Precursors, *The Journal of cell biology* 108 (1989).

19. M. J. Paszek et al., Tensional homeostasis and the malignant phenotype., *Cancer cell* 8, 241-54 (2005).

20. S. Mitra, K. Stemke-Hale, G. B. Mills, S. Claerhout, Interactions between tumor cells and microenvironment in breast cancer: A new opportunity for targeted therapy., *Cancer science* 103, 400-7 (2012).

21. A. Albini, M. B. Sporn, The tumour microenvironment as a target for chemoprevention., *Nature reviews. Cancer* 7, 139-47 (2007).

22. D. E. Ingber, Can cancer be reversed by engineering the tumor microenvironment?, *Seminars in cancer biology* 18, 356-64 (2008).

23. R. P. Tucker et al., Phylogenetic analysis of the tenascin gene family: evidence of origin early in the chordate lineage., *BMC evolutionary biology* 6, 60 (2006).

24. K. S. Pollard, M. J. Hubisz, K. R. Rosenbloom, A. Siepel, Detection of nonneutral substitution rates on mammalian phylogenies., *Genome research* 20, 110-21 (2010).

25. G. G. Loots, I. Ovcharenko, rVISTA 2.0: evolutionary analysis of transcription factor binding sites., *Nucleic acids research* 32, W217-21 (2004).

26. A. Ghatnekar, M. Trojanowska, GATA-6 is a novel transcriptional repressor of the human Tenascin-C gene expression in fibroblasts., *Biochimica et biophysica acta* 1779, 145-51 (2008).

27. P. McDonel, I. Costello, B. Hendrich, Keeping things quiet: roles of NuRD and Sin3 co-repressor complexes during mammalian development., *The international journal of biochemistry & cell biology* 41, 108-16 (2009).

28. A. Scherberich et al., Murine tenascin-W: a novel mammalian tenascin expressed in kidney and at sites of bone and smooth muscle development., *Journal of cell science* 117, 571-81 (2004).

29. A. Scherberich et al., Tenascin-W is found in malignant mammary tumors, promotes alpha8 integrin-dependent motility and requires p38MAPK activity for BMP-2 and TNF-alpha induced expression in vitro., *Oncogene* 24, 1525-32 (2005).

30. E. Martina, R. Chiquet-Ehrismann, F. Brellier, Tenascin-W: an extracellular matrix protein associated with osteogenesis and cancer., *The international journal of biochemistry & cell biology* 42, 1412-5 (2010).

31. C. Scotti et al., Recapitulation of endochondral bone formation using human adult mesenchymal stem cells as a paradigm for developmental engineering., *Proceedings of the National Academy of Sciences of the United States of America* 107, 7251-6 (2010).

32. M. A. Bourdon, C. J. Wikstrand, H. Furthmayr, T. J. Matthews, D. D. Bigner, Human Glioma-Mesenchymal Extracellular Matrix Antigen Defined by Monoclonal Antibody Human Glioma-Mesenchymal Monoclonal Antibody Extracellular Matrix Antigen Defined by, *Cancer Research* , 2796-2805 (1983).

33. R. Chiquet-Ehrismann, M. Chiquet, Tenascins: regulation and putative functions during pathological stress., *The Journal of pathology* 200, 488-99 (2003).

34. M. Degen et al., Tenascin-W is a novel marker for activated tumor stroma in low-grade human breast cancer and influences cell behavior., *Cancer research* 67, 9169-79 (2007).

35. M. Degen et al., Tenascin-W, a new marker of cancer stroma, is elevated in sera of colon and breast cancer patients., *International journal of cancer.* 122, 2454-61 (2008).

36. D. S. Guttery, J. a Shaw, K. Lloyd, J. H. Pringle, R. a Walker, Expression of tenascin-C and its isoforms in the breast., *Cancer metastasis reviews* 29, 595-606 (2010).

37. S. S. Brack, M. Silacci, M. Birchler, D. Neri, Tumor-targeting properties of novel antibodies specific to the large isoform of tenascin-C., *Clinical cancer research* 12, 3200-8 (2006).

38. K. Tanaka, N. Hiraiwa, H. Hashimoto, Y. Yamazaki, M. Kusakabe, Tenascin-C regulates angiogenesis in tumor through the regulation of vascular endothelial growth factor expression., *International journal of cancer.* 108, 31-40 (2004).

39. D. Zagzag et al., Tenascin-C Promotes Microvascular Cell Migration and Phosphorylation of Focal Adhesion Kinase Tenascin-C Promotes Microvascular Cell Migration and Phosphorylation of Focal, *Proteins* , 2660-2668 (2002).

40. D. A. M. Mustafa et al., Angiogenesis proteome A proteome comparison between physiological angiogenesis and angiogenesis in glioblastoma Angiogenesis proteome, *Biochemistry* (2012).

41. F. Brellier et al., The adhesion modulating properties of tenascin-w., *International journal of biological sciences* 8, 187-94 (2012).

42. G. Orend, R. Chiquet-Ehrismann, Tenascin-C induced signaling in cancer., *Cancer letters* 244, 143-63 (2006).

43. F. Brellier, R. Chiquet-Ehrismann, How do tenascins influence the birth and life of a malignant cell?, *Journal of cellular and molecular medicine* 16, 32-40 (2012).

44. K. S. Midwood, T. Hussenet, B. Langlois, G. Orend, Advances in tenascin-C biology., *Cellular and molecular life sciences* 68, 3175-99 (2011).

45. D. A. Reardon, M. R. Zalutsky, D. D. Bigner, Antitenascin-C monoclonal antibody radioimmunotherapy for malignant glioma patients, *Expert Review of Anticancer Therapy* , 675-687 (2007).

46. C. Schliemann et al., Three clinical-stage tumor targeting antibodies reveal differential expression of oncofetal fibronectin and tenascin-C isoforms in human lymphoma., *Leukemia research* 33, 1718-22 (2009).

47. M. Steiner, D. Neri, Antibody-radionuclide conjugates for cancer therapy: historical considerations and new trends., *Clinical cancer research* 17, 6406-16 (2011).

48. H. Y. Ko, K.-J. Choi, C. H. Lee, S. Kim, A multimodal nanoparticle-based cancer imaging probe simultaneously targeting nucleolin, integrin αvβ3 and tenascin-C proteins., *Biomaterials* 32, 1130-8 (2011).

49. B. J. Hicke et al., Tumor targeting by an aptamer., *Journal of nuclear medicine* 47, 668-78 (2006).

50. R. Gherzi, M. Ponassi, B. Gaggero, L. Zardi, The first untranslated exon of the human tenascin-C gene plays a regulatory role in gene transcription., *FEBS letters* 369, 335-9 (1995).

51. D. W. Copertino, S. Jenkinson, F. S. Jones, G. M. Edelman, Structural and functional similarities between the promoters for mouse tenascin and chicken cytotactin., *Proceedings of the National Academy of Sciences of the United States of America* 92, 2131-5 (1995).

52. D. W. Copertino, G. M. Edelman, F. S. Jones, Multiple promoter elements differentially regulate the expression of the mouse tenascin gene., *Proceedings of the National Academy of Sciences of the United States of America* 94, 1846-51 (1997).

53. F. S. Jones, K. L. Crossin, B. a Cunningham, G. M. Edelman, Identification and characterization of the promoter for the cytotactin gene., *Proceedings of the*

*National Academy of Sciences of the United States of America* 87, 6497-501 (1990).

54. R. Gherzi et al., Human Tenascin Gene. Structure of the 5'-region, identification, and characterization of the transcription regulatory sequences, *The Journal of biological chemistry* 270, 3429-3434 (1995).

55. R. C. Hardison, Conserved noncoding sequences are reliable guides to regulatory elements., *Trends in genetics* 16, 369-72 (2000).

56. K. R. Bradnam, I. Korf, Longer first introns are a general property of eukaryotic gene structure., *PloS one* 3, e3093 (2008).

57. M. Mojsin et al., Rapid detection and purification of sequence specific DNA binding proteins using magnetic separation, *Journal of the Serbian Chemical Society* 71, 135-141 (2006).

58. D. E. Reed, X. M. Huang, J. a Wohlschlegel, M. S. Levine, K. Senger, DEAF-1 regulates immunity gene expression in Drosophila., *Proceedings of the National Academy of Sciences of the United States of America* 105, 8351-6 (2008).

59. M. Mangelsdorf, E. Chevrier, A. Mustonen, D. J. Picketts, Börjeson-Forssman-Lehmann Syndrome due to a novel plant homeodomain zinc finger mutation in the PHF6 gene., *Journal of child neurology* 24, 610-4 (2009).

60. P. Van Vlierberghe et al., PHF6 mutations in adult acute myeloid leukemia., *Leukemia* 25, 130-4 (2011).

61. Y. Zhang, It takes a PHD to interpret histone methylation., *Nature structural & molecular biology* 13, 572-4 (2006).

62. L. Bruhn, a Munnerlyn, R. Grosschedl, ALY, a context-dependent coactivator of LEF-1 and AML-1, is required for TCRalpha enhancer function., *Genes & Development* 11, 640-653 (1997).

63. S. a Denslow, P. a Wade, The human Mi-2/NuRD complex and gene regulation., *Oncogene* 26, 5433-8 (2007).

64. J. Ramírez, J. Hagman, The Mi-2/NuRD complex, *DNA Sequence* 4, 532-536 (2009).

65. M. Brackertz, J. Boeke, R. Zhang, R. Renkawitz, Two highly related p66 proteins comprise a new family of potent transcriptional repressors interacting with MBD2 and MBD3., *The Journal of biological chemistry* 277, 40958-66 (2002).

66. H. Richly, L. Aloia, L. Di Croce, Roles of the Polycomb group proteins in stem cells and cancer., *Cell death & disease* 2, e204 (2011).

67. N. Reynolds et al., NuRD-mediated deacetylation of H3K27 facilitates recruitment of Polycomb Repressive Complex 2 to direct gene repression, *The EMBO Journal* 31, 593-605 (2011).

68. P. Weber, D. Montag, M. Schachner, R. R. Bernhardt, Zebrafish tenascin-W, a new member of the tenascin family., *Journal of neurobiology* 35, 1-16 (1998).

69. C. V. Meloty-Kapella, M. Degen, R. Chiquet-Ehrismann, R. P. Tucker, Avian tenascin-W: expression in smooth muscle and bone, and effects on calvarial cell spreading and adhesion in vitro., *Developmental dynamics* 235, 1532-42 (2006).

70. T. Katagiri et al., Bone morphogenetic protein-2 converts the differentiation pathway of C2C12 myoblasts into the osteoblast lineage., *The Journal of cell biology* 127, 1755-66 (1994).

71. A. Mikura et al., Association of tenascin-W expression with mineralization in mouse calvarial development., *Congenital anomalies* 49, 77-84 (2009).

72. J. M. Morgan, A. Wong, C. E. Yellowley, D. C. Genetos, Regulation of tenascin expression in bone., *Journal of cellular biochemistry* 22305 (2011), doi:10.1002/jcb.23265.

73. S. a Bergfeld, Y. a DeClerck, Bone marrow-derived mesenchymal stem cells and the tumor microenvironment., *Cancer metastasis reviews* 29, 249-61 (2010).

74. D. Gao, V. Mittal, The role of bone-marrow-derived cells in tumor growth, metastasis initiation and progression., *Trends in molecular medicine* 15, 333-43 (2009).

75. S. Kidd et al., Direct evidence of mesenchymal stem cell tropism for tumor and wounding microenvironments using in vivo bioluminescent imaging., *Stem cells* 27, 2614-23 (2009).

76. X. Wu et al., In vivo tracking of superparamagnetic iron oxide nanoparticle-labeled mesenchymal stem cell tropism to malignant gliomas using magnetic resonance imaging. Laboratory investigation., *Journal of neurosurgery* 108, 320-9 (2008).